



BC Geological Survey
Assessment Report
34783a

**Assessment Report on Geophysical work conducted during 2013 at the
Jay Project**

Event Number: 5496488

Liard Mining Division
British Columbia, Canada

Latitude / Longitude (center): 57°17'47"N, -125°7'39"W
UTM, NAD 83 Zone 9N (center): 371800E, 6352390N
1:250,000 NTS Map Sheet 104G-035, -025, -015

Claims Worked On:

976058, 976059, 976063, 976071, 976074, 976334, 976337, 976353, 976355, 976357, 976359,
976360, 976075, 976132, 976155, 976158, 976160, 976162, 976164

Owner: Teck Resources Limited
Suite 3300, 550 Burrard Street
Vancouver, British Columbia, V6C 0B3

Prepared By: Victoria Sterritt, Mike Takaichi, Stephen Beckman

Vancouver, British Columbia

June 24, 2014

Table of Contents

Table of Contents	2
List of Figures	3
List of Tables	3
SUMMARY	4
1.0 INTRODUCTION	4
2.0 PROPERTY LOCATION, DESCRIPTION, AND OWNERSHIP	4
2.1 Location	4
2.2 Description	4
2.3 Ownership.....	6
3.0 ACCESS, INFRASTRUCTURE, CLIMATE, AND PHYSIOGRAPHY	8
3.1 Access.....	8
3.2 Infrastructure	8
3.3 Climate.....	8
3.4 Physiography	8
4.0 EXPLORATION HISTORY	9
5.0 REGIONAL GEOLOGY	9
5.1 Regional Mineralization	9
• The Galore Creek deposit	9
• The Schaft Creek deposit.....	10
6.0 GEOLOGICAL SUMMARY OF THE JAY PROPERTY	10
6.1 Geology.....	10
6.2 Alteration and Mineralization.....	10
7.0 2013 EXPLORATION PROGRAM: AIRBORNE ZTEM SURVEY	10
7.1 Inversion of Magnetic Data	11
7.2 Inversion of ZTEM Data.....	13
REFERENCES	14
COST STATEMENT.....	15

List of Figures

Figure 1: Location map of the Jay property in British Columbia.....	5
Figure 2: Map of mineral claims comprising the Jay Property.....	7
Figure 3: Magnetic Inversion Histogram.....	11
Figure 1: Isosurface of the magnetic susceptibility inversion	12

List of Tables

Table 1: List of mineral claims comprising the Jay property.....	5
--	---

List of Appendices

Appendix I: 1:25,000 scale map of mineral claims comprising the Jay property	
Appendix II: 1:25,000 scale map of airborne survey flight lines	
Appendix III: Geotech ZTEM Survey Report	

SUMMARY

The Jay property is located in the Liard Mining Division within the Coast Range Mountains region of northwestern British Columbia. The property is located approximately 70 km south of Telegraph creek. The project property is comprised of 19 contiguous mineral claims totalling approximately 6,977 hectares. The mineral claims which comprise the project are 100% owned by Teck Resources. Work in 2013 consisted of an airborne geophysical ZTEM and magnetic survey.

1.0 INTRODUCTION

This report summarizes work conducted on the Jay project by Teck from August 24th to December 19th, 2013. Work during this time period included an airborne ZTEM survey and 3D inversion modelling of these data.

Additional information contained in this report includes a summary of the exploration history in the project area, descriptions of the regional geology, project geology and mineralization. Appendices for this report include geophysical maps and reports.

2.0 PROPERTY LOCATION, DESCRIPTION, AND OWNERSHIP

2.1 Location

The Jay property is located in the Liard Mining Division within the Coast Range Mountains region of northwestern British Columbia. The property is located approximately 70 km south of Telegraph creek (Figure 2).

2.2 Description

The Jay property consists of 18 mineral claims situated on crown land. The claims comprise a contiguous block encompassing a total of 6768.3 hectares. The claims are situated on the Klastline Plateau to the west of Kinaskan Lake, and extend south to the Willow Ridge near the southern end of Kinaskan Lake. The claim block is elongate and irregularly shaped, extending approximately 22.5km north to south, and is 7 km wide at its widest point (Figure 2, Appendix I). A complete list of tenure numbers, issue dates, expiry dates, and claim size for these mineral claims is contained in Table 1.

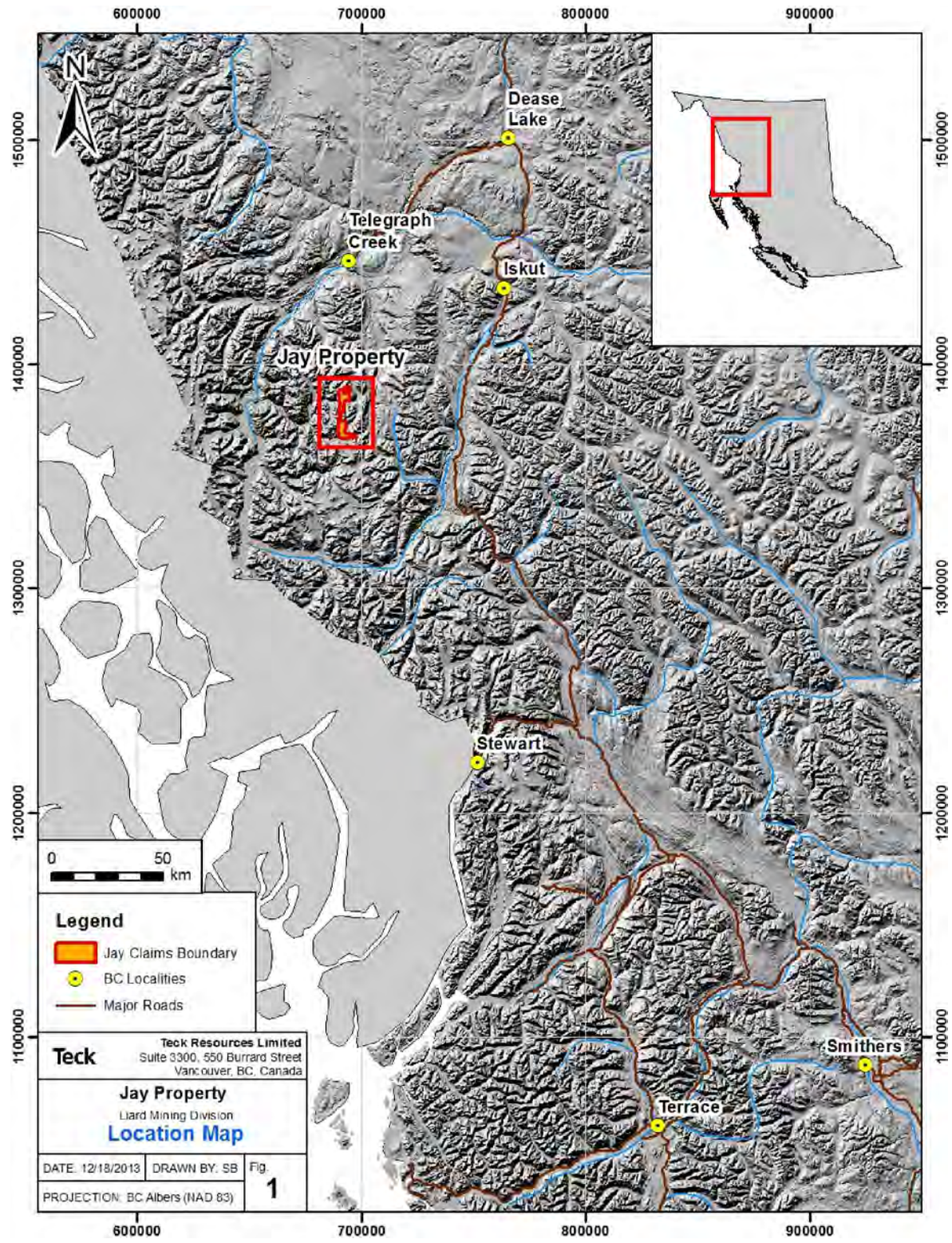


Figure 2: Location map of the Jay property within British Columbia.

Table 1: List of mineral claims comprising the Jay property.

Tenure Name	Claim Name	Issue Date	Good to Date	New Good to Date	Area (ha)
976058	HURON 021	2012/apr/02	2014/apr/02	2022/dec/30	420.3
976059	HURON 022	2012/apr/02	2014/apr/02	2022/dec/30	419.8
976063	HURON 023	2012/apr/02	2014/apr/02	2022/dec/30	419.5
976071	HURON 025	2012/apr/02	2014/apr/02	2022/dec/30	384.3
976074	HURON 026	2012/apr/02	2014/apr/02	2022/dec/30	296.7
976075	JAY019	2012/apr/02	2014/apr/02	2022/dec/30	438.3
976132	JAY020	2012/apr/02	2014/apr/02	2022/dec/30	438.2
976155	JAY021	2012/apr/02	2014/apr/02	2022/dec/30	438.2
976158	JAY022	2012/apr/02	2014/apr/02	2022/dec/30	420.5
976160	JAY023	2012/apr/02	2014/apr/02	2022/dec/30	437.8
976162	JAY024	2012/apr/02	2014/apr/02	2022/dec/30	280.2
976164	JAY025	2012/apr/02	2014/apr/02	2022/dec/30	262.6
976334	HURON 043	2012/apr/02	2014/apr/02	2022/dec/30	314.1
976337	HURON 044	2012/apr/02	2014/apr/02	2022/dec/30	383.7
976353	HURON 045	2012/apr/02	2014/apr/02	2022/dec/30	419.0
976355	HURON046	2012/apr/02	2014/apr/02	2022/dec/30	314.3
976357	HURON047	2012/apr/02	2014/apr/02	2022/dec/30	209.4
976359	HURON048	2012/apr/02	2014/apr/02	2022/dec/30	366.5
976360	HURON 049	2012/apr/02	2014/apr/02	2022/dec/30	314.0

2.3 Ownership

All nineteen claims comprising the Jay property are owned 100% by Teck Resources.

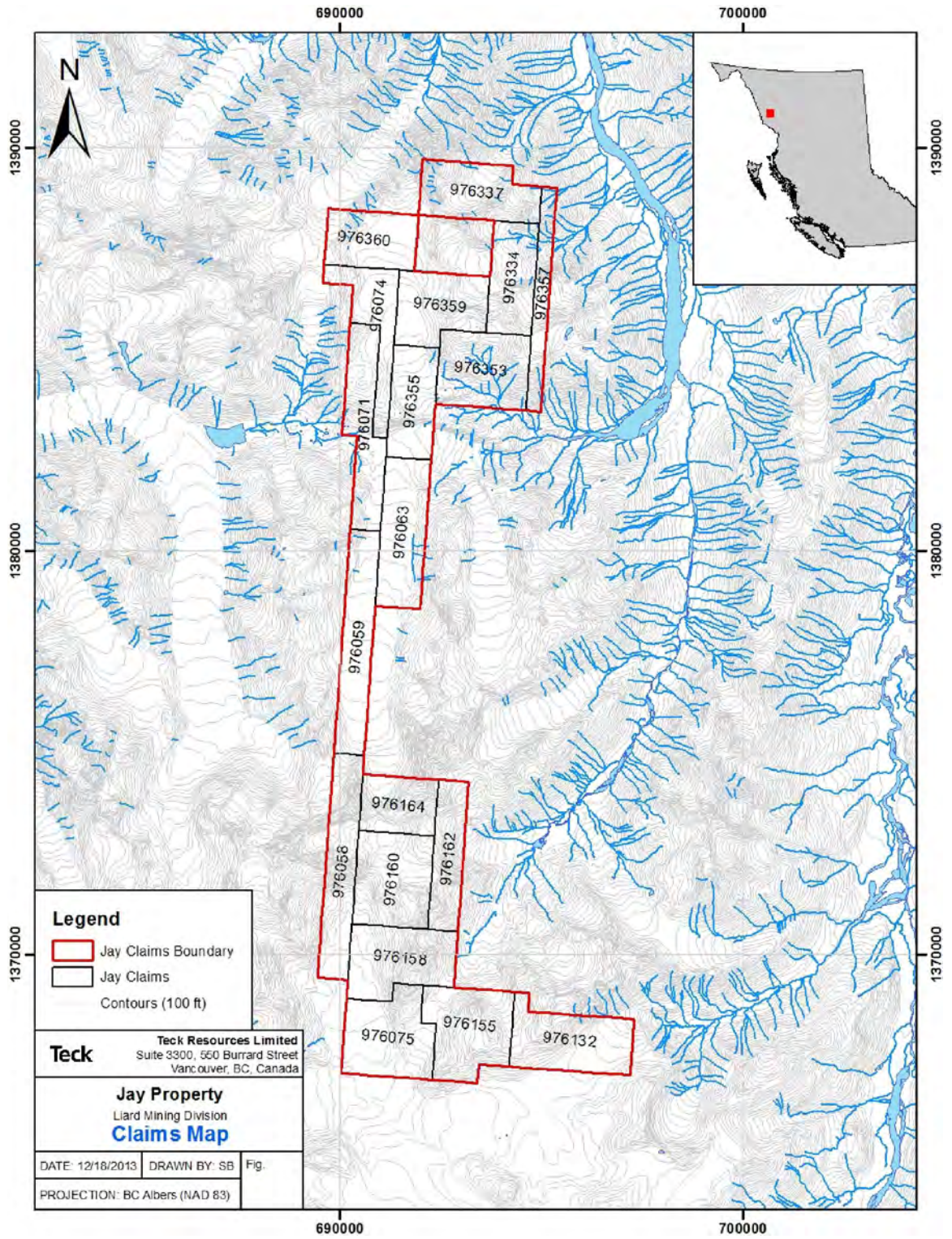


Figure 3: Map of mineral claims comprising the Jay property. See Appendix 1 for large-scale map detailing the claim boundary and individual claim numbers.

3.0 ACCESS, INFRASTRUCTURE, CLIMATE, AND PHYSIOGRAPHY

3.1 Access

Access to the property is via helicopter from the Schaft Creek camp 14 km to the northeast, the Galore Creek camp 25 km to the west and the Scud River airstrip 45 km to the west. These strips are all accessible to fixed wing aircraft from Smithers or Dease Lake.

3.2 Infrastructure

The main access route in the area is the Highway 37 in the next valley to the east. It connects the nearby communities of Dease Lake, Iskut Village, Bob Quinn, and Smithers. Smithers and Dease Lake have paved airports with regularly scheduled flights. Iskut and Bob Quinn have gravel airstrips capable of handling small aircraft.

A roadbed for an unfinished railway is located approximately 30 km east of the property near Dease Lake. This roadbed was part of a planned railway connecting Dease Lake and Fort St. James. Track for this railway ends approximately 240 km southeast of Dease Lake, and is owned by Canadian National Railway.

Resources are available in several nearby communities. Dease Lake is home to a hardware/grocery store, RCMP office, Government of British Columbia forestry office, small hospital, Tahltan First Nations Band office, school, gas station, and hotel accommodations. Telegraph Creek has a gas station/grocery store, nursing station, accommodation and a small gravel airstrip.

As of 2012, construction is underway for the BC Hydro Northwest Transmission Line (NTL). The NTL is a 287 kilovolt transmission line that will connect Bob Quinn to the Skenna Substation, located near the city of Terrace. Further extension of the NTL beyond Bob Quinn to the Tatogga Substation is ongoing to facilitate development of Imperial Metals' Red Chris project, which is due for commissioning in 2014.

3.3 Climate

The climate in the area is northern temperate, with moderately warm summers and cold dry winters. Typical daytime temperature ranges are from -20°C to 20°C throughout the year. Precipitation is estimated at over 200 cm per year, occurring mostly during the winter (October to April) as snowfall.

3.4 Physiography

The property is situated within the Schaft Creek drainage basin and covers the headwaters of Hickman Creek. The topography of the area is rugged with glacially steepened valleys and jagged

mountain peaks. Elevations range from 1370 to 2377 m above sea level. The whole property is above treeline and consists of barren rock with patchy coverage of alpine grasses, stunted spruce and glacial ice.

4.0 EXPLORATION HISTORY

Exploration in the Stikine River region began in the 1860's when placer gold was discovered south of Telegraph Creek. During the 1950's the focus shifted from placer to lode gold deposits and subsequently Hudson Bay Mining and Smelting Co. and Kennco Explorations Ltd explored for porphyry copper deposits in the region, leading to the discovery of the Galore Creek, Copper Canyon, and Schaft Creek copper-gold deposits. The BC Geological Survey conducted a regional geochemical survey in the area in 1987. Prospecting was done by United Mineral Services Ltd. in 1988 and Coast Mountain Geological in 1990.

5.0 REGIONAL GEOLOGY

The area consists of Upper Paleozoic to Tertiary Stikina Terrane rock units bounded to the west by the Coast Range Plutonic Complex and to the east by the Intermontane Belt. The oldest rocks comprise deformed Pre-Permian to Mid-Jurassic Stikine sediments, tuffs, intermediate volcanics, and limestone. Mid-Triassic rocks include silty shale, argillites and limey siltstone. Upper Triassic rocks include augite andesite and basaltic andesite flows, volcanic breccias, and tuffs with locally-derived sandstones and siltstones. Intrusive rocks include Lower Jurassic to Upper Triassic syenite stocks and dikes and Jurassic to Lower Cretaceous quartz diorite and granodiorite plutons of the Coast Plutonic Complex with numerous satellite intrusions of Eocene quartz monzonite and granodiorite.

5.1 Regional Mineralization

The region surrounding the Jay project hosts several significant porphyry Cu-Au-Mo deposits and porphyry/epithermal Cu-Au-Ag deposits. Many of these deposits are Late Triassic to Early Jurassic in age, and are associated with calc-alkalic to alkalic plutonic rocks. These plutonic rocks and associated deposits are situated within the "Stikine Arch", which is defined as a domain of folding, faulting, and Late Triassic to Early Jurassic magmatism located on the north to northwest margin of the Bowser Basin. Significant porphyry-related deposits hosted in the Stikine Arch within the vicinity of the Jay project include the following:

- The **Galore Creek** deposit, located approximately 25 km southwest of the Jay property, with proven and probable reserves of 528 Mt grading 0.585% Cu, 0.321 g/t Au, and 6.02 g/t Au, with an additional measured and indicated resource of 286.7 Mt grading 0.33% Cu, 0.27 g/t Au, and 3.64 g/t Ag, with an additional inferred resource of 346.6 Mt grading 0.42% Cu,

0.24 g/t Au, and 4.28 g/t Ag. The Galore Creek deposit is a silica-undersaturated alkalic porphyry Cu-Au deposit hosted in a Late Triassic alkalic complex. Mineralization occurs in several zones, and is associated with syenite porphyry dikes with a U-Pb age of 210 ± 1 Ma, and pipe-shaped polyolithic magmatic and hydrothermal breccias (Gill et al., 2011).

- The **Schaft Creek** deposit, located approximately 12 km west-northwest of the Jay property, with a measured resource of 143 Mt grading 0.310% Cu, 0.244 g/t Au, and 0.017% Mo, an additional indicated resource of 1,021 Mt grading 0.265% Cu, 0.182 g/t Au, and 0.017% Mo, and an additional inferred resource of 538 Mt grading 0.232% Cu, 0.179 g/t Au, and 0.017% Mo, all at a 0.2% Cu cut-off grade (Copper Fox Metals, 2013). The Schaft Creek deposit is a porphyry Cu-Au-Mo deposit associated with porphyritic granodiorite dikes and hydrothermal breccias. The Re-Os age of molybdenite mineralization at Schaft Creek is 222.0 ± 0.8 Ma (Scott et al., 2008).

6.0 GEOLOGICAL SUMMARY OF THE JAY PROPERTY

6.1 Geology

Most of the property comprises Middle Triassic hornblende-quartz diorite to granodiorite and tonalite dated at 206 Ma (unpublished K-Ar) (Massey, 2005). There are also slivers of metamorphosed Stuhini Group volcanic rocks, biotite schist, chlorite schist and Polaris Suite Alaskan-type ultramafic rocks of Mt Hickman. The intrusive, trending northeasterly, is in fault contact with Upper Triassic pyroxene porphyry flows, fragmentals, tuffs and lahar

6.2 Alteration and Mineralization

Historic work in the area has shown that alteration is limited to small chlorite-epidote stringers concentrated on fracture surfaces or more pervasive chlorite-epidote of rock matrix in zones of intense fracturing. Mineralization within the intrusive and the mafic volcanic rocks consists of disseminated pyrite and trace chalcopyrite. Shear and fracture-hosted quartz and quartz-carbonate veins of white bull quartz and clots of sulfides are also present.

7.0 2013 EXPLORATION PROGRAM: AIRBORNE ZTEM SURVEY

Work on the Jay property in 2013 consisted of an airborne geophysical survey to collect Z-axis Tipper electromagnetic (ZTEM) and magnetic data. Aeromagnetic data are useful for lithological and fault interpretation, especially in areas that are largely covered by vegetation and quaternary sediments. ZTEM data can be processed to produce apparent resistivity images at various frequencies which can also help to interpret rock type and the presence of major faults.

The ZTEM data were collected using a vertical-dipole air-core receiver coil 7.4 m in diameter slung beneath the helicopter. Two orthogonal air-core horizontal-dipole coils of 3.5 m diameter were set up on the survey block to measure the horizontal EM reference fields at 57°21.1930 N, 131°00.9750 W. Subsequently, the T_{zx} and T_{zy} tippers were calculated for six frequencies (30, 45, 90, 180, 360, and 720 Hz).

The magnetic sensor was a Geometrics caesium vapour sensor mounted on a separate bird 55 m below to the helicopter and nominally 15 m above the ZTEM bird.

The survey was flown along 250 m spaced east-west traverse lines and 2500 m north-south tie lines from August 24th to September 13th, 2013. In total, 293.551 km were flown on the Jay tenure block. The mean terrain clearance of the ZTEM bird was 443 m although the intended flight height was 80 m. Further details on the survey technique and processing can be found in Appendix A (Report on a Helicopter Borne Z-Axis Tipper Electromagnetic (ZTEM) and Aeromagnetic Geophysical Survey).

7.1 Inversion of Magnetic Data

The aeromagnetic data were inverted in-house using the Voxi algorithm provided by Geosoft. The benefit of unconstrained inversion modelling of magnetic data is that variations in sensor height, which are extreme through this survey area and affect the amplitude of the measured field, are accounted for in the resulting susceptibility model thus allowing for more accurate interpretation of the data.

The mag2 data were used as input for the inversion modelling as these are diurnally corrected but unlevelled. The magnetic sensor height was calculated as 15 m above the altitude of the EM bird above topography, which is the nominal distance at a consistent survey speed. Errors of 5% + 15 nT were applied. An IGRF of 56647 nT with an inclination of 74.6 and declination of 20.2 were used. A regional background was removed using an intercept of 56505, x-slope of 0.0012921 and y-slope of 0.005048. A mesh of 100 x 100 x 50 m was used; although smaller cells could be justified the cell size was dictated by the total number of cells needed to invert the entire survey. A lower bound of zero was imposed to return only positive (i.e. real) susceptibilities.

The inversion converged in three iterations and the resulting model looked smooth and reasonable. The predicted data fit the residual observed data to within generally three standard deviations (Figure 4). The most poorly fit points are generally those of high magnetic amplitude over the central portion of the survey area so the modelled susceptibilities in these areas are not accurate.

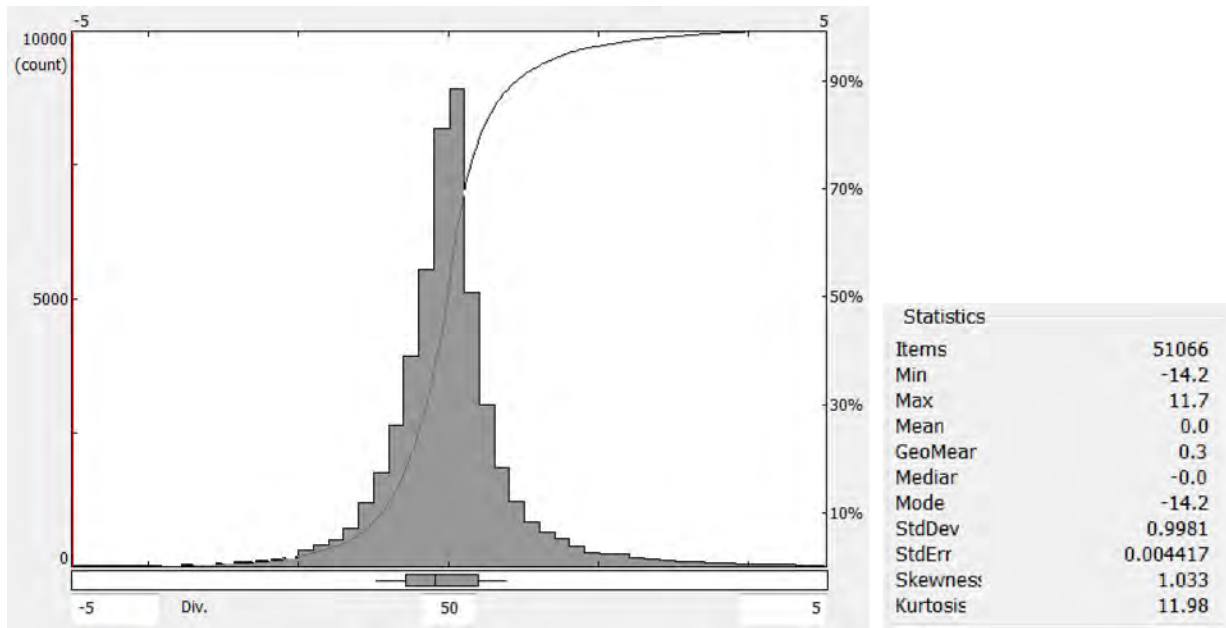


Figure 4: Histogram of the Z-score defined as the difference between the observed and predicted data normalized to the assigned error. The inset shows the summary statistics for the Z-score.

Depth slices of the Voxi susceptibility inversion model were generated for 50, 300, 550, 800, 1050, 1300, 1550, 1800 m below the DEM-SRTM topography grid. In 3D, isosurfaces at magnetic susceptibility cutoffs of 0.1×10^{-3} SI and 50×10^{-3} SI were also produced (Figure 5).

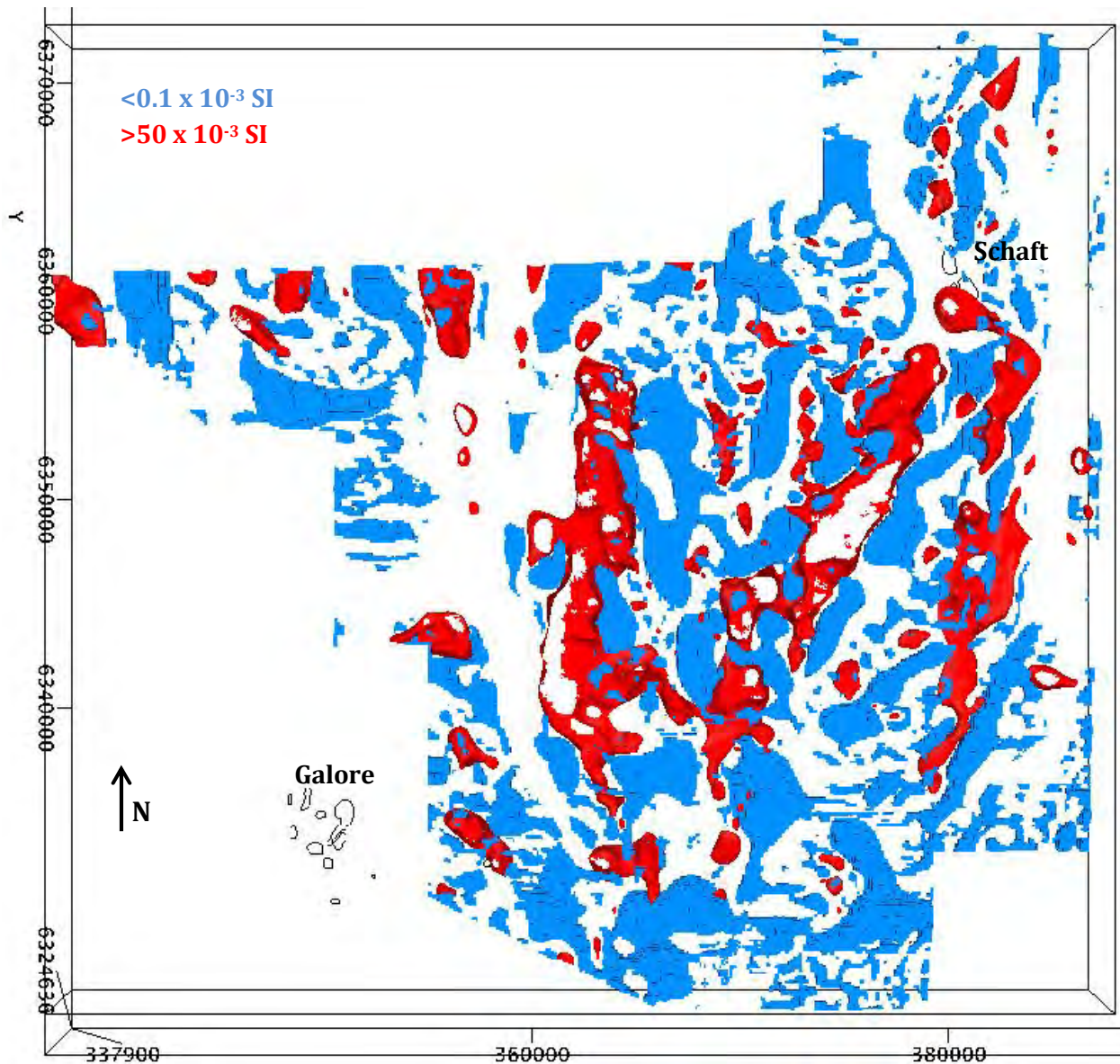


Figure 5: Isosurface of the magnetic susceptibility inversion model at a cutoff of 0.1×10^{-3} SI (blue) and 50×10^{-3} SI (red) for elevations above 1000 m a.s.l.

7.2 Inversion of ZTEM Data

Computational Geosciences Inc (CGI) was contracted to perform 3D inversion modelling of the ZTEM data using the OcTree codes from UBC. This modelling was performed to produce a 3D model of apparent resistivity that combines the resistivity information from all frequencies and both X- and Y-components while accounting for topographic effects which are present in the grid

Three starting (1000, 2000, 4000 ohm-m) models were initially tested on a coarse mesh to determine the appropriate background resistivity for the block. Ultimately, a fine mesh of 100 x 100 x 40 m cells was employed with a 2000 ohm-m starting model.

Depth slices were produced from the final inversion model and will be used for interpretation. Specifically, the main axes of conductive trends were traced as these likely represent major faults in the area that facilitate the flow of currents.

REFERENCES

Brown, D.A., Gunning, M.H., Greig, C.J., 1996. The Stikine Project: Geology of Western Telegraph Creek Map Area, Northwestern British Columbia; British Columbia Geological Survey, Bulletin 95, 182 p.

Copper Fox Metals, 2013. Feasibility Study on the Schaft Creek project, British Columbia, Canada; report prepared by Tetra Tech for Copper Fox Metals, Inc., 604 p.

Gill, R., Kulla, G., Wortman, G., Melnyk, J., and Rogers, D., 2011. Galore Creek Project, British Columbia, NI 43-101 Technical Report on Pre-Feasibility Study; prepared for NovaGold Resources Inc., 380 p.

Logan, J.M., Drobe, J.R., and McClelland, W.C., 1997. Geology of the Forrest Kerr-Mess Creek Area, Northwestern British Columbia; British Columbia Ministry of Energy and Mines, Energy and Minerals Division, Geological Survey Branch, Bulletin 104, 164 p.

Scott, J.E., Richards, J.P., Heaman, L.M., Creaser, R.A., and Salazar, G.S., 2008. The Schaft Creek porphyry Cu-Mo-(Au) deposit, northwestern British Columbia; Exploration and Mining Geology, vol. 17, no 3-4, p. 163-196.

Teck, 2011. Annual Report on the 2011 Exploration Program at the GJ/Kinaskan Property, British Columbia, Canada; Internal report for Teck Resources Limited, 51 p.

COST STATEMENT

Exploration Work type	Comment	Days			Totals
Office Studies		List Personnel (note - Office only, do not include field days)			
Literature search			\$0.00	\$0.00	
Database compilation	V Sterritt	14.2	\$450.00	\$6,375.00	
Computer modelling	Voxi inversion of magnetics	2.0	\$272.00	\$544.00	
Reprocessing of data			\$0.00	\$0.00	
General research			\$0.00	\$0.00	
Report preparation	V Sterritt	9.5	\$450.00	\$4,275.00	
Other (specify)				\$11,194.00	
				\$22,388.00	\$22,388.00
Airborne Exploration Surveys		Line Kilometres / Enter total invoiced amount			
Aeromagnetics			\$0.00	\$0.00	
Radiometrics			\$0.00	\$0.00	
Electromagnetics (ZTEM)	5420 km		\$0.00	\$676,928.00	
Gravity			\$0.00	\$0.00	
Digital terrain modelling			\$0.00	\$0.00	
Other (specify)	3D Inversion Modelling of ZTEM		\$0.00	\$56,910.00	
				\$733,838.00	\$733,838.00
Transportation		No.	Rate	Subtotal	
Airfare	V. Sterritt airfare to site		\$0.00	\$1,213.92	
Taxi			\$0.00	\$0.00	
truck rental			\$0.00	\$0.00	
kilometers			\$0.00	\$0.00	
ATV			\$0.00	\$0.00	
fuel			\$0.00	\$0.00	
Helicopter (hours)	PWH Helicopter Transportation	3	\$1,495.00	\$4,485.00	
Fuel (litres/hour)		567.00	\$1.80	\$1,020.60	
Other					
				\$6,719.52	\$6,719.52
Accommodation & Food		Rates per day			
Hotel			\$0.00	\$0.00	
Camp	VS and Geotech crew at Schaft Camp		\$0.00	\$28,250.00	
Meals	day rate or actual costs-specify		\$0.00	\$0.00	
				\$28,250.00	\$28,250.00
TOTAL Expenditures					\$791,195.52

Statement of Qualifications

I, Victoria Sterritt, do certify that:

I graduated from Queen's University in 2004 with a B.Sc.E in Geological Engineering, specializing in Applied Geophysics, and from the University of British Columbia in 2007 with an M.Sc. in Economic Geology.

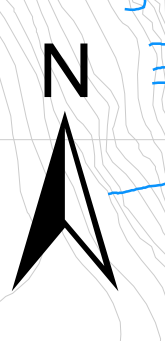
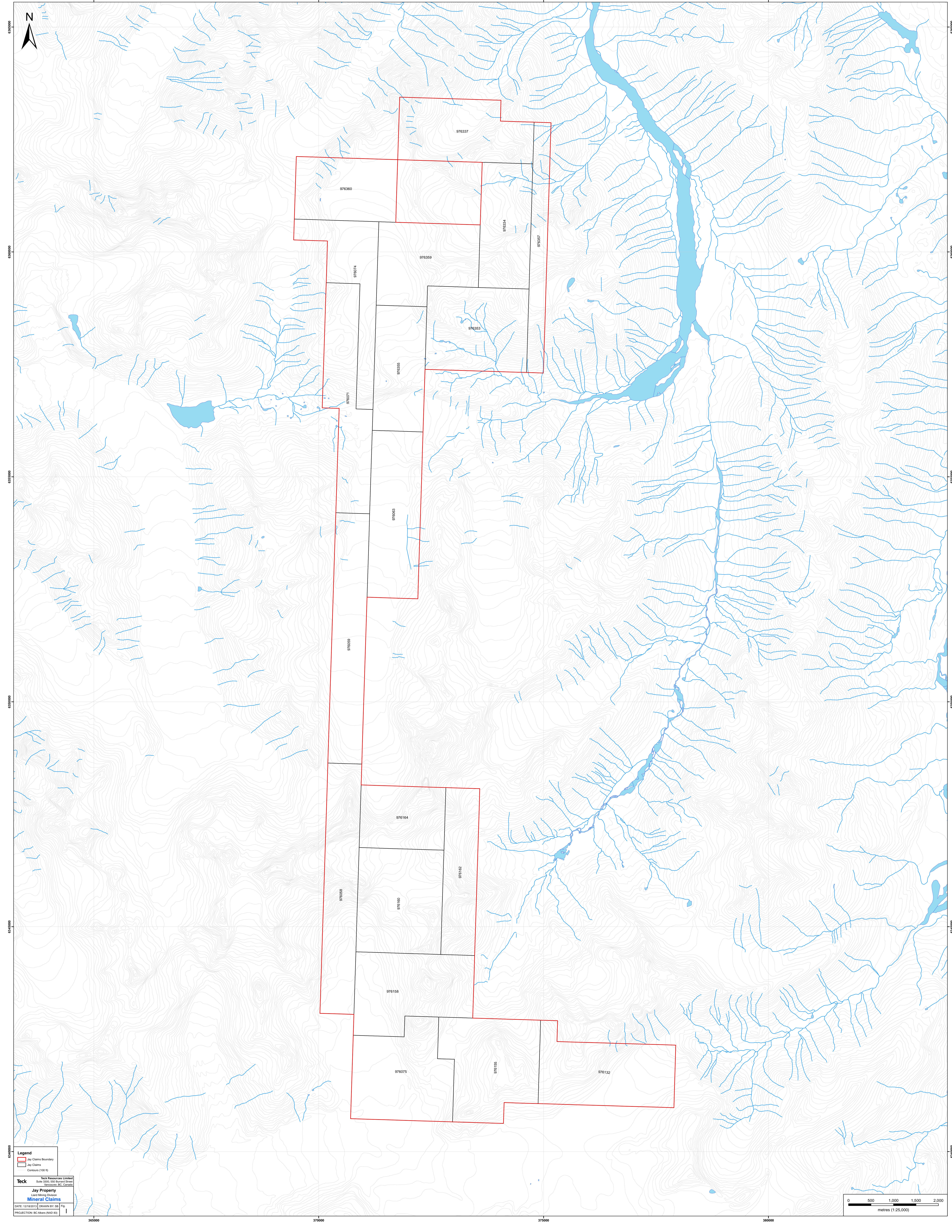
I have worked as a Geophysicist continuously since graduation and have worked for Teck Resources since 2010.

The data in this report and conclusions drawn from them are true and accurate to the best of my knowledge.

I hold no direct or indirect interest in the Jay property or any of the adjacent properties.

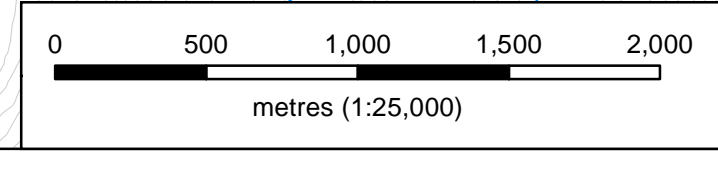
I reside in Vancouver.

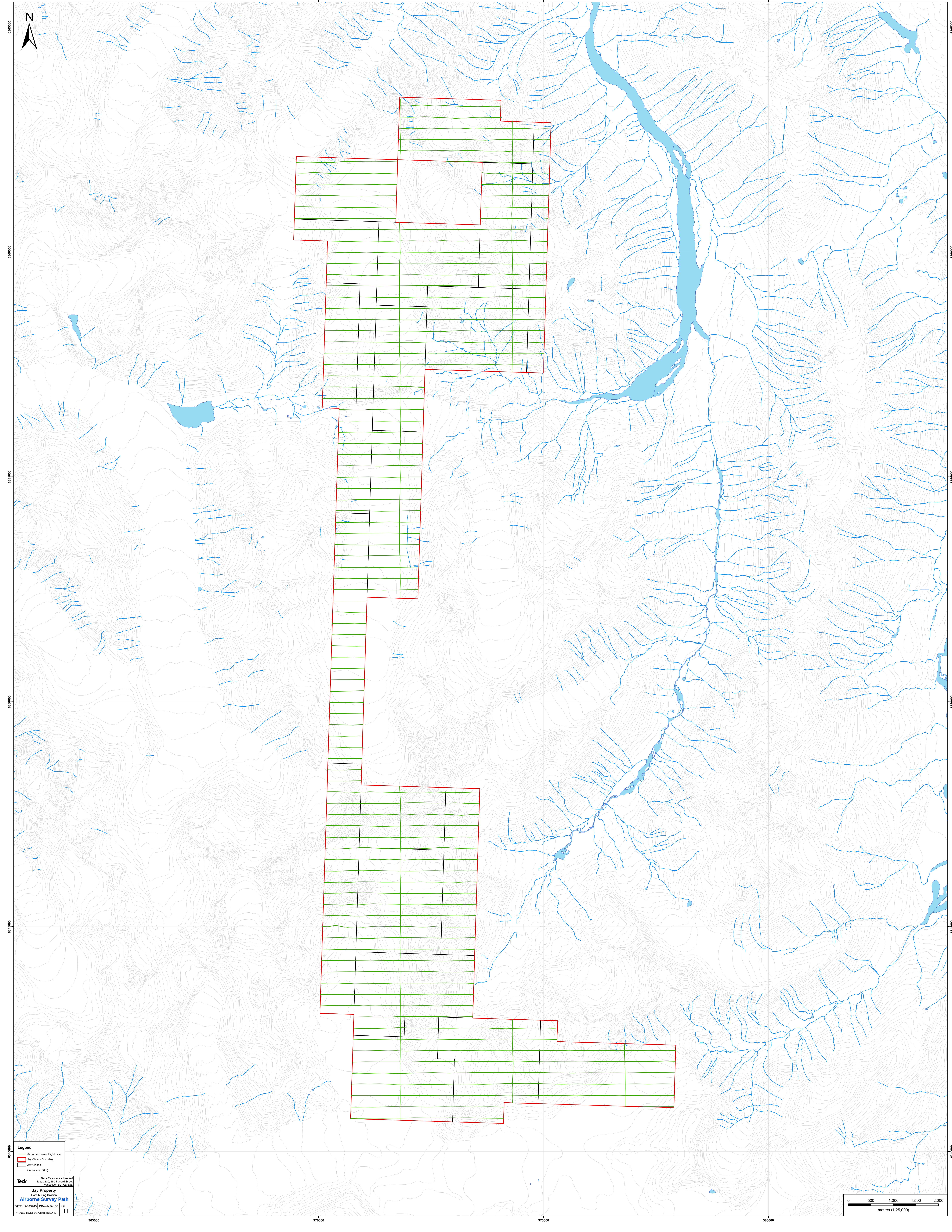
Victoria Sterritt
B.Sc.E., M.Sc., P.Eng
Vancouver, British Columbia



Legend
Jay Claims Boundary
Jay Claims
Contours (100 ft)

Teck Teck Resources Limited
Sault Ste. Marie, Ontario
Vancouver, BC, Canada
Jay Property
Lund Mining Division
Mineral Claims
DATE: 12/16/2011 DRAWN BY: SS Pfg
PROJECTION: BC Albers (NAD 83)





Legend

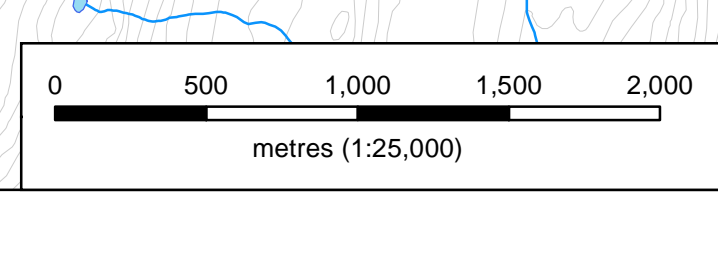
- ▬ Airborne Survey Flight Line
- ▭ Jay Claims Boundary
- ▭ Jay Claims
- ▭ Contours (100 ft)

Teck Teck Resources Limited
Suite 200, 550 Burrard Street
Vancouver, BC Canada

Jay Property
Lund Mining Division

Airborne Survey Path

DATE: 12/16/2011 DRAWN BY: SB Pfg
PROJECTION: BC Albers (NAD 83)



REPORT ON A HELICOPTER-BORNE Z-AXIS TIPPER ELECTROMAGNETIC (ZTEM) AND AEROMAGNETIC GEOPHYSICAL SURVEY

Scud Block

Scud Peak, British Columbia, Canada

For:

Teck Resources Limited

By:

Geotech Ltd.

245 Industrial Parkway North
Aurora, Ont., CANADA, L4G 4C4

Tel: 1.905.841.5004

Fax: 1.905.841.0611

www.geotech.ca

Email: info@geotech.ca



Survey flown August – September 2013
Project GL130332
October 2013

TABLE OF CONTENTS

EXECUTIVE SUMMARY	III
1. INTRODUCTION	1
1.1 General Considerations	1
1.2 Survey Location	2
1.3 Topographic Relief and Cultural Features	3
2. DATA ACQUISITION	4
2.1 Survey Area	4
2.2 Survey Operations	4
2.3 Flight Specifications	5
2.4 Aircraft and Equipment	5
2.4.1 Survey Aircraft	5
2.4.2 Airborne Receiver	5
2.4.3 Base Station Receiver	6
2.4.4 Airborne magnetometer	7
2.4.5 Radar Altimeter	7
2.4.6 GPS Navigation System	8
2.4.7 Digital Acquisition System	8
2.4.8 Mag Base Station	8
3. PERSONNEL	9
4. DATA PROCESSING AND PRESENTATION	10
4.1 Flight Path	10
4.2 In-field Processing and Quality Control	10
4.3 GPS Processing	10
4.4 ZTEM Electromagnetic Data	11
4.4.1 Preliminary Processing	11
4.4.2 Geosoft Processing	11
4.4.3 Final Processing	12
4.4.4 ZTEM Profile Sign Convention	12
4.4.5 ZTEM Quadrature Sign Dependence	13
4.4.6 Total Divergence and Phase Rotation Processing	14
4.4.7 2D EM Inversion	15
4.5 Magnetic Data	15
5. DELIVERABLES	16
5.1 Survey Report	16
5.2 Maps	16
6. CONCLUSIONS AND RECOMMENDATIONS	20
6.1 Conclusions	20
6.2 Recommendations	20
7. REFERENCES AND SELECTED BIBLIOGRAPHY	21

LIST OF FIGURES

Figure 1: Property Location	1
Figure 2: Scud Block, with ZTEM and Magnetic Base Station Locations	2
Figure 3: Google Earth image of the Scud block	3
Figure 4: ZTEM System Configuration	6
Figure 5: ZTEM base station receiver coils	7
Figure 6: ZTEM Crossover Polarity Convention for T _{xz} and T _{zy} for tie-lines (Left) and survey line (Right)	13
Figure 7: Illustration of ZTEM In-Phase & Quadrature Tipper transfer function polarity convention (e-iωt) relative to equivalent MT Tipper Quadrature polarity convention (e+iωt) for a graphitic conductor in Athabasca Basin, SK.	14

LIST OF TABLES

Table 1: Survey Specifications	4
Table 2: Survey Schedule	4
Table 3: Acquisition and Processing Sampling Rates.....	8
Table 4: Geosoft GDB Data Format.....	17

APPENDICES

A. Survey location maps.....	
B. Survey Block Coordinates.....	
C. Geophysical Maps	
D. ZTEM Theoretical Considerations	
E. ZTEM Tests over Unconformity Uranium Deposits	
F. 2D Inversions	

REPORT ON A HELICOPTER-BORNE Z-AXIS, TIPPER ELECTROMAGNETIC (ZTEM) AND AEROMAGNETIC GEOPHYSICAL SURVEY

Scud Block
Scud Peak, British Columbia, Canada

Executive Summary

During August 24th to September 13th, 2013 Geotech Ltd. carried out a helicopter-borne geophysical survey for Teck Resources Limited over the Scud block situated at Scud Peak, British Columbia, Canada.

Principal geophysical sensors included a Z-Axis Tipper electromagnetic (ZTEM) system, and a caesium magnetometer. Ancillary equipment included a GPS navigation system and a radar altimeter. A total of 5420 line-kilometres of geophysical data were acquired during the survey.

The survey operations were based out of Schaft Creek Camp and Huron Camp, British Columbia. In-field data quality assurance and preliminary processing were carried out on a daily basis during the acquisition phase. Preliminary and final data processing, including generation of final digital data and map products were undertaken from the office of Geotech Ltd. in Aurora, Ontario.

The processed survey results are presented as the following maps:

- Total Magnetic Intensity
- 3D View of In-Phase Total Divergence versus Skin Depth
- In-Phase Total Divergence (30Hz, 90Hz and 360Hz)
- Tzx In-line In-Phase & Quadrature Profiles over 90Hz Phase Rotated Grid
- Tzy Cross-line In-Phase & Quadrature Profiles over 90Hz Phase Rotated Grid

The survey report describes the procedures for data acquisition, processing, final image presentation and the specifications for the digital data set. 2D inversions over selected lines were performed in support of the ZTEM survey results.

1. INTRODUCTION

1.1 General Considerations

These services are the result of the agreement made between Geotech Ltd. and Teck Resources Limited to perform a helicopter-borne geophysical survey over the Scud block located at Scud Peak, British Columbia, Canada (Figure 1).

Victoria Sterritt represented Teck Resources Limited during the data acquisition and data processing phases of this project.

The geophysical surveys consisted of helicopter borne AFMAG Z-axis Tipper electromagnetic (ZTEM) system and aero magnetics using a caesium magnetometer. A total of 5420 line kilometres of geophysical data were acquired during the survey. The survey area is shown in Figure 2.

In a ZTEM survey, a single vertical-dipole air-core receiver coil is flown over the survey area in a grid pattern, similar to regional airborne EM surveys. Two orthogonal, air-core horizontal axis coils are placed close to the survey site to measure the horizontal EM reference fields. Data from the three coils are used to obtain the Tzx and Tzy Tipper (Vozoff, 1972) components at six frequencies in the 30 to 720 Hz band. The ZTEM is useful in mapping geology using resistivity contrasts and magnetometer data provides additional information on geology using magnetic susceptibility contrasts.



Figure 1: Property Location

The crew was based out Schaft Creek Camp and Huron Camp, British Columbia for the acquisition phase of the survey. Survey flying was started on August 24th, 2013 and was completed on September 13th, 2013.

Data quality control and quality assurance, and preliminary data processing were carried out on a daily basis during the acquisition phase of the project. Final reporting, data presentation and archiving were completed from the Aurora office of Geotech Ltd. in October, 2013.

1.2 Survey Location

The Scud block is located at Scud Peak, British Columbia, Canada as shown in Figure 2.

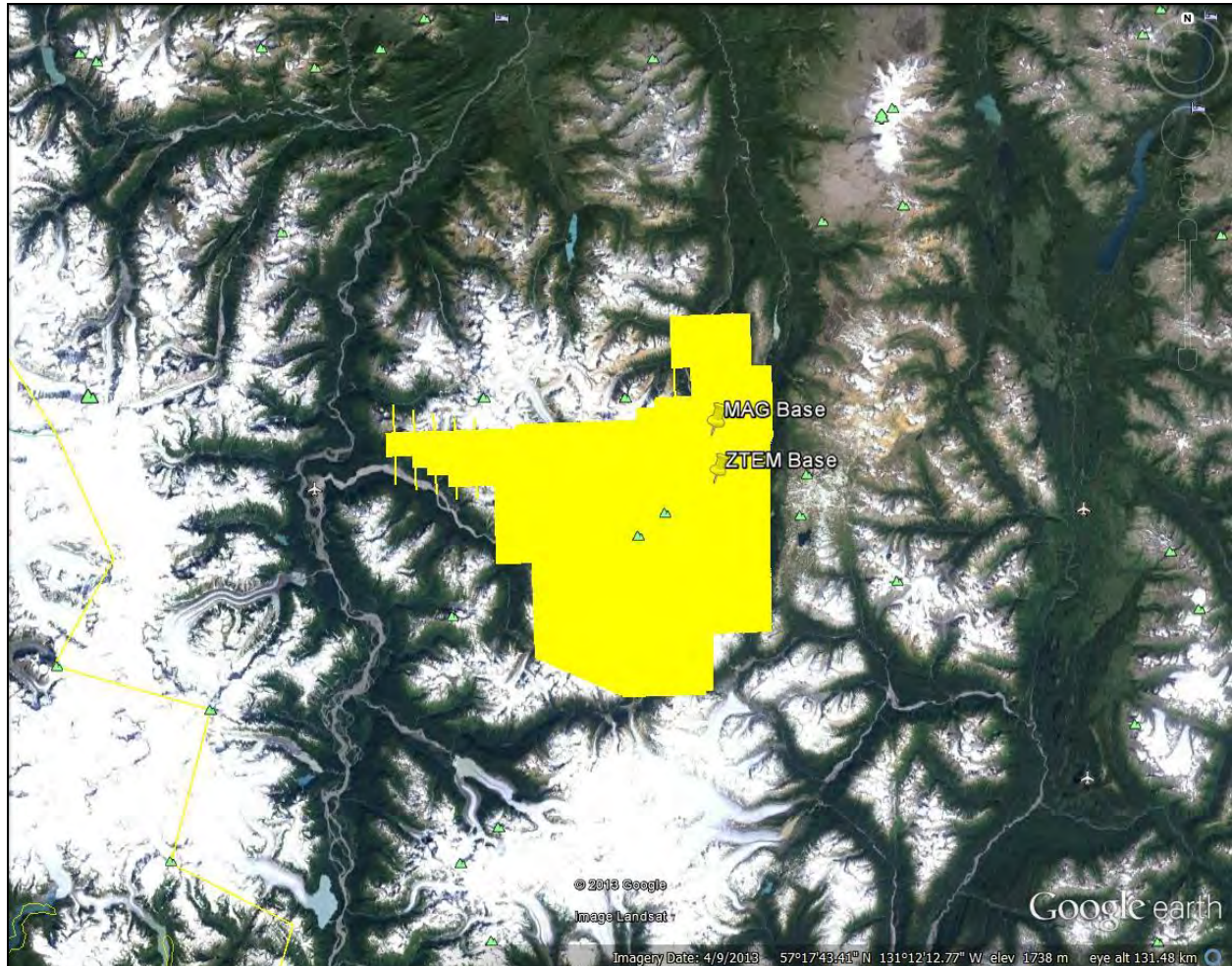


Figure 2: Scud Block, with ZTEM and Magnetic Base Station Locations

The block was flown in an east to west (N 90° E azimuth) direction, with a flight line spacing of 250 metres, as depicted in Figure 3. Tie lines were flown perpendicular to the traverse lines at a spacing of 2500 metres, in a north to south (N 0° E azimuth) direction. For more detailed information on the flight spacing and direction see Table 1.

1.3 Topographic Relief and Cultural Features

Topographically, the block exhibits a high relief with an elevation ranging from 239 to 2820 metres above mean sea level over an area of 1230 square kilometres (Figure 3). The survey area has various rivers and streams running throughout which connects various water bodies. There are limited signs of culture such as small roads and buildings, mainly concentrated in the southwest area of the block (Figure 3).

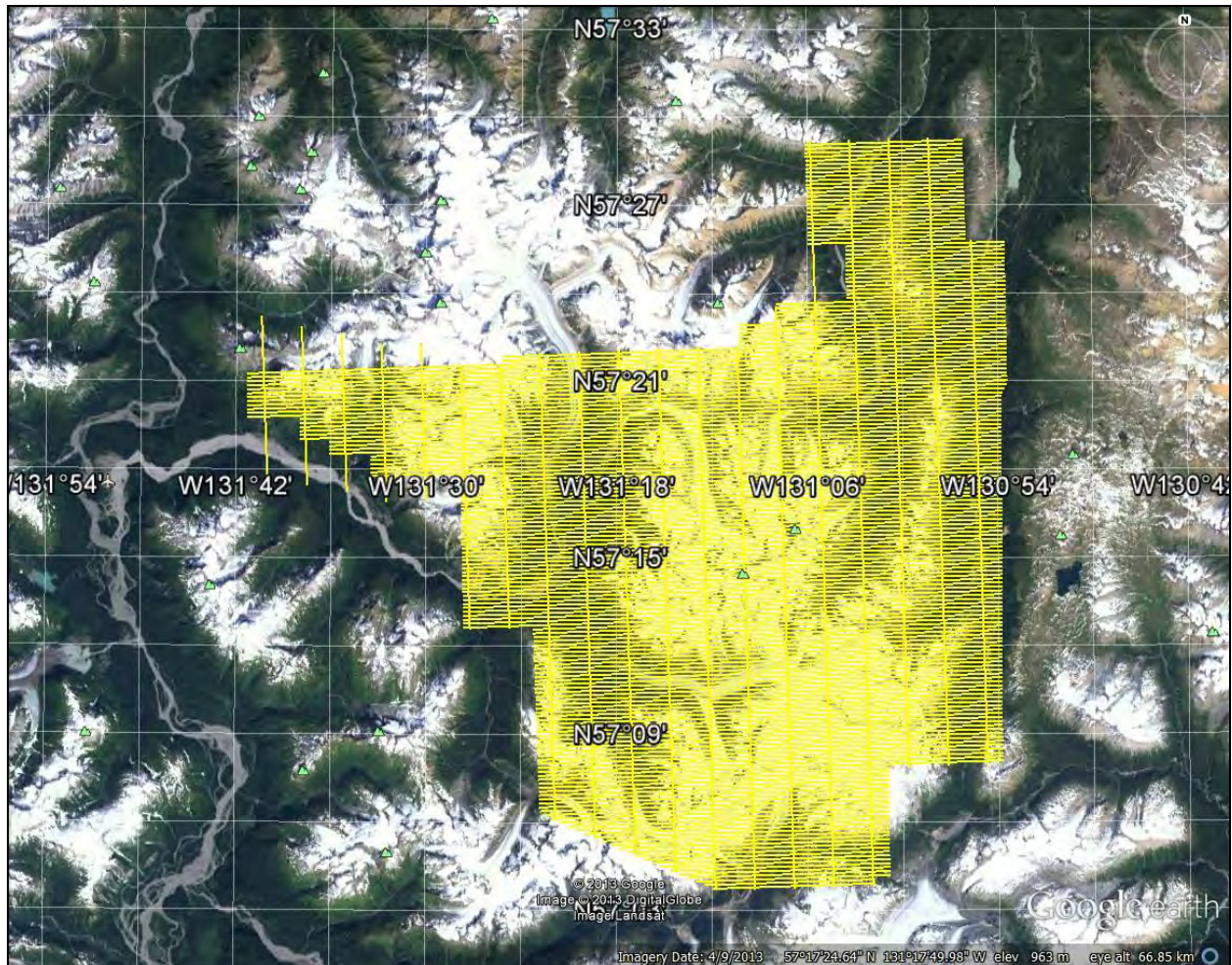


Figure 3: Google Earth image of the Scud block

The survey area is covered by numerous mining claims which are plotted on all maps. The survey area is covered by NTS (National Topographic Survey) of Canada sheet 104G02, 104G03, 104G04, 104G05, 104G06, and 104G07.

2. DATA ACQUISITION

2.1 Survey Area

The survey block (see Location map in Appendix A and Figure 2) and general flight specifications are as follows:

Table 1: Survey Specifications

Survey block	Traverse Line spacing (m)	Area (Km ²)	Planned Line-km	Actual ¹ Line-km	Flight direction	Line numbers
Scud Block	Traverse: 250	1230	5420	5513	N 90° E / N 270° E	L1000 – L2870
	Tie: 2500				N 0° E / N 180° E	T3000 – T3180
TOTAL		1230	5420	5513		

Survey block boundaries co-ordinates are provided in Appendix B.

2.2 Survey Operations

Survey operations were based out of Shaft Creek Camp and Huron Camp, British Columbia on August 24th to September 13th, 2013. The following table shows the timing of the flying.

Table 2: Survey Schedule

Date	Flight #	Flown km	Crew location	Comments
23-Aug-2013			Shaft Creek Camp, BC	Crew arrived
24-Aug-2013			Shaft Creek Camp, BC	Mobilized to Bell2
25-Aug-2013			Shaft Creek Camp, BC	System assembly
26-Aug-2013			Shaft Creek Camp, BC	Mobilized to Huron Camp
27-Aug-2013			Huron Camp, BC	Coordinated logistics & system assembly
28-Aug-2013			Huron Camp, BC	Client safety meeting& system assembly
29-Aug-2013			Huron Camp, BC	Client safety meeting& system assembly
30-Aug-2013			Huron Camp, BC	Client safety meeting & testing
31-Aug-2013	1		Huron Camp, BC	Test flight
1-Sep-2013	2,3,4	576	Huron Camp, BC	576km flown
2-Sep-2013	5,6,7	594	Huron Camp, BC	594km flown
3-Sep-2013	8,9		Huron Camp, BC	Data not accepted due to technical issues
4-Sep-2013			Huron Camp, BC	Client safety meeting & technical issues
5-Sep-2013	10	130	Huron Camp, BC	130km flown
6-Sep-2013	11,12,13	672	Huron Camp, BC	672km flown
7-Sep-2013	14,15,16	594	Huron Camp, BC	594km flown
8-Sep-2013			Huron Camp, BC	No production due to weather

¹ Actual line-km represents the total line-km contained in the final databases. These line-km normally exceed the Planned line-km's, as indicated in the survey NAV files.

Date	Flight #	Flown km	Crew location	Comments
9-Sep-2013	17,18,19	849	Huron Camp, BC	849km flown
10-Sep-2013	20,21	471	Huron Camp, BC	471km flown
11-Sep-2013			Huron Camp, BC	Pilot Rest Day
12-Sep-2013	22,23,24	740	Huron Camp, BC	740km flown
13-Sep-2013	25,26,27	798	Huron Camp, BC	Remaining kms were flown – flying complete

2.3 Flight Specifications

During the survey the helicopter was maintained at a mean height of 498 metres above the ground with a nominal survey speed of 80 km/hour for the survey block. This allowed for a nominal EM sensor terrain clearance of 428 metres and a magnetic sensor clearance of 443 metres.

The on board operator was responsible for monitoring the system integrity. He also maintained a detailed flight log during the survey, tracking the times of the flight as well as any unusual geophysical or topographic feature.

On return of the aircrew to the base camp the survey data was transferred from a compact flash card (PCMCIA) to the data processing computer. The data were then uploaded via ftp to the Geotech office in Aurora for daily quality assurance and quality control by trained personnel.

2.4 Aircraft and Equipment

2.4.1 Survey Aircraft

The survey was flown using a Eurocopter Aerospatiale (Astar) 350 B3 helicopter, registration number C-FVTM. The helicopter was operated by Geotech Aviation. Installation of the geophysical and ancillary equipment was carried out by a Geotech Ltd crew.

2.4.2 Airborne Receiver

The airborne ZTEM receiver coil measures the vertical component (Z) of the EM field. The receiver coil is a Geotech Z-Axis Tipper (ZTEM) loop sensor which is isolated from most vibrations by a patented suspension system and is encased in a fibreglass shell. It is towed from the helicopter using an 85 metre long cable as shown in Figure 4. The cable is also used to transmit the measured EM signals back to the data acquisition system.

The coil has a 7.4 metre diameter with an orientation to the Vertical Dipole. The digitizing rate of the receiver is 2000 Hz. Attitudinal positioning of the receiver coil is enabled using 3 GPS antennas mounted on the coil. The output sampling rate is 0.4 seconds (see Section 2.4.7)

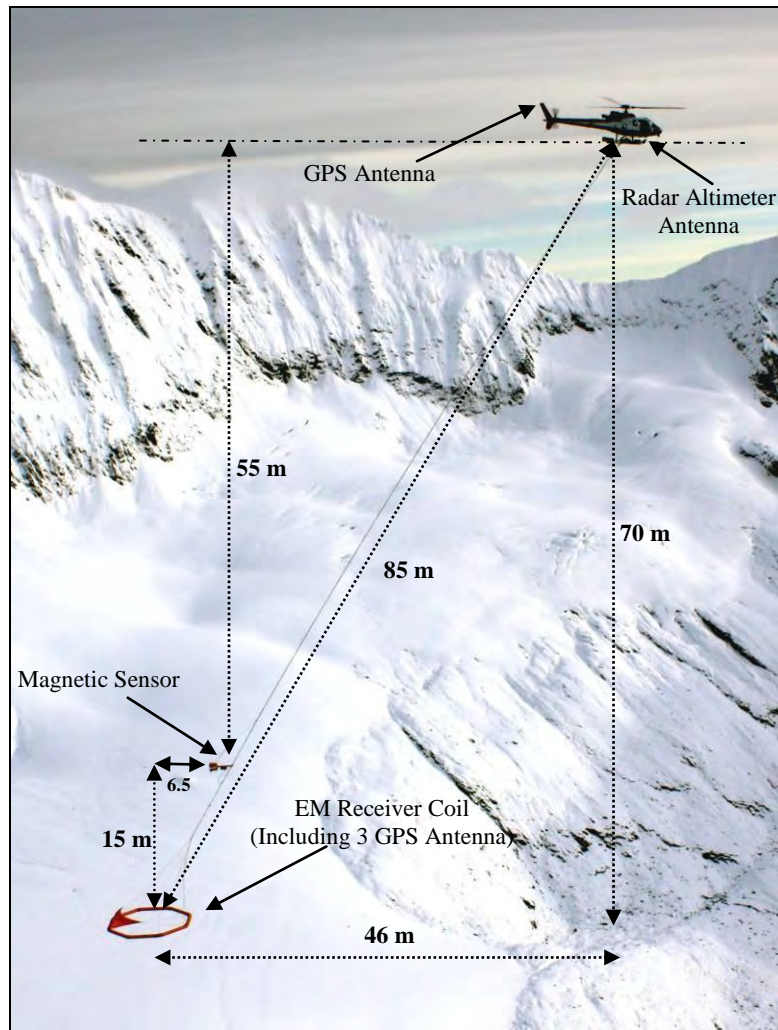


Figure 4: ZTEM System Configuration

2.4.3 Base Station Receiver

The two Geotech ZTEM base station receiver coils measure the orthogonal, horizontal X and Y components of the EM reference field. They are set up perpendicular to each other and roughly oriented according to the flight line direction. The orientation of both units is not critical as the horizontal field can be further decomposed into the two orientations of the survey flight. The orientation of the base stations were measured using a compass.

The base station coils each have a diameter of 3.5 meters, with the coil orientations to the horizontal dipole, as shown in Figure 5.

The base station receiver coils for the block were installed at the block (57°18'00.50 N, 131°00'41.10 W). The azimuth of the reference coil was N62°E (named as A) and for the orthogonal component it was N332°E (named as B). Angles A and B are taken into account together with the survey lines azimuth to calculate the in-line (Tzx) and cross-line (Tzy) field utilizing a proprietary software.



Figure 5: ZTEM base station receiver coils.

2.4.4 Airborne magnetometer

The magnetic sensor utilized for the survey was a Geometrics split-beam optically pumped caesium vapour magnetic field sensor, mounted in a separate bird, and towed on a cable at a mean distance of 55 metres below the helicopter (Figure 4). The sensitivity of the magnetic sensor is 0.02 nanoTesla (nT) at a sampling interval of 0.1 seconds. The magnetometer will perform continuously in areas of high magnetic gradient with the ambient range of the sensor approximately 20k-100k nT. The Aerodynamic magnetometer noise is specified to be less than 0.5 nT. The magnetometer sends the measured magnetic field strength as nanoTesla to the data acquisition system via the RS-232 port.

2.4.5 Radar Altimeter

A Terra TRA 3000/TRI 40 radar altimeter was used to record terrain clearance. The antenna was mounted beneath the bubble of the helicopter cockpit.

2.4.6 GPS Navigation System

The navigation system used was a Geotech PC104 based navigation system utilizing a NovAtel's WAAS(Wide Area Augmentation System) enable OEM4-G2-3151W GPS receiver, Geotech navigate software, a full screen display with controls in front of the pilot to direct the flight and an NovAtel GPS antenna mounted on the helicopter tail (Figure 5). As many as 11 GPS and two WAAS satellites may be monitored at any one time. The positional accuracy or circular error probability (CEP) is 1.8 m, with WAAS active, it is 1.0 m. The co-ordinates of the block were set-up prior to the survey and the information was fed into the airborne navigation system.

2.4.7 Digital Acquisition System

The power supply and the data acquisition system are mounted on an equipment rack which is installed into the helicopter. Signal and power wires are run through the helicopter to connect on to the tow cable outside. The tow cable supports the ZTEM and magnetometer birds during flight via a safety shear pin connected to the helicopter hook. The major power and data cables have a quick disconnect safety feature as well. The installation was undertaken by the Geotech Ltd. crew and was certified before surveying.

A Geotech data acquisition system recorded the digital survey data on an internal compact flash card. Data is displayed on an LCD screen as traces to allow the operator to monitor the integrity of the system. The data type and sampling interval as provided in Table 3.

Table 3: Acquisition and Processing Sampling Rates

DATA TYPE	ACQUISITION SAMPLING	PROCESSING SAMPLING
ZTEM Receiver	0.0005 sec	0.4 sec
Magnetometer	0.1 sec	0.4 sec
GPS Position	0.2 sec	0.4 sec
Radar Altimeter	0.2 sec	0.4 sec
ZTEM Base station	0.0005 sec	--

2.4.8 Mag Base Station

A combined magnetometer/GPS base station was utilized on this project. A Geometrics Caesium split-beam vapour magnetometer was used as a magnetic sensor with a sensitivity of 0.001 nT. The base station was recording the magnetic field together with the GPS time at 1 Hz on a base station computer.

The base station magnetometer sensors for the block were installed at the block area (57°21.1930 N, 131°00.9750 W) away from electric transmission lines and moving ferrous objects such as motor vehicles. The base station data were backed-up to the data processing computer at the end of each survey day.

3. PERSONNEL

The following Geotech Ltd. personnel were involved in the project.

Field:

Project Manager:	Scott Trew (Office)
Data QC:	Thomas Wade (Office)
Crew chief:	Colin Lennox
Operator:	Benjamin Bruder

The survey pilot and the mechanical engineer were employed directly by the helicopter operator – Geotech Aviation.

Pilot:	Bruno Prieur
Mechanical Engineer:	Chris Ward

Office:

Preliminary Data Processing:	Thomas Wade
Final Data Processing:	Nick Venter
Final Data QC:	Geoffrey Plastow
2D Inversions:	Shengkai Zhao
Reporting/Mapping:	Karl Monje

Data acquisition phase was carried out under the supervision of Andrei Bagrianski, P. Geo, Chief Operating Officer. Processing and 2D Inversions phases were carried out under the supervision of Geoffrey Plastow, P.Geo, Data Processing Manager and Jean Legault, P.Geo, P.Eng, Chief Geophysicist (Interpretation). The overall contract management and customer relations were by Sales.

4. DATA PROCESSING AND PRESENTATION

Data compilation and processing were carried out by the application of Geosoft OASIS Montaj and programs proprietary to Geotech Ltd.

4.1 Flight Path

The flight path, recorded by the acquisition program as WGS 84 latitude/longitude, was converted into the WGS 84, UTM Zone 9 North coordinate system in Oasis Montaj.

The flight path was drawn using linear interpolation between x, y positions from the navigation system. Positions are updated every second and expressed as UTM easting's (x) and UTM northing's (y).

4.2 In-field Processing and Quality Control

In-Field data processing and quality control are done on a flight by flight basis by a qualified data processor (see Section 3.0). Processing steps and check-up procedures are designed to assure the best possible final quality of ZTEM survey data. A general overview of those steps is presented in the following paragraphs.

The In-Field quality control can be separated into several phases:

- a. GPS Processing Phase: GPS Data are first examined and evaluated during the GrafMov processing.
- b. Raw data, ZTEM viewer phase:

Data can be viewed, examined for consistency, individual channel spectra examined and overall noise estimated in the viewer provided by the ZTEM proprietary software, on the raw flight data and raw base station data separately, on the merged data, and finally on the data that have undergone ZTEM processing.
- c. Field Geosoft phase:

Magnetic data, Radar altimeter data, GPS positioning data are re-examined and processed in this phase. Prior to splitting the lines EM data are examined flight by flight and the effectiveness of applying the attitude correction evaluated. After splitting the lines, a set of grids are generate for each parameter and their consistency evaluated. Data profiles are also re-evaluated on a line to line basis. A power line monitor channel is available in order to identify power line noise.

4.3 GPS Processing

Three GPS sensor (mounted on the airborne receiving loop) measurements were differentially corrected using the Waypoint GrafMov™ software in order to yield attitude corrections to recorded EM data.

4.4 ZTEM Electromagnetic Data

The ZTEM data were processed using proprietary software. Processing steps consist of the following preliminary and final processing steps:

4.4.1 Preliminary Processing

- a. Airborne EM, Mag, radar altimeter and GPS data are first merged with EM base station data into one file.
- b. Merged data are viewed and examined for consistency in an incorporated viewer
- c. In the next, processing phase, the following entities are taken into account:
 - the Base station coils orientation with respect to the Magnetic North,
 - the Local declination of the magnetic field,
 - Suggested direction of the X coordinate (North or line direction),
 - Sensitivity coefficient that compensates for the difference in geometry between the base station and airborne coils.
 - Rejection filters for the 60 Hz and helicopter generated frequencies.
- d. Six frequencies (30, 45, 90, 180, 360, and 720 Hz) are extracted from the airborne EM time-series coil response using windows of 0.4 seconds and the base station coils using windows of 1.0 seconds.
- e. The real (In-Phase) and imaginary (Quadrature) parts of the tipper transfer functions are derived from the In-line (X or Tzx) and Cross-line (Y or Tzy) components.
- f. Such processed EM data are then merged with the GPS data, magnetic base station data and exported into a Geosoft xyz file.

4.4.2 Geosoft Processing

Next stage of the preliminary data processing is done in a Geosoft™ environment, using the following steps:

- a. Import the output xyz file from the AFMAG processing, as well as the base Mag data into one database.
- b. Split lines according to the recorded line channel,
- c. GPS processing, flight path recovery (correcting, filtering, calculating Bird GPS coordinates, line splitting)
- d. Radar altimeter processing, yielding the altitude values in metres.
- e. Magnetic spike removal, filtering (applied to both airborne and base station data). Calculation of a base station corrected mag.
- f. Apply preliminary attitude corrections to EM data (In phase and Quadrature), filter and make preliminary grids and profiles of all channels.

4.4.3 Final Processing

Final data processing and quality control were undertaken by Geotech Ltd headquarters in Aurora, Ontario by qualified senior data processing personnel.

A quality control step consisted of re-examining all data in order to validate the preliminary data processing and to allow for final adjustments to the data.

Attitude corrections were re-evaluated, and re-applied, on component by component, flight by flight, and frequency by frequency bases. Any remaining line to line system noise was removed by applying a mild additional levelling correction.

Due to the mountainous terrain, the flight elevations occasionally caused the aircraft's on-board radar to fall out of range. The absence of radar data resulted in no-values being recorded for the digital elevation model (DEM), EM bird altitude (alt_b) and the radar altimeter channel. In such cases the "DEM", "alt_b" and radar have been replaced by dummy (*) values.

To make up for their absence, for 2D inversion and other interpolation purposes, the digital elevation model was approximated using the available satellite radar topographic model "SRTM 90m World Elevation" from the Geosoft DAP server and the alt_b was then recalculated using the receiver bird on-board GPS. The resulting "dem_SRTM", "alt_b_SRTM" and "radar_SRTM" channels have been added to the final database.

4.4.4 ZTEM Profile Sign Convention

Tzx and Tzy tipper components do not exhibit maxima or minima above conductors, resistors or at contacts; in fact they produce cross-over type anomalies (Ward, 1959; Vozoff, 1972; Labson, 1985). The sign of the cross-over (positive-to-negative or neg-to-pos) or its polarity (normal or reversed) depends on the line direction and follows a well-defined convention. The crossover polarity sign convention for ZTEM is according to the right hand Cartesian rule (Z positive –up) that is commonly used for multi-component transient electromagnetic methods.

For the west to east lines of the block the sign convention for the In-phase Tzx in-line component crossover is positive-negative pointing N90°E for tabular conductors' perpendicular to the profile (Figure 6-right). The corresponding Tzy component in-phase cross-over polarity is positive-negative pointing N0°E (90 degrees counter clockwise to Tzx) according to the right hand Cartesian rule.

For the south to north tie-lines of the block the sign convention for the In-phase Tzx in-line component crossover is positive-negative pointing N0°E for tabular conductors' perpendicular to the profile (Figure 6-left). The corresponding Tzy component in-phase cross-over polarity is positive-negative pointing N270°E (90 degrees counter clockwise to Tzx) according to the right hand Cartesian rule.

Conversely, tabular resistive bodies produce In-Phase cross-overs for the In-line Tzx and Cross-line Tzy components that are opposite in sign to conductors, i.e., negative to positive cross-overs.

On the other hand, the Quadrature part of the tipper transfer function can produce cross-overs in Tzx and Tzy that are of either polarity over a conductor or resistor. For this reason, the ZTEM profile sign convention only applies to the In-phase part of the tipper response. A

brief discussion of ZTEM and AFMAG, along with selected forward model responses is presented in Appendix D.

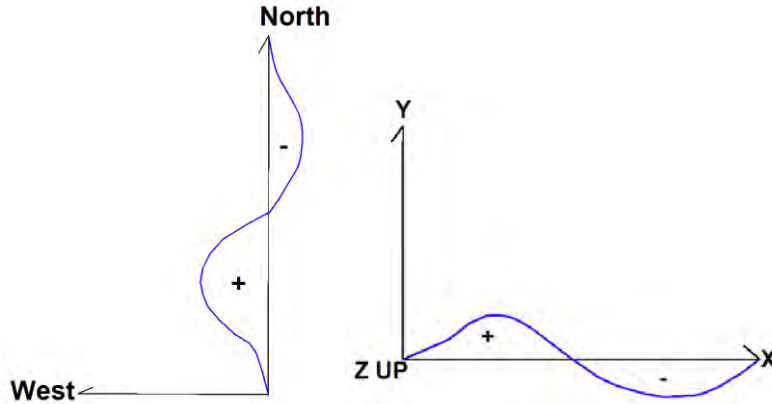


Figure 6: ZTEM Crossover Polarity Convention for T_{zx} and T_{zy} for tie-lines (Left) and survey line (Right)

4.4.5 ZTEM Quadrature Sign Dependence

One important note regarding the sign of the ZTEM Quadrature, relative to the In-Phase component, particularly with regards to computer modeling and inversion.

The sign of the magnetotelluric Quadrature relative to the In-Phase tipper transfer function component pertains to the Fourier transformation of the time series to give frequency domain spectra. There are two widely used conventions for time dependence in the transformations, **$\exp(+i\omega t)$** and **$\exp(-i\omega t)$** . That which is implemented largely is a matter of personal preference and precedent. The importance of the In-Phase and Quadrature sign convention is not critical, provided that it is known and documented.

In ZTEM, the data processing code used for the Fourier transformation the time-series data to frequency domain spectra adopts a **$\exp(-i\omega t)$** time dependence (J. Dodds, Geo Equipment Manufacturing, pers. comm., Nov-2009). Whereas in the forward modeling and inversion program Zvert2d, the sign of the Quadrature relative to the In-Phase transfer function assumes an **$\exp(+i\omega t)$** dependence².

As a result, for users interested in computer modeling and inversion of ZTEM data, the sign of the Quadrature will need to be reversed, relative to the In-Phase component, in order to provide a proper result (Figure 7). Indeed this reverse Quadrature polarity convention is assumed in all forward modeling and inversion of ZTEM data, as described in Figures 5-7 in Appendix D.

² Phillip E. Wannamaker (2009): Two-dimensional Inversion of ZTEM data: Synthetic Model Study and Test Profile Images, Internal Geotech technical report by Emblem Exploration Services Inc., January 22, 2009, 32 pp.

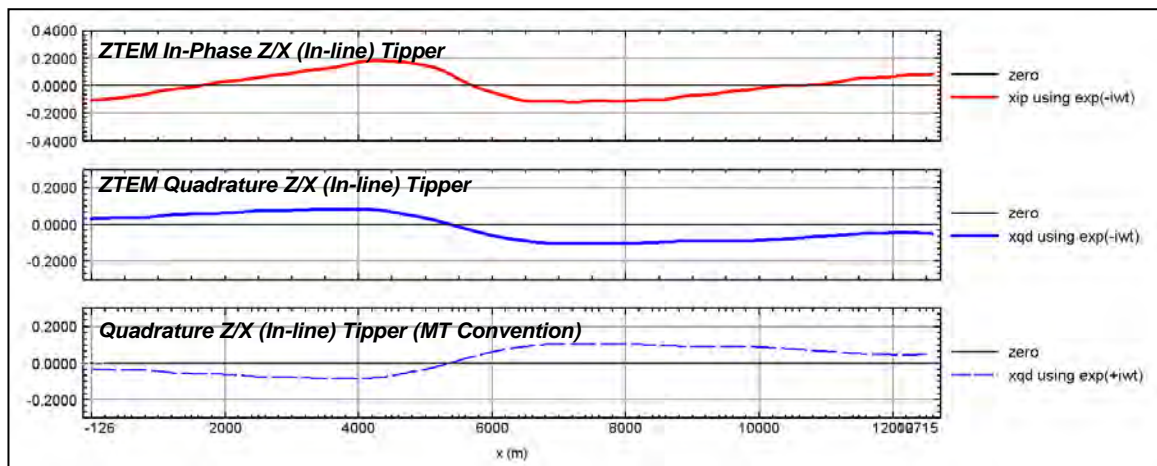


Figure 7: Illustration of ZTEM In-Phase & Quadrature Tipper transfer function polarity convention ($e^{-i\omega t}$) relative to equivalent MT Tipper Quadrature polarity convention ($e^{+i\omega t}$) for a graphitic conductor in Athabasca Basin, SK.

4.4.6 Total Divergence and Phase Rotation Processing

In a final processing step DT (Total Divergence) and PR (Phase Rotation) processing are applied to the multi-frequency In-phase and Quadrature ZTEM data. This is due to the crossover nature of the Tipper Responses; these additional processing steps are applied to convert them into local maxima for easier interpretation.

To present the data from both tipper components into one image, the Total Divergence parameter, termed the DT is calculated from the horizontal derivatives of the Tzx and Tzy tippers (Lo and Zang, 2008). It is analogous to the “Peaker” parameter in VLF (Pedersen, 1998).

<p style="text-align: center;"><u>Total Divergence DT:</u></p>	$DT = DIV (Tzx, Tzy)$ $= d(Tzx)/dx + d(Tzy)/dy$
---	---

This DT parameter was introduced by Petr Kuzmin (Milicevic, 2007, p. 13) and is derived for each of the In Phase and Quadrature components at individual frequencies. These in turn allow for minima over conductors and maxima over resistive zones. DT grids for each of the extracted frequencies were generated accordingly, using a reverse colour scheme with warm colours over conductors and cool colours over resistors.

The DT gives a clearer image of conductor’s location and shape but, as a derivative, it does not preserve some of the long wavelength information and is also sensitive to noise.

As an alternative, a 90 degree Phase Rotation (PR) technique is also applied to the grids of each individual component (Tzx and Tzy). It transforms bipolar (cross over) anomalies into single pole anomalies with a maximum over conductors, while preserving long wavelength information (Lo et al., 2009). The two orthogonal grids are then usually added to obtain a Total Phase Rotated (TPR) grid for the In-Phase and Quadrature.

<p style="text-align: center;"><u>Total Phase-Rotation TPR:</u> = PR (Tzx) + PR (Tzy)</p>
--

A presentation of the ZTEM test survey results over unconformity uranium deposits that illustrates DT and TPR examples, as documented by Lo et al. (2009) is provided in Appendix E.

4.4.7 2D EM Inversion

2d inversions of the ZTEM results were performed over selected lines using the Geotech Av2dtopo software developed by Phil Wannamaker, U. of Utah, for Geotech Ltd. The inversion algorithm is based on the 2D inversion code with Jacobians of de Lugao and Wannamaker (1996), the 2D forward code of Wannamaker et al (1987), and the Gauss-Newton parameter step equations of Tarantola (1987). Av2dtopo has been developed/modified for use with our ZTEM platform by taking into account the ground topography and the air-layer between the receiver bird and the ground surface. It also implements a depth-of-investigation (DOI) index, using the 1.5x MT maximum skin depth and integrated 1D conductance method of Spies (1989). This is shown using a dashed DOI line and opaque coloring in the 2d inversion section of Appendix F.

The 2D code only considers the In-Line (Tzx) data and assumes that the strike lengths of bodies are infinite and orthogonal to the profile. The code is designed to account for the ZTEM vertical coil receiver and fixed base station reference measurements. The inversion uses a model-mesh consisting of 440 cells laterally and 112 cells vertically. Typically the ZTEM data are de-sampled to 192 pts, in order to allow the inversion to run in 20 minutes or less. Typically, between 1-2% errors are added to the In-line in-phase (XIP) and Quadrature (XQD) data obtained at 30,45,90,180,360 & 720Hz. Errors are adjusted until numerical convergence (<1.0 rms) is attained in 5 iterations or less. All inversions are based on an a priori homogeneous starting half-space model, usually between 100 – 1000ohm metres, as determined by the interpreter, based on model testing, as described in Appendix F.

4.5 Magnetic Data

The processing of the total magnetic field intensity (TMI) data involved the correction for diurnal variations by using the digitally recorded ground base station magnetic values. The base station magnetometer data was edited and merged into the Geosoft GDB database on a daily basis. The aeromagnetic data was corrected for diurnal variations by subtracting the observed magnetic base station deviations.

Tie line levelling was carried out by adjusting intersection points along traverse lines. A micro-levelling procedure was applied to remove persistent low-amplitude components of flight-line noise remaining in the data.

The corrected magnetic data was interpolated between survey lines using a random point gridding method to yield x-y grid values for a standard grid cell size of 50 metres. The Minimum Curvature algorithm was used to interpolate values onto a rectangular regular spaced grid.

5. DELIVERABLES

5.1 Survey Report

The survey report describes the data acquisition, processing, and final presentation of the survey results. The survey report is provided in two paper copies and digitally in PDF format.

5.2 Maps

Final maps were produced at scale of 1:50,000. The coordinate/projection system used was NAD83, UTM Zone 9 North. All maps show the mining claims, flight path trace and topographic data; latitude and longitude are also noted on maps.

The preliminary and final results of the survey are presented as profile plans for the EM data that were generated for individual real (In-Phase) and imaginary parts (Quadrature) of the Tzx and Tzy components. Colour contour maps of the corresponding DT (Total Divergence) or TPR (Total Phase Rotated) grids for three of the six frequencies, (30, 45, 90, 180, 360 and 720Hz), as well as for corresponding Phase Rotated Grids for individual components.

3D views have been constructed by plotting the either DT or TPR grids at their respective penetration depths using a 2000 ohm-m half space, using the Bostick skin depth rule (Bostick, 1977) see Appendix D.

Final maps were chosen, in consultation with the client, to represent all collected data, are listed in Section 5.3.

Sample maps of the related 3D view, Magnetic and Total Divergence are included in this report and presented in Appendix C.

Digital Data

- Two copies of the data and maps on a DVD were prepared to accompany the report. Each DVD contains a digital file of the line data in GDB Geosoft Montaj.
- DVD structure.
There are two (2) main directories;

Data	contains databases and grids, as described below.
Report	contains a copy of the report and appendices in PDF format.

Databases in Geosoft GDB format, containing the channels listed in Table 4.

Table 4: Geosoft GDB Data Format

Column	Description
X	UTM Easting NAD83 Zone 9N, (Centre of the ZTEM loop) (meters)
Y	UTM Northing NAD83 Zone 9N, (Centre of the ZTEM loop) (meters)
Z	Elevation- WGS84 (Centre of the ZTEM loop) (metres)
Longitude	Longitude – WGS84 (Centre of the ZTEM loop) (Decimal degree)
Latitude	Latitude – WGS84 (Centre of the ZTEM loop) (Decimal degree)
Alt_B:	Calculated ZTEM Bird terrain clearance (metres)
Alt_b_SRTM	ZTEM Bird terrain clearance Calculated from SRTM (metres)
DEM	Digital Elevation Model (above mean sea level, meters)
DEM_SRTM	Digital Elevation Model calculated from SRTM (above mean sea level, meters)
Radar	Helicopter terrain clearance from radar altimeter (metres - AGL)
Radar_SRTM	Helicopter terrain clearance from SRTM (metres – AGL)
basemag	Magnetic base station data, nT
Gtime	UTC Time (seconds of the day)
Mag1	Measured total magnetic field, nT
Mag2	Diurnally-corrected total magnetic field, nT
TMI	Levelled total magnetic field, nT
TMI_IGRF	Levelled total magnetic field IGRF correct, nT
xlp_030Hz*	Tzx In-Phase 30 Hz final corrected
xlp_045Hz*	Tzx In-Phase 45 Hz final corrected
xlp_090Hz*	Tzx In-Phase 90 Hz final corrected
xlp_180Hz*	Tzx In-Phase 180 Hz final corrected
xlp_360Hz*	Tzx In-Phase 360 Hz final corrected
xlp_720Hz*	Tzx In-Phase 720 Hz final corrected
xQd_030Hz*	Tzx Quadrature 30 Hz final corrected
xQd_045Hz*	Tzx Quadrature 45 Hz final corrected
xQd_090Hz*	Tzx Quadrature 90 Hz final corrected
xQd_180Hz*	Tzx Quadrature 180 Hz final corrected
xQd_360Hz*	Tzx Quadrature 360 Hz final corrected
xQd_720Hz*	Tzx Quadrature 720 Hz final corrected
ylp_030Hz*	Tzy In-Phase 30 Hz final corrected
ylp_045Hz*	Tzy In-Phase 45 Hz final corrected
ylp_090Hz*	Tzy In-Phase 90 Hz final corrected
ylp_180Hz*	Tzy In-Phase 180 Hz final corrected
ylp_360Hz*	Tzy In-Phase 360 Hz final corrected
ylp_720Hz*	Tzy In-Phase 720 Hz final corrected
yQd_030Hz*	Tzy Quadrature 30 Hz final corrected
yQd_045Hz*	Tzy Quadrature 45 Hz final corrected
yQd_090Hz*	Tzy Quadrature 90 Hz final corrected
yQd_180Hz*	Tzy Quadrature 180 Hz final corrected
yQd_360Hz*	Tzy Quadrature 360 Hz final corrected
yQd_720Hz*	Tzy Quadrature 720 Hz final corrected
PLM	Power Line Monitor (60Hz)

*also includes raw and compensated data (i.e. xlp_030 and xlp_030_c respectively).

Grids in Geosoft GRD format, as follows:

TMI:	Total Magnetic Intensity
DEM:	Digital Elevation Model
PLM:	Power Line Monitor
XIP_30Hz_PR:	Tzx In-Phase Component Phase Rotated grid at 30 Hz
XIP_45Hz_PR:	Tzx In-Phase Component Phase Rotated grid at 45 Hz
XIP_90Hz_PR:	Tzx In-Phase Component Phase Rotated grid at 90 Hz
XIP_180Hz_PR:	Tzx In-Phase Component Phase Rotated grid at 180 Hz
XIP_360Hz_PR:	Tzx In-Phase Component Phase Rotated grid at 360 Hz
XIP_720Hz_PR:	Tzx In-Phase Component Phase Rotated grid at 720 Hz
XQd_30Hz_PR:	Tzx Quadrature component Phase Rotated grid at 30 Hz
XQd_45Hz_PR:	Tzx Quadrature component Phase Rotated grid at 45 Hz
XQd_90Hz_PR:	Tzx Quadrature component Phase Rotated grid at 90 Hz
XQd_180Hz_PR:	Tzx Quadrature component Phase Rotated grid at 180 Hz
XQd_360Hz_PR:	Tzx Quadrature component Phase Rotated grid at 360 Hz
XQd_720Hz_PR:	Tzx Quadrature component Phase Rotated grid at 720 Hz
YIP_30Hz_PR:	Tzy In-Phase Component Phase Rotated grid at 30 Hz
YIP_45Hz_PR:	Tzy In-Phase Component Phase Rotated grid at 45 Hz
YIP_90Hz_PR:	Tzy In-Phase Component Phase Rotated grid at 90 Hz
YIP_180Hz_PR:	Tzy In-Phase Component Phase Rotated grid at 180 Hz
YIP_360Hz_PR:	Tzy In-Phase Component Phase Rotated grid at 360 Hz
YIP_720Hz_PR:	Tzy In-Phase Component Phase Rotated grid at 720 Hz
YQd_30Hz_PR:	Tzy Quadrature component Phase Rotated grid at 30 Hz
YQd_45Hz_PR:	Tzy Quadrature component Phase Rotated grid at 45 Hz
YQd_90Hz_PR:	Tzy Quadrature component Phase Rotated grid at 90 Hz
YQd_180Hz_PR:	Tzy Quadrature component Phase Rotated grid at 180 Hz
YQd_360Hz_PR:	Tzy Quadrature component Phase Rotated grid at 360 Hz
YQd_720Hz_PR:	Tzy Quadrature component Phase Rotated grid at 720 Hz
IP_30Hz_DT:	Total Divergence grid from In-phase components at 30 Hz
IP_45Hz_DT:	Total Divergence grid from In-phase components at 45 Hz
IP_90Hz_DT:	Total Divergence grid from In-phase components at 90 Hz
IP_180Hz_DT:	Total Divergence grid from In-phase components at 180 Hz
IP_360Hz_DT:	Total Divergence grid from In-phase components at 360 Hz
IP_720Hz_DT:	Total Divergence grid from In-phase components at 720 Hz
QD_30Hz_DT:	Total Divergence grid from Quadrature components at 30 Hz
QD_45Hz_DT:	Total Divergence grid from Quadrature components at 45 Hz
QD_90Hz_DT:	Total Divergence grid from Quadrature components at 90 Hz
QD_180Hz_DT:	Total Divergence grid from Quadrature components at 180 Hz
QD_360Hz_DT:	Total Divergence grid from Quadrature components at 360 Hz
QD_720Hz_DT:	Total Divergence grid from Quadrature components at 720 Hz
IP_30Hz_TPR:	Total Phase Rotated grid from In-phase components at 30 Hz
IP_45Hz_TPR:	Total Phase Rotated grid from In-phase components at 45 Hz
IP_90Hz_TPR:	Total Phase Rotated grid from In-phase components at 90 Hz
IP_180Hz_TPR:	Total Phase Rotated grid from In-phase components at 180 Hz
IP_360Hz_TPR:	Total Phase Rotated grid from In-phase components at 360 Hz
IP_720Hz_TPR:	Total Phase Rotated grid from In-phase components at 720 Hz
QD_30Hz_TPR:	Total Phase Rotated grid from Quadrature components at 30 Hz
QD_45Hz_TPR:	Total Phase Rotated grid from Quadrature components at 45 Hz
QD_90Hz_TPR:	Total Phase Rotated grid from Quadrature components at 90 Hz
QD_180Hz_TPR:	Total Phase Rotated grid from Quadrature components at 180 Hz
QD_360Hz_TPR:	Total Phase Rotated grid from Quadrature components at 360 Hz
QD_720Hz_TPR:	Total Phase Rotated grid from Quadrature components at 720 Hz

A Geosoft .GRD file has a .GI metadata file associated with it, containing grid projection information. A grid cell size of 50 metres was used.

- Maps at 1:50,000 scale in Geosoft MAP format, as follows:

GL130332_50k_3D_IP_DT: 3D view of In-Phase Total Divergence versus Skin Depth (30-720Hz)
GL130332_50k_TMI: Total Magnetic Intensity (TMI)
GL130332_50k_30Hz_IP_DT: 30Hz In-Phase Total Divergence Grid
GL130332_50k_90Hz_IP_DT: 90Hz In-Phase Total Divergence Grid
GL130332_50k_360Hz_IP_DT: 360Hz In-Phase Total Divergence Grid
GL130332_50k_XIP_profiles_XIP_PR: Tzx (In-line) In-Phase Profiles over 90Hz Phase Rotated In-Phase Grid
GL130332_50k_XQD_profiles_XQD_PR: Tzx (In-line) Quadrature Profiles over a 90Hz Phase Rotated Quadrature Grid.
GL130332_50k_YIP_profiles_YIP_PR: Tzy (Cross-line) In-Phase Profiles over 90Hz Phase Rotated In-Phase Grid
GL130332_50k_YQD_profiles_YQD_PR: Tzy (Cross-line) Quadrature Profiles over 90Hz Phase Rotated Quadrature Grid.

- 2D Resistivity Inversion maps: 2D Inversions were performed on all survey lines.
- Maps are also presented in PDF format.
- 1:50,000 topographic vectors were taken from the NRCAN Geogratis database at: <http://geogratis.gc.ca/geogratis/en/index.html>.
- Background shading is derived from NASA SRTM (Shuttle Radar Topography Mission) data.
- A Google Earth file “*GL130332_FP.kml*” is included, showing the flight path of each block. Free versions of Google Earth software from: <http://earth.google.com/download-earth.html>

6. CONCLUSIONS AND RECOMMENDATIONS

6.1 Conclusions

A helicopter-borne ZTEM and aeromagnetic geophysical survey has been completed over the Scud block located near Scud Peak, British Columbia, Canada.

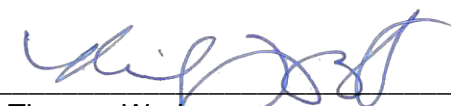
The total area coverage is 1230 km². Total survey line coverage is 5420 line kilometres. The principal sensors included a Z-Axis Tipper electromagnetic (ZTEM) system and a caesium magnetometer. Results have been presented as stacked profiles and contour colour images at a scale of 1:50,000.

There is no summary interpretation included in this report, however 2D inversions over all lines have been provided in Appendix F.

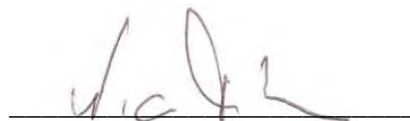
6.2 Recommendations

Based on the geophysical results obtained, a number of interesting conductive structures were identified across the property. The magnetic results also contain worthwhile information in support of exploration targets of interest. We therefore recommend a more detailed interpretation of the available geophysical data, including additional 3D inversion in conjunction with the geology, prior to ground follow up and drill testing.

Respectfully submitted³,



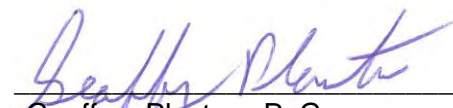
Thomas Wade
Geotech Ltd.



Nick Venter
Geotech Ltd.



Shengkai Zhao
Geotech Ltd.



Geoffrey Plastow, P. Geo
Data Processing Manager
Geotech Ltd.



Jean Legault, P. Geo, P. Eng
Chief Geophysicist (Interpretation)
Geotech Ltd.

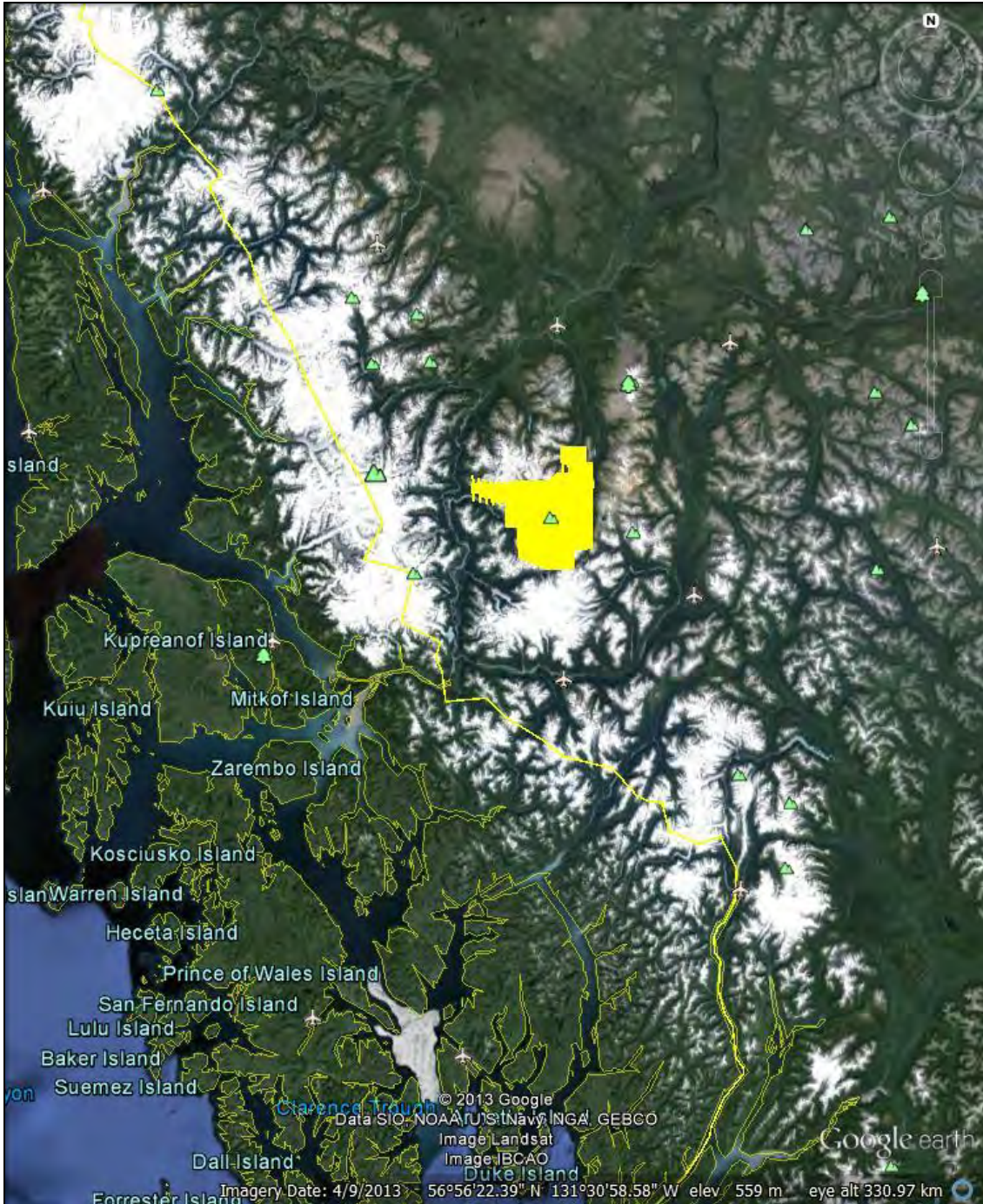
October 2013

³Final data processing of the EM and magnetic data were carried out by Geoffrey Plastow, Data Processing Manager from the office of Geotech Ltd. in Aurora, Ontario. 2D Inversions were carried out by Shengkai Zhao from the office of Geotech Ltd. in Aurora, Ontario, under the supervision of Jean Legault P. Geo, P. Eng, Chief Geophysicist (Interpretation).

7. References and Selected Bibliography

- Anav, A., Cantarano, S., Cerruli-Irelli, P., and Pallotino, G.V.(1976). A correlation method for measurement of variable magnetic fields: *Inst. Elect. and Electron. Eng. Trans., Geosc. Elect.* GE14, 106-114.
- Bostick, F.X. (1977). A Simple almost exact method of MT analysis, Proceedings of the University of Utah Workshop on Electrical Methods in Geothermal Exploration, 175-188.
- De Lugao, P.P.,and Wannamaker, P.E.(1996). Calculating the two-dimensional magnetotelluric Jacodian in finite elements using reciprocity: *Geophys. J. Int.*, **127**, 806-810
- Karous, M.R., and S. E. Hjelt (1983). Linear filtering of VLF dip-angle measurements: *Geophysical Prospecting*, **31**, 782-794.
- Kuzmin, P., Lo, B. and Morrison, E. (2005). Final Report on Modeling, interpretation methods and field trials of an existing prototype AFMAG system, Miscellaneous Data Release 167, Ontario Geological Survey, 2005.
- Labson, V. F., Becker A., Morrison, H. F., and Conti, U. (1985). Geophysical exploration with audiofrequency natural magnetic fields. *Geophysics*, **50**, 656-664.
- Legault, J.M., Kumar, H., Milicevic, B., and Hulbert, L. (2009), ZTEM airborne tipper AFMAG test survey over a magmatic copper-nickel target at Axis Lake in northern Saskatchewan, SEG Expanded Abstracts, **28**, 1272-1276
- Legault, J.M., Kumar, H., Milicevic, B., and Wannamaker, P.,(2009), ZTEM tipper AFMAG and 2D inversion results over an unconformity uranium target in northern Saskatchewan, SEG Expanded Abstracts, **28**, 1277-1281.
- Lo, B., Legault, J.M., Kuzmin, P. and Combrick, M. (2009). ZTEM (Airborne AFMAG) tests over unconformity uranium deposits, Extended abstract submitted to 20th ASEG International Conference and Exhibition, Adelaide, AU, 4pp.
- Lo, B., and Zang, M., (2008), Numerical modeling of Z-TEM (airborne AFMAG) responses to guide exploration strategies, SEG Expanded Abstracts, **27**, 1098-1101.
- Milicevic, B. (2007). Report on a helicopter borne Z-axis, Tipper electromagnetic (ZTEM) and magnetic survey at Safford, Giant Hills, Baldy Mountains and Sierrita South Areas, Arizona, USA., Geotech internal survey report (job A226), 33pp.
- Pedersen, L.B., Qian, W., Dynesius, L. and Zhang, P. (1994). An airborne sensor VLF system. From concept to realization. *Geophysical Prospecting*, **42**, i.8, 863-883
- Pederson, L.B. (1998). Tensor VLF measurements: first experiences, *Exploration Geophysics*, **29**, 52-57.
- Spies, B., 1989, Depth of investigation in electromagnetic sounding methods, *Geophysics*, **54**, 872-888.
- Strangway, D. W., Swift Jr., C. M., and Holmer, R. C. (1973). The Application of Audio-Frequency Magnetotellurics (AMT) to Mineral Exploration. *Geophysics*, **38**, 1159-1175.
- Tarantola, A.,(1987) Inverse problem theory: Elsevier, New York, 613 pp.
- Vozoff, K.(1972). The magnetotelluric method in the exploration of sedimentary basins. *Geophysics*, **37**, 98-141.
- Vozoff, K. (1991). The magnetotelluric method. In: Electromagnetic Methods in Applied Geophysics - Volume 2 Applications, edited by Nabighian, M.N., Society of Exploration Geophysicists, Tulsa., 641-711.
- Ward, S. H. (1959). AFMAG - Airborne and Ground. *Geophysics*, **24**, 761-787.
- Ward, S. H, O'Brien, D.P., Parry, J.R. and McKnight, B.K. (1968). AFMAG Interpretation. *Geophysics*, **33**, 621-644.
- Wannamaker, P.E., Stodt, J.A., and Rijo, L., (1987). A stable finite element solution for two-dimensional magnetotelluric modeling: *Geophy. J. Roy. Astr. Soc.*,**88**, 277-296.
- Zhang, P. and King, A. (1998). Using magnetotellurics for mineral exploration, Extended Abstracts from 1998 Meeting of Society of Exploration Geophysics

APPENDIX A
SURVEY BLOCK LOCATION MAP



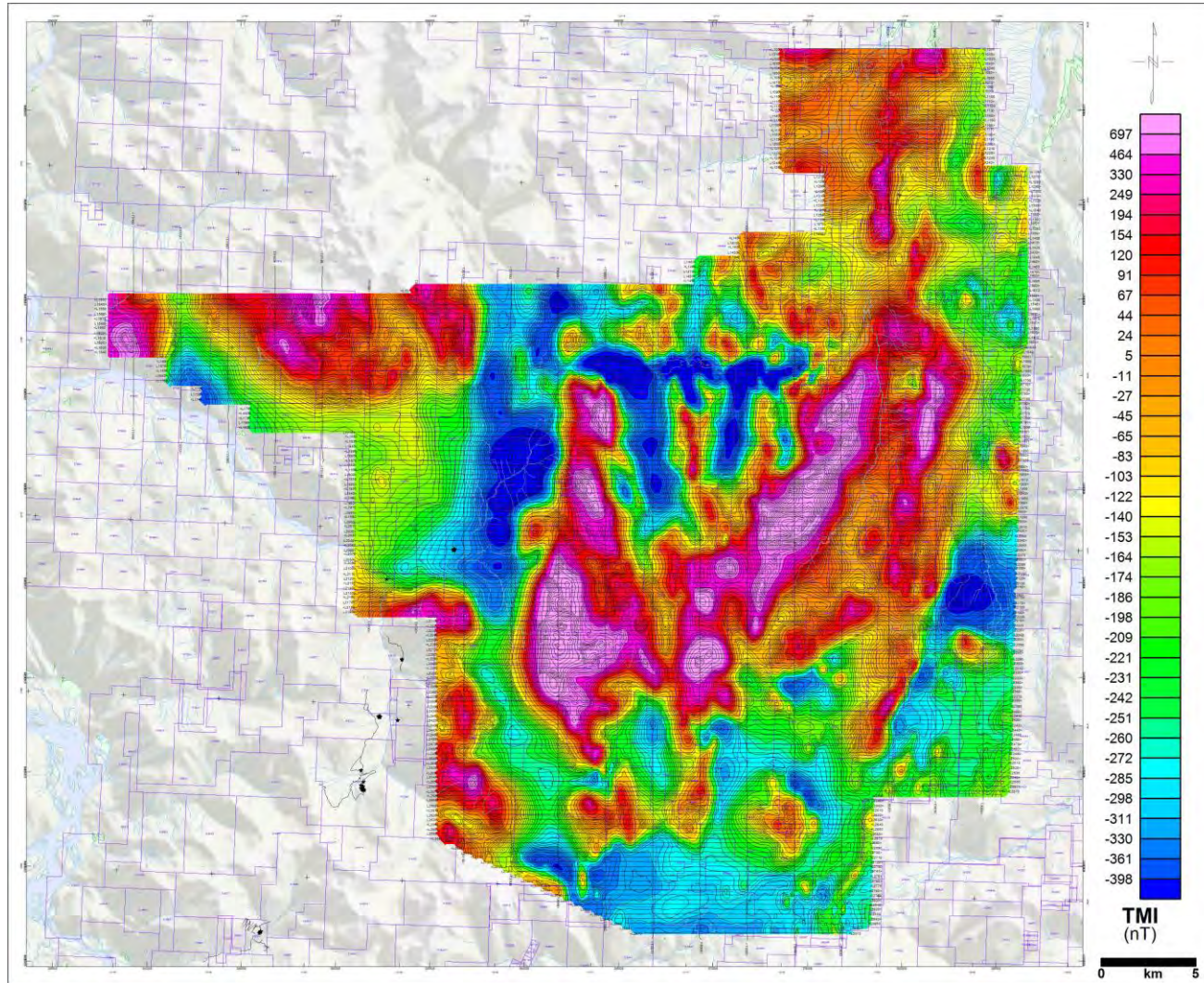
Survey Overview Location Map

APPENDIX B

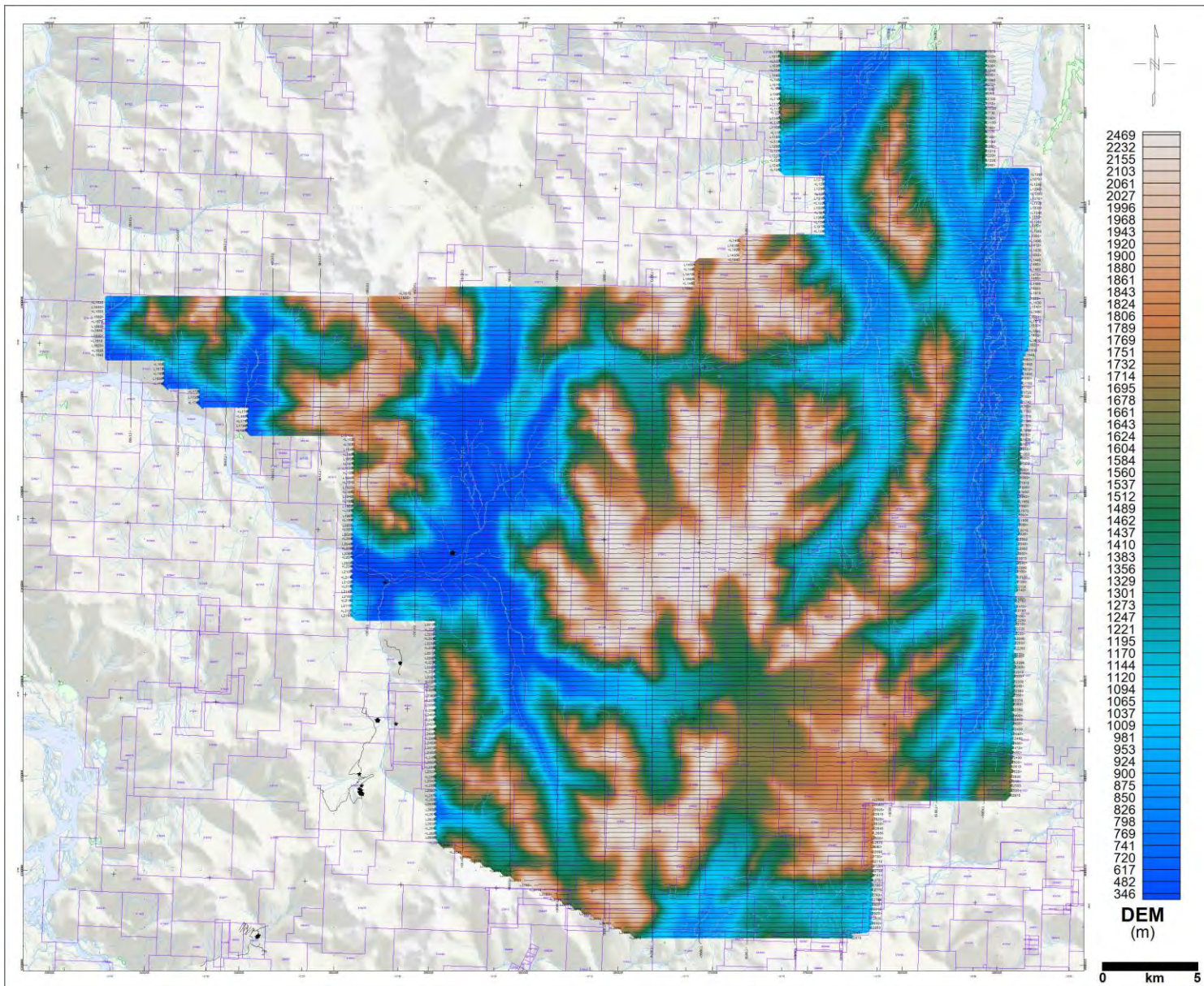
SCUD SURVEY BLOCK COORDINATES (WGS84 Zone 9N)

X	Y
385244	6333744.4
378036.7	6333839.6
377882.1	6326809.6
376882.5	6326838.9
376839.9	6326257
366918	6326336.4
355816.1	6331606.9
355783.1	6343304.4
351379.8	6343364.7
351493.7	6352988.1
345846.5	6353210.5
345898.4	6354587.8
343263.7	6354687.8
343299.2	6355615.1
341417.7	6355687.5
341471.7	6357078.5
338173.2	6357207.6
338218.9	6360000
354382.8	6360000
354407.5	6360708
369355.1	6360708
369437.2	6362042.2
371756.5	6362050.7
371807.9	6363354.5
376295.2	6363396.8
376316.4	6366941.8
373962.5	6366941.8
373962.5	6373472.2
383962.5	6373472.2
383962.5	6366941.8
386417	6366941.8
386301.2	6357783.4
385904.8	6357064.7

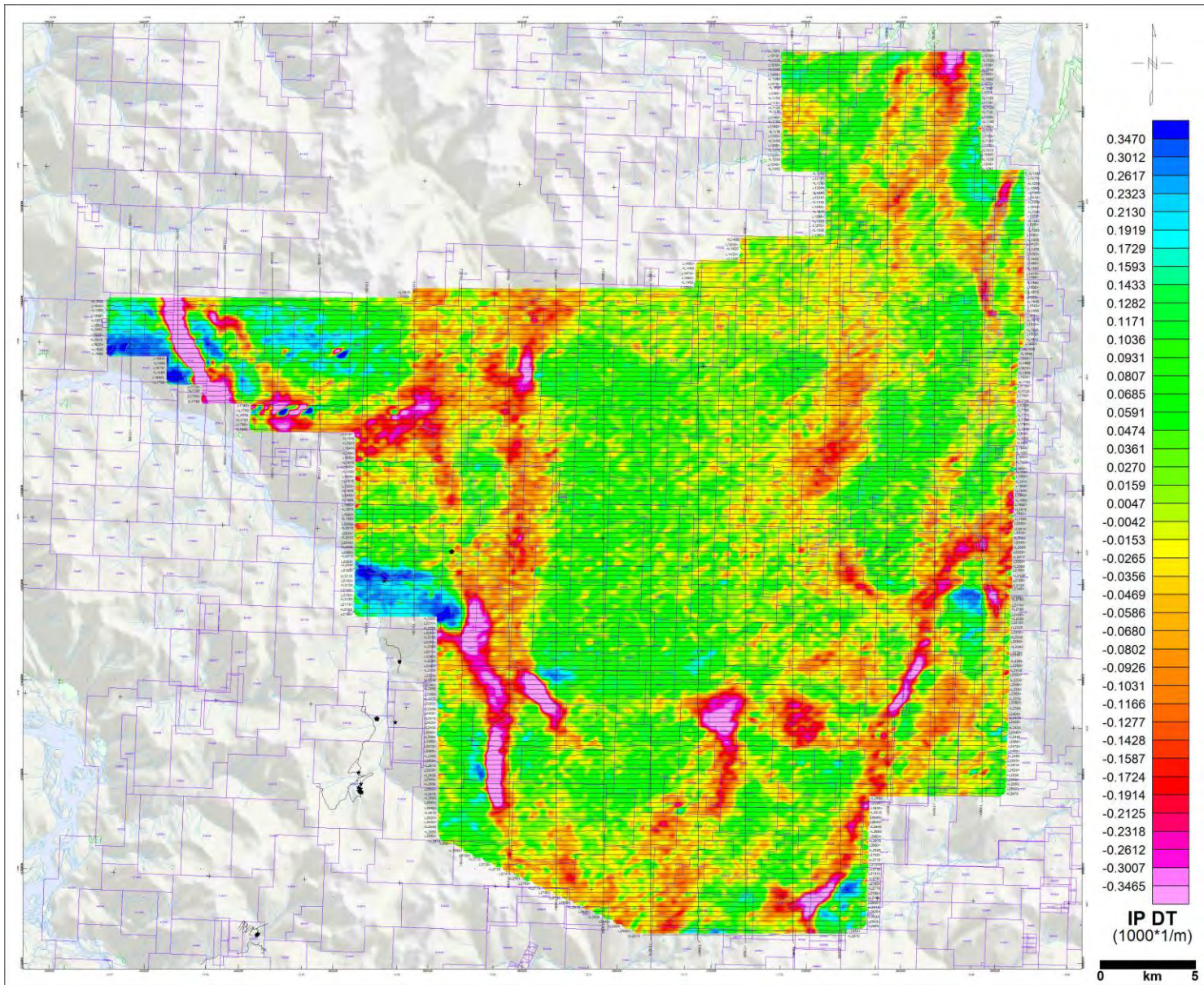
APPENDIX C GEOPHYSICAL MAPS¹



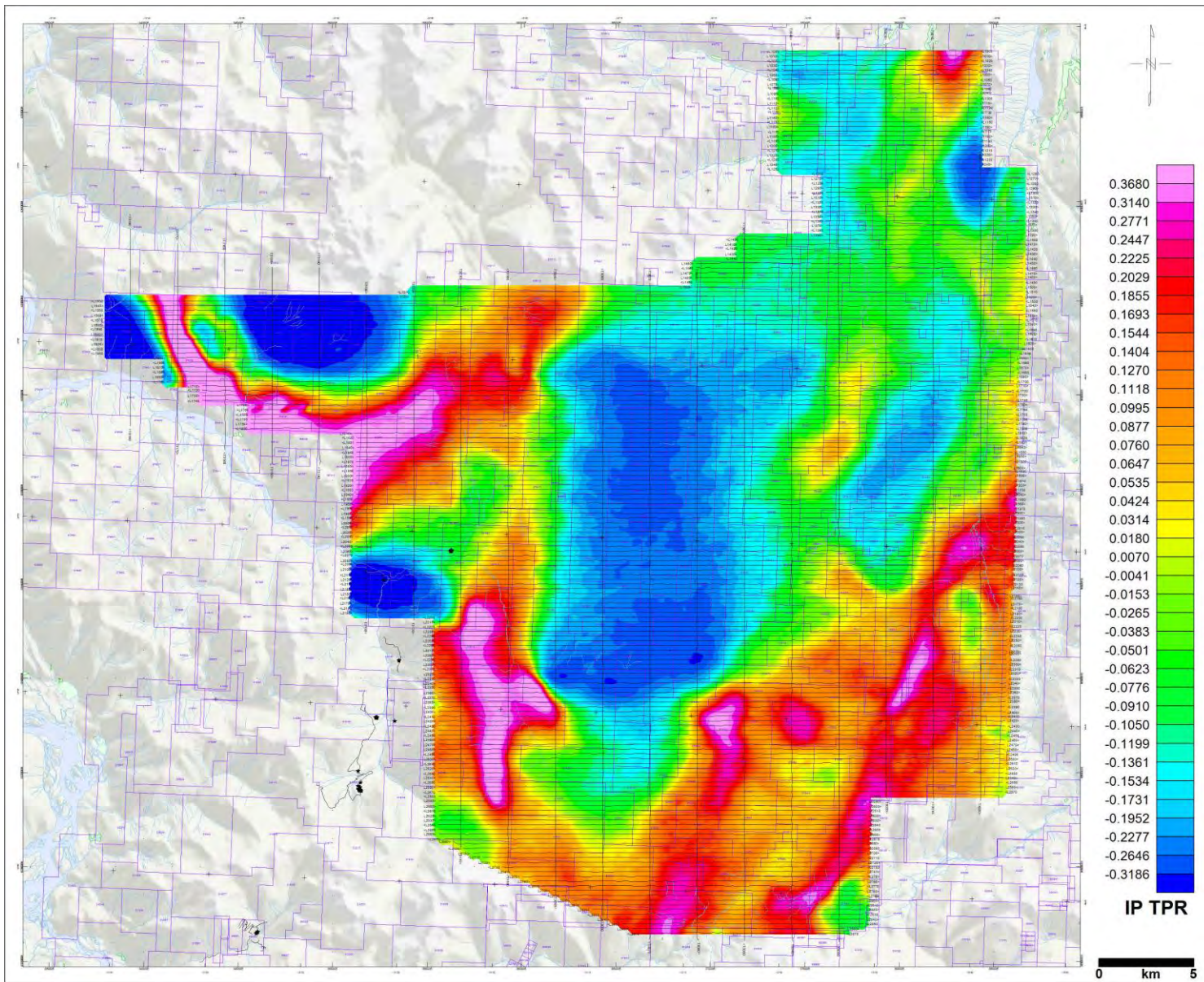
¹ Full size geophysical maps are also available in PDF format on the final DVD



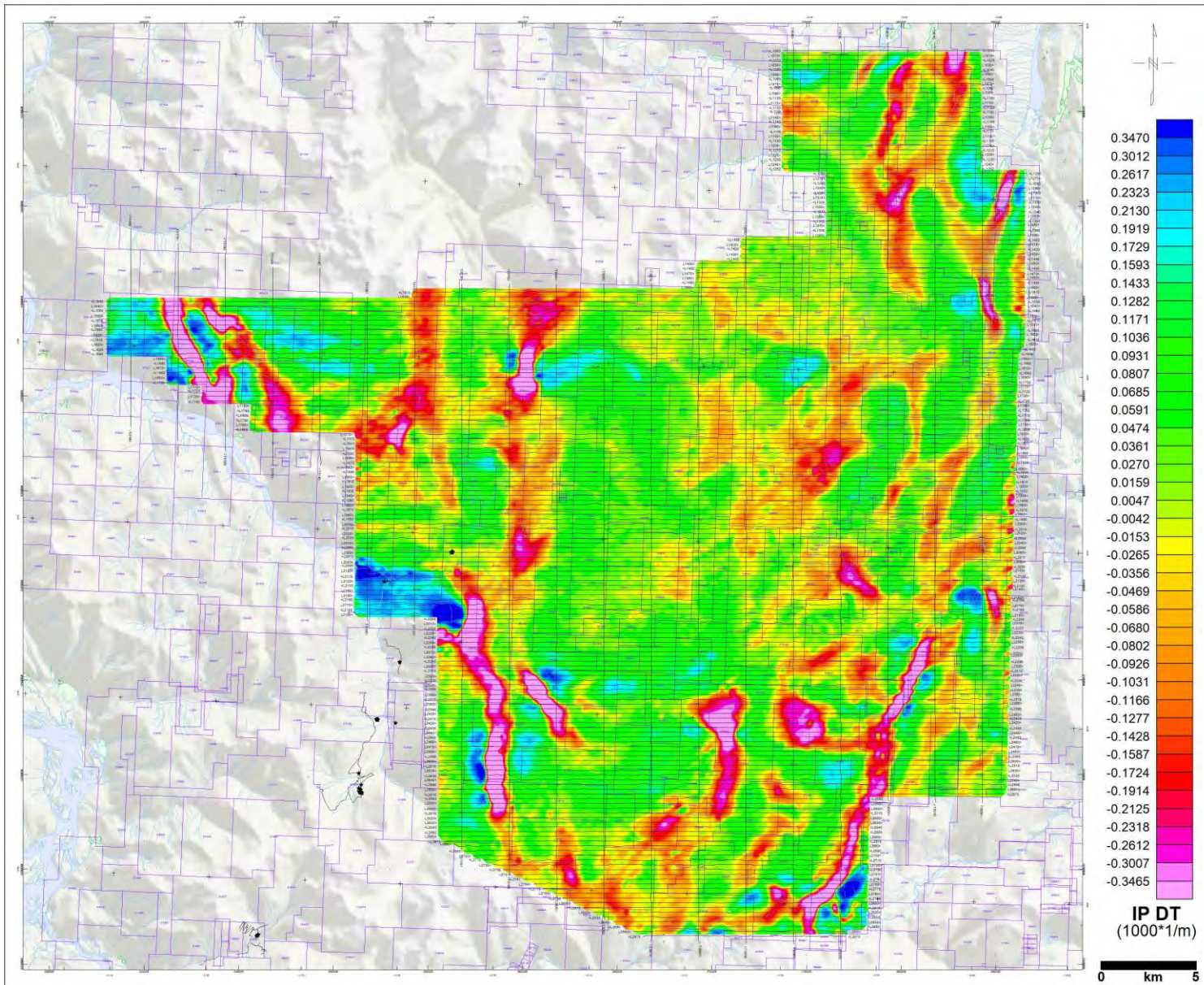
Digital Elevation Model (DEM)



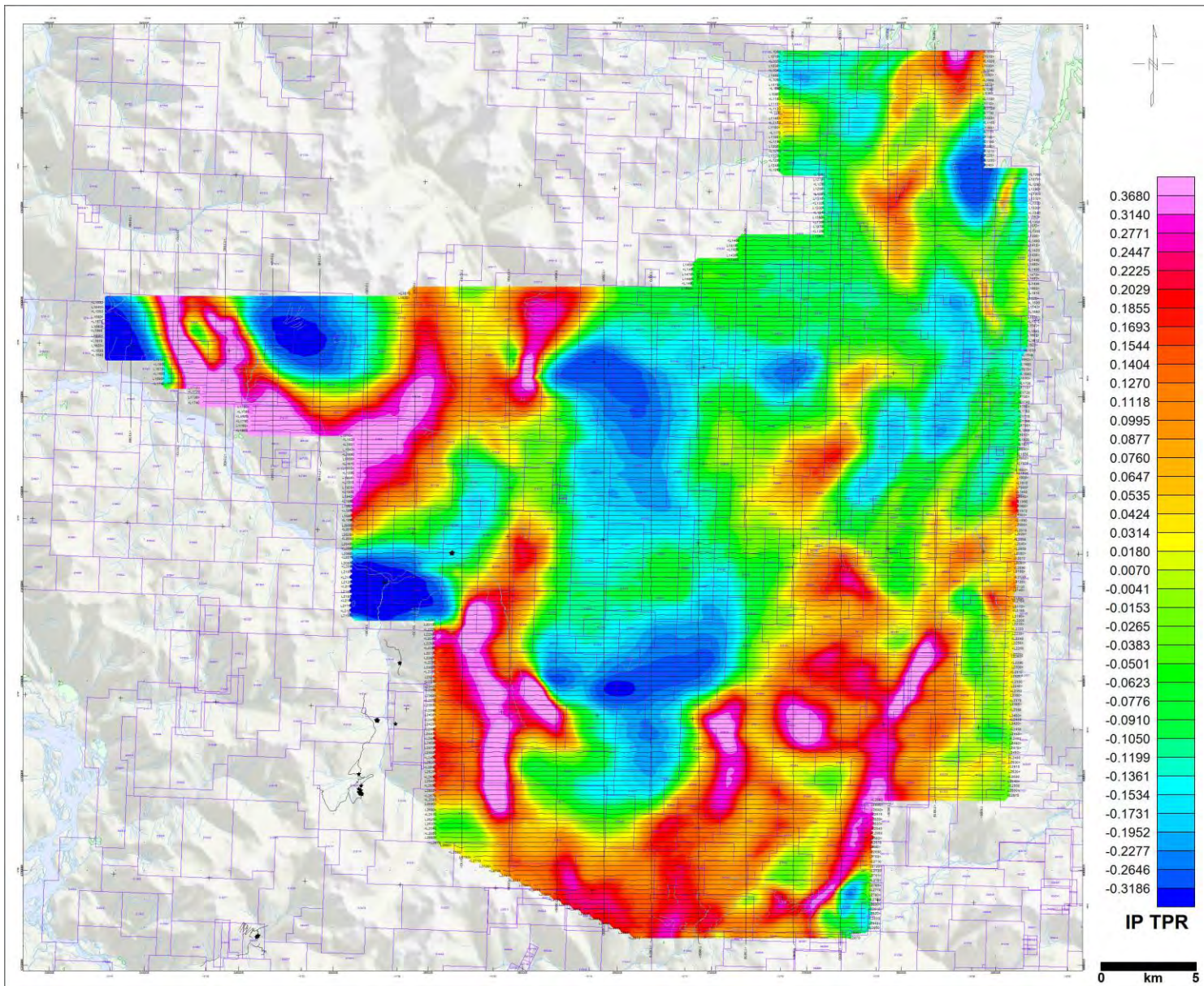
30Hz In-Phase Total Divergence (DT)



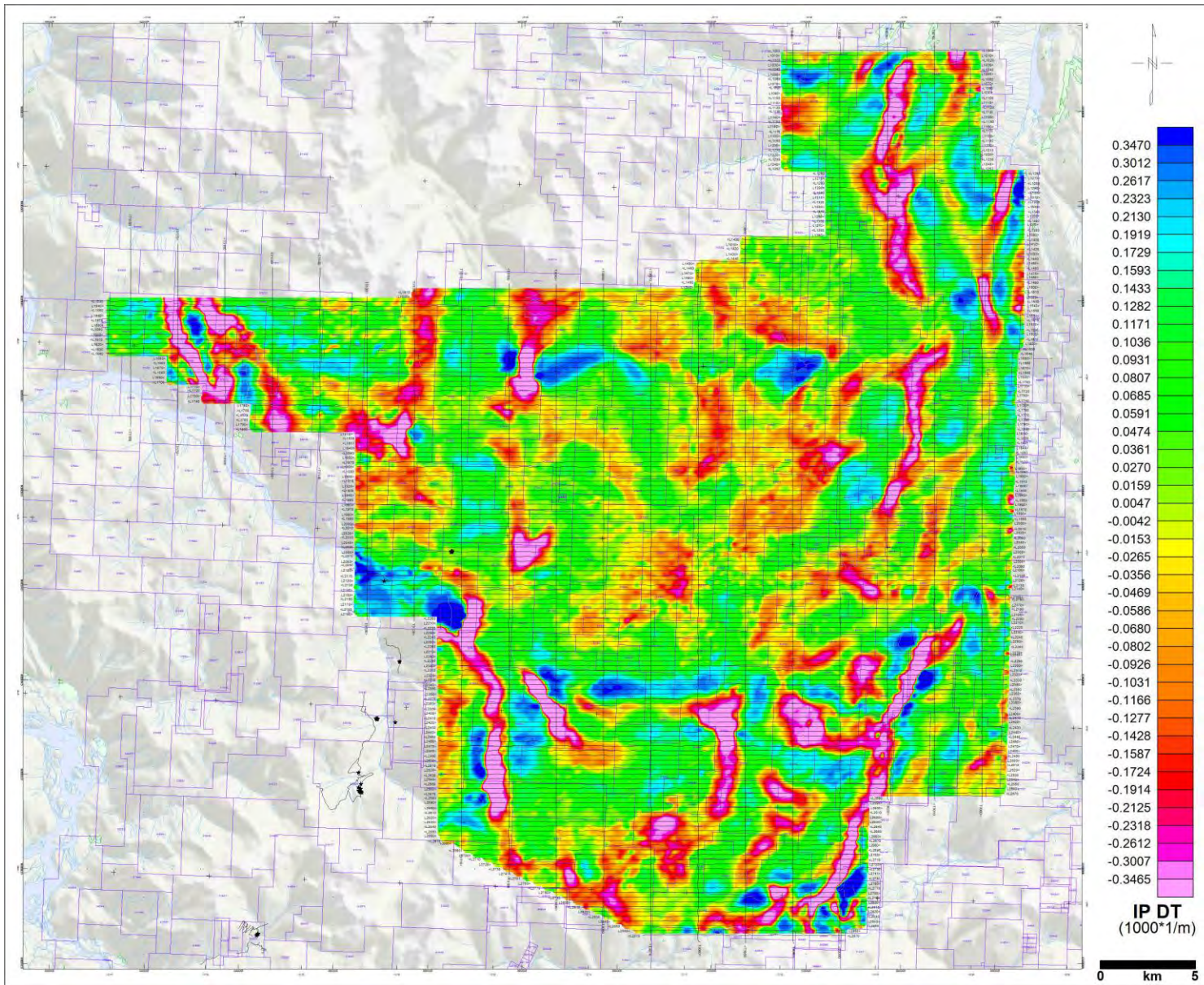
30Hz In-Phase Total Phase Rotated (TPR)



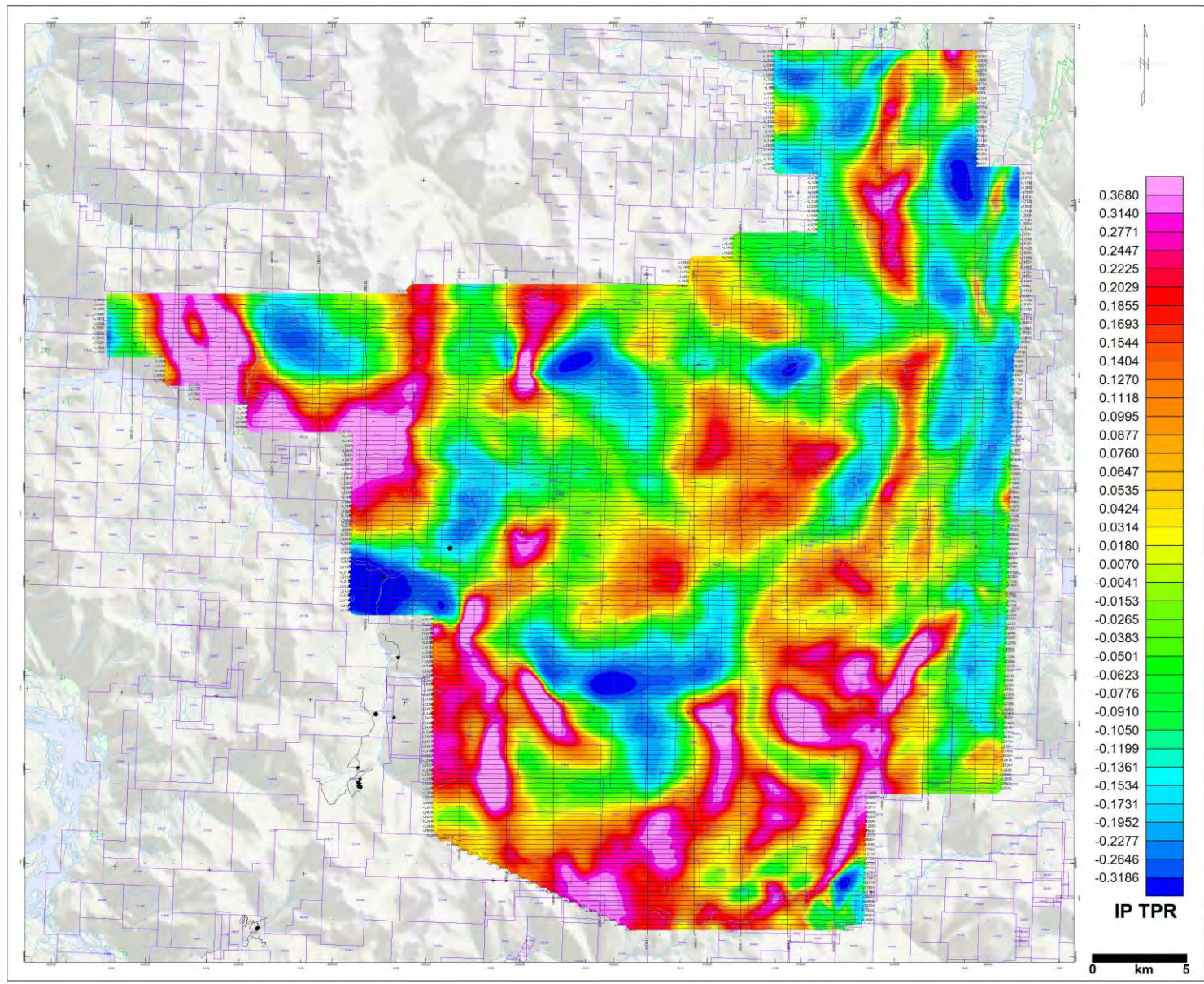
90Hz In-Phase Total Divergence (DT)



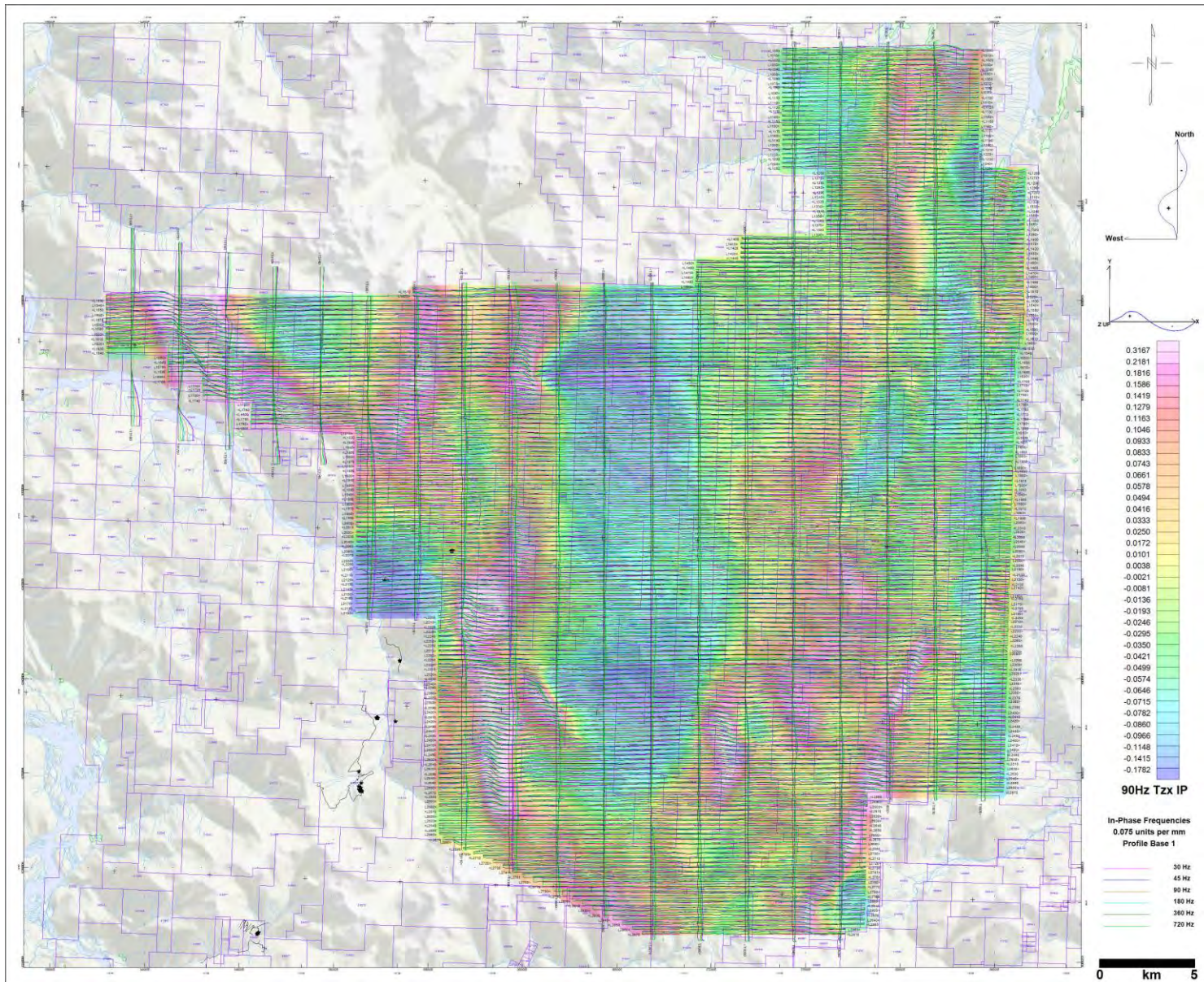
90Hz In-Phase Total Phase Rotated (TPR)



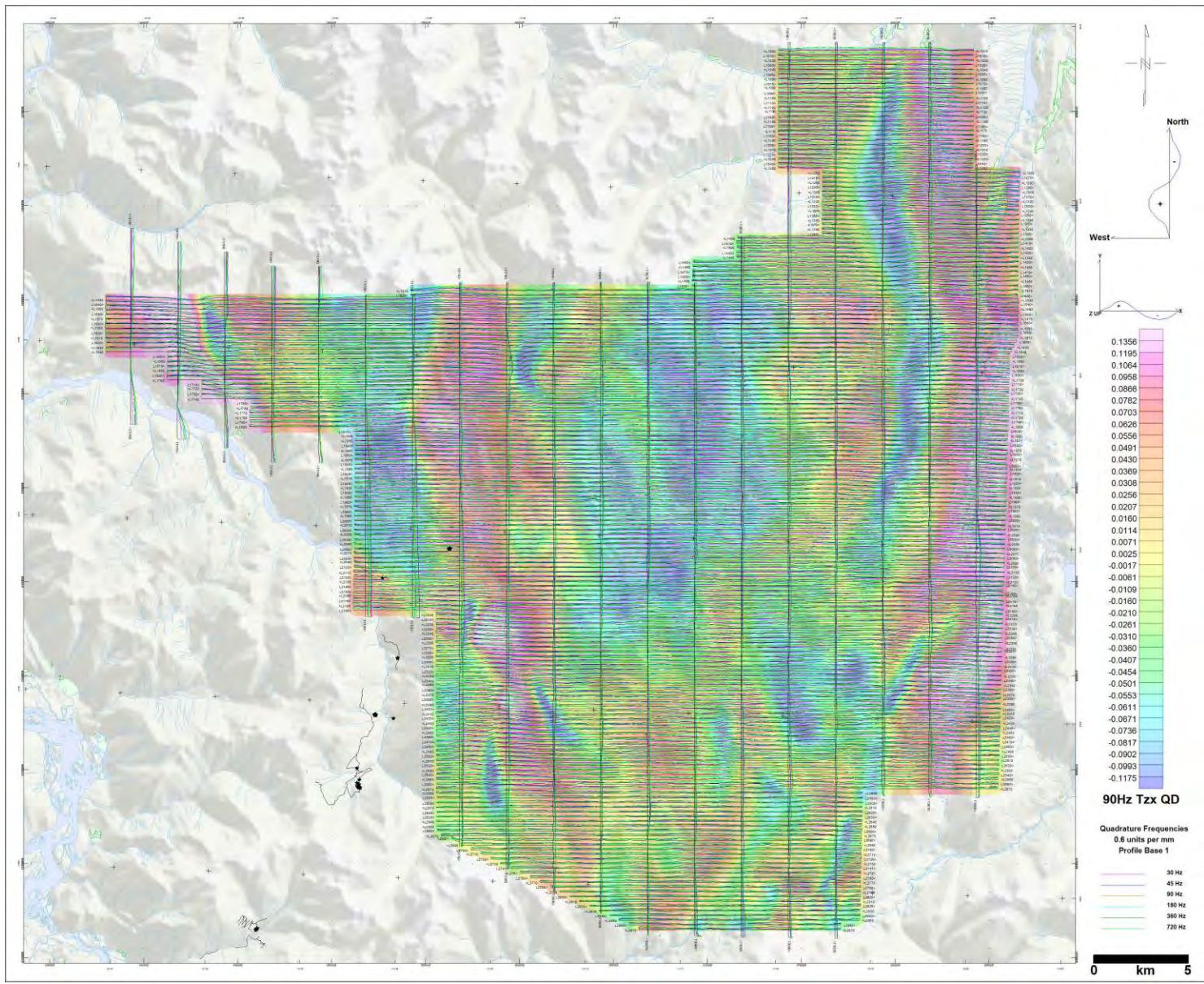
360Hz In-Phase Total Divergence (DT)



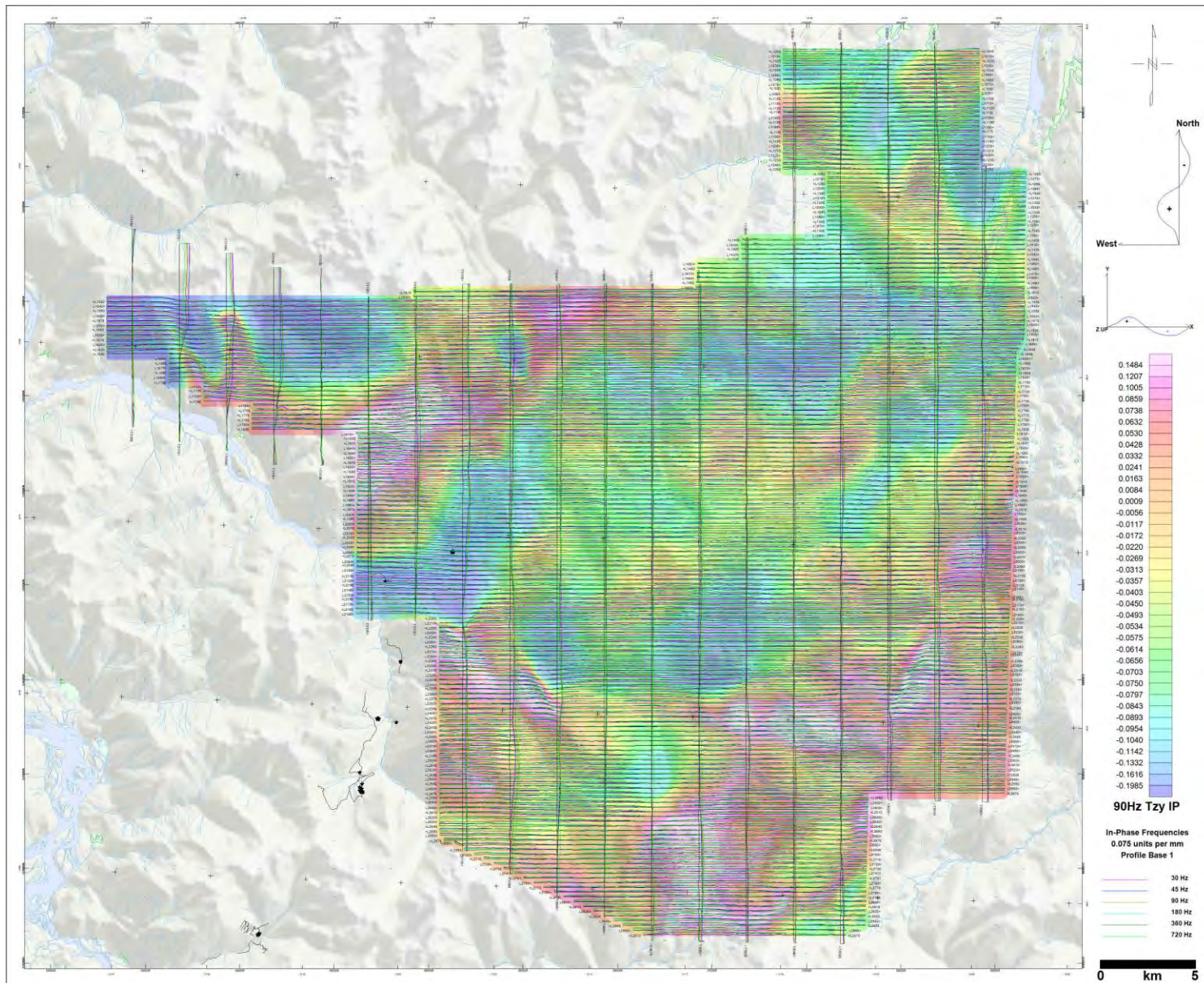
360Hz In-Phase Total Phase Rotated (TPR)



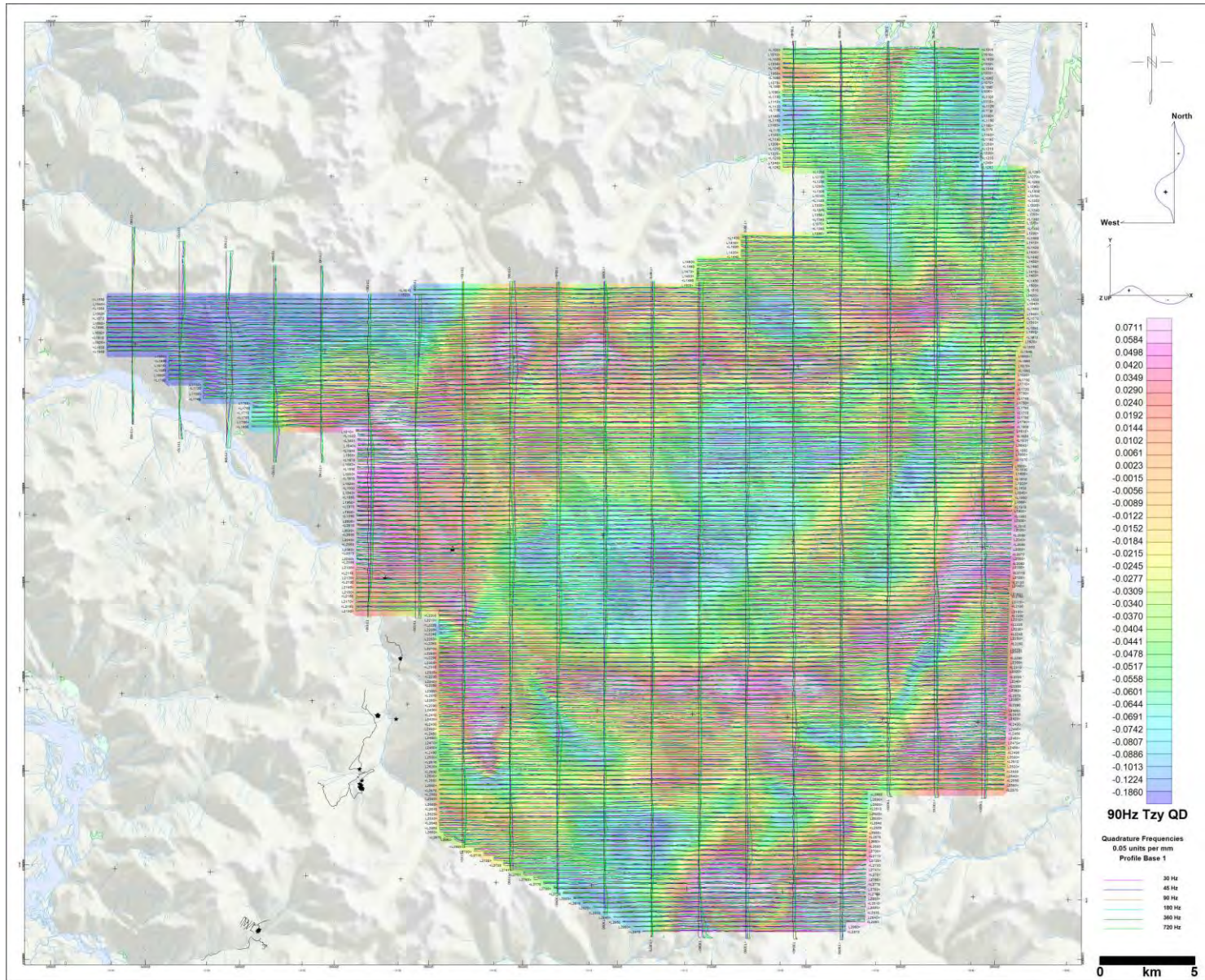
Tzx (In-line) In-Phase Profiles over 90Hz Phase Rotated In-Phase Grid



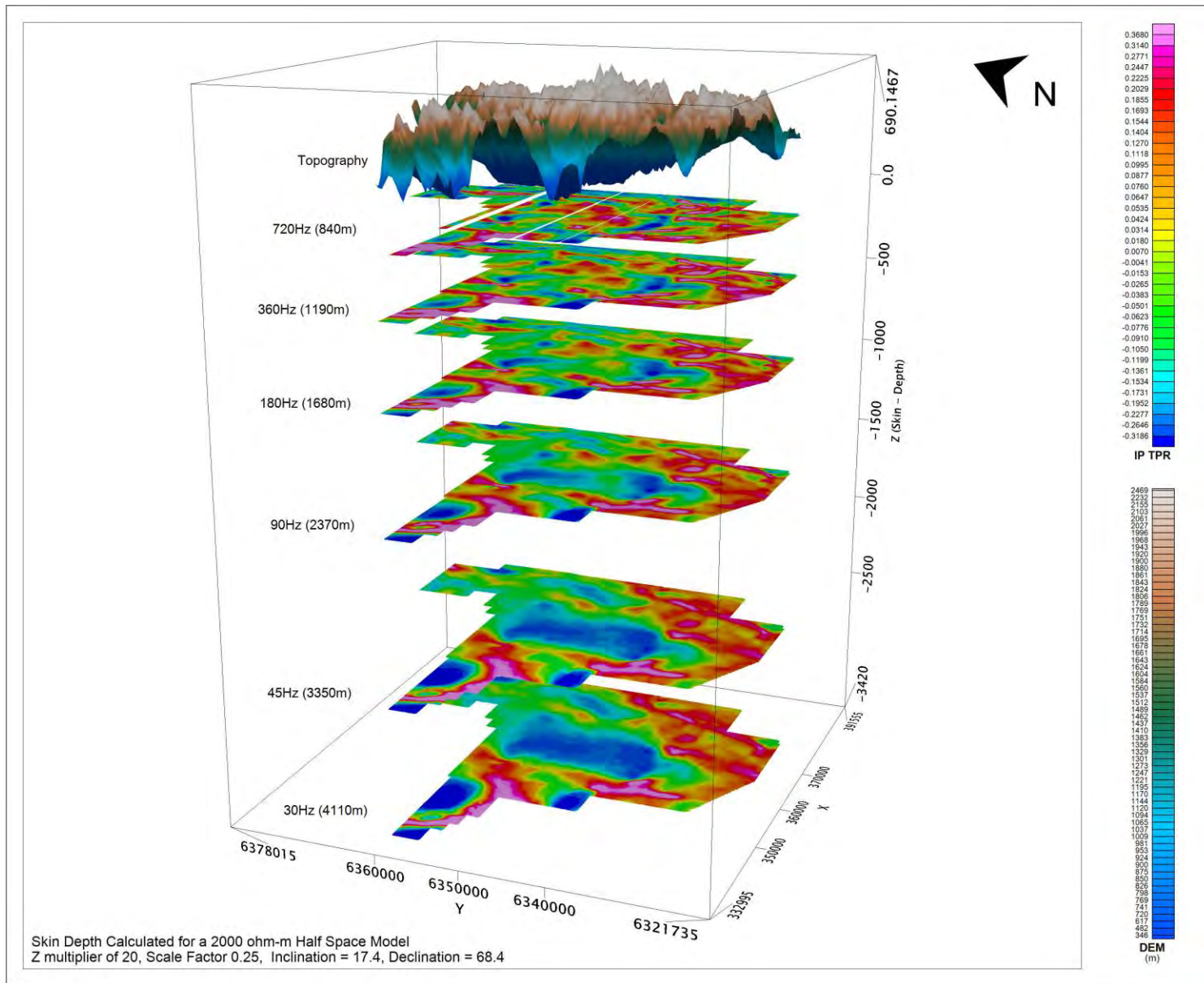
Tzx (In-line) Quadrature profiles over 90Hz Phase Rotated Quadrature Grid



Tzy (Cross-line) In-Phase Profiles over 90Hz Phase Rotated In-Phase Grid



Tzy(Cross-line) Quadrature Profiles over 90Hz Phase Rotated Quadrature Grid



3D View of In-Phase Total Phase Rotated versus Skin Depth (30-720Hz)

APPENDIX D

ZTEM THEORETICAL CONSIDERATIONS

A brief section on the theory behind the AFMAG technique is provided for completeness and a more comprehensive development of the theory can be found in standard texts. The natural EM field is normally horizontally polarized. Subsurface lateral variations of conductivity generate a vertical component, which is linearly related to the horizontal field. Although the fields look like random signals, they may be treated as the sum of sinusoids. At each frequency the field can be expressed as a complex number with magnitude and argument equal to the amplitude and phase of the sinusoid. The relation between the field components can then be expressed by a linear complex equation with two complex coefficients at any one frequency. These coefficients are dependent upon the subsurface and not upon the horizontal field present at any particular time and are appropriate parameters to measure (Vozoff, 1972).

$$H_z(f) = T_x(f) H_x(f) + T_y(f) H_y(f), \quad (1)$$

Where

$H_x(f)$, $H_y(f)$ and $H_z(f)$ are x, y and z components of the field,

$T_x(f)$ and $T_y(f)$ are the “tipper” coefficients.

In the case of a horizontally homogeneous environment, T_x and T_y are equal to zero because $H_z = 0$. They show certain anomalies only by the presence of changes in subsurface conductivity in the horizontal direction. The real parts of the coefficients correspond to tangents of tilt angles measured with a controlled source. The complex tensor $[T_x, T_y]$ known as the “tipper” defines the vertical response to horizontal fields in the x and y directions respectively.

T_x and T_y are two unknown coefficients in one equation, and we therefore must combine two or more sets of measurements to solve them. To reduce effects of noise, multiple sets of measurements can be made, and the coefficients, which minimize the squared error in predicting the measured Z from X and Y, can be found. This leads to next formulas for estimating the coefficients.

$$T_x = ([H_z H_x^*] [H_y H_y^*] - [H_z H_y^*] [H_x H_x^*]) / ([H_x H_x^*] [H_y H_y^*] - [H_x H_y^*] [H_y H_x^*]), \quad (2)$$

and

$$T_y = ([H_z H_y^*] [H_x H_x^*] - [H_z H_x^*] [H_x H_y^*]) / ([H_x H_x^*] [H_y H_y^*] - [H_x H_y^*] [H_y H_x^*]). \quad (3)$$

Where

$[H_x H_y^*]$ (For example) denotes a sum of the product of H_x with the complex conjugate of H_y .

In practical processing algorithms, all numbers Hx, Hy and Hz can be obtained by applying the same digital band-pass filters to three incoming parallel data signals. FFT algorithms are also applicable. All sums like [HxHy*] can be calculated on the basis of a discrete time interval in the range from 0.1 to 1 sec or on a sliding time base.

Using platform attitude data in the EM data processing can be done at different stages of the signal processing. The most obvious idea is to transform parallel data from local coordinates of the platform into absolute geographical coordinates before the main signal processing procedure. Unfortunately, the proper algorithms of attitude data obtained, often require some post-processing algorithms such as using post-calculated accelerations based on GPS data etc. That is why it is preferable to treat x-y-z coordinates in formulas above in the local coordinate system of the platform and to recalculate resulting local tilt angles into a geographical or global coordinate system later, during the data post processing.

In weak field conditions where the level of the signal is comparable with input noise levels in preamplifiers, the bias in the estimated values of Tx and Ty caused by noise in the horizontal signals become substantial and cannot be reduced by any averaging. This bias can be removed by the use of separate reference signals containing noise uncorrelated with noise in signals Hx and Hy. (Anav et al., 1976).

$$T_x = ([HzRx^*] [HyRy^*] - [HzRy^*] [HyRx^*]) / ([HxRx^*] [HyRy^*] - [HxRy^*] [HyRx^*]), \quad (4)$$

and

$$T_y = ([HzRy^*] [HxRx^*] - [HzRx^*] [HxRy^*]) / ([HxRx^*] [HyRy^*] - [HxRy^*] [HyRx^*]). \quad (5)$$

Where:

Rx is the reference field x component,
Ry is the reference field y component.

An additional two electromagnetic sensors, providing these reference signals can be placed at some distance away from the main x, y and z sensors. Currently, though, no additional remote-reference processing are applied to ZTEM data.

Numerical Modelling

In order to understand the airborne AFMAG responses to conductors for a variety of geological environments, EMIGMA™ modelling code from PetRos EiKon (Toronto, ON) was obtained to conduct the formulated model studies.

Below are some of the modelling results from their study.

Modelling assumption:

The assumptions for the modelling are that:

3 components of the magnetic field are measured and they are processed according to:

$$Hz(f) = T_x(f) H_x(f) + T_y(f) H_y(f)$$

The vector (Tx,Ty) is usually referred to as the 'tipper' vector and is determined in the frequency domain through processing. This is normally done by determining transfer functions from an extended time series.

For the modelling exercise, the 3 components of the magnetic vector (Hx,Hy,and Hz) are modelled twice for 2 orthogonal polarizations of a plane wave source field and then the tipper is calculated from a matrix calculation using the results of the 2 source polarizations' models. For the 2D forward modelling results, the tipper vectors are shown as a function of frequency

Basic Model Response

For the initial models, we assume a thin plate-like model. The model is perpendicular to the flight direction. Initially, we will assume very long strike directions. From this quasi-2D model, there are 2 basic responses. The so-called TE response and the so-called TM response.

For the initial models, we will assume the strike is in the y (North) directions and the flight is in the x (East) direction Sensor heights are 30m above ground.

TE Mode: For the TE response, the electric field excitation flows along strike (current channelling) and the horizontal H field (Hx) flows perpendicular to strike thus causing induction through Faraday's law. The Hz response is generated both from channelling and induction.

TM Mode: For this response, the electric field excitation flows perpendicular to strike generating quasi-static charges on faces and the horizontal H field (Hx) flows parallel to strike. Since, the XZ face is very small for this model, little current is induced. The charges on the faces have a small dipole moment due to the thinness of the model.

For the rest of the models unless otherwise noted, the parameters used are:

Strike Length: 1km

Depth Extent: 1km

Conductance: 100S

Depth to Top: 10m

Background: Thin-overburden (10m), Resistive Basement (1000 Ohm-m)

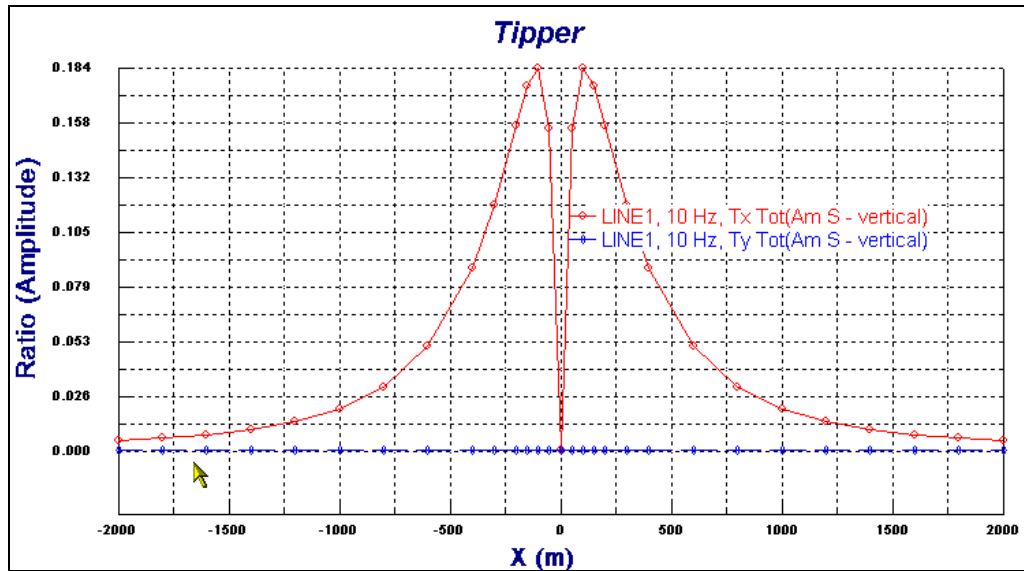


Figure D-1 – Calculated Tipper components at 10 Hz for above model parameters.

Figure D1 shows the Tipper (Tx,Ty) Amplitudes at 10Hz using a 10Ωm overburden. Note small Ty (ie quasi-TM response)

Amplitude Response

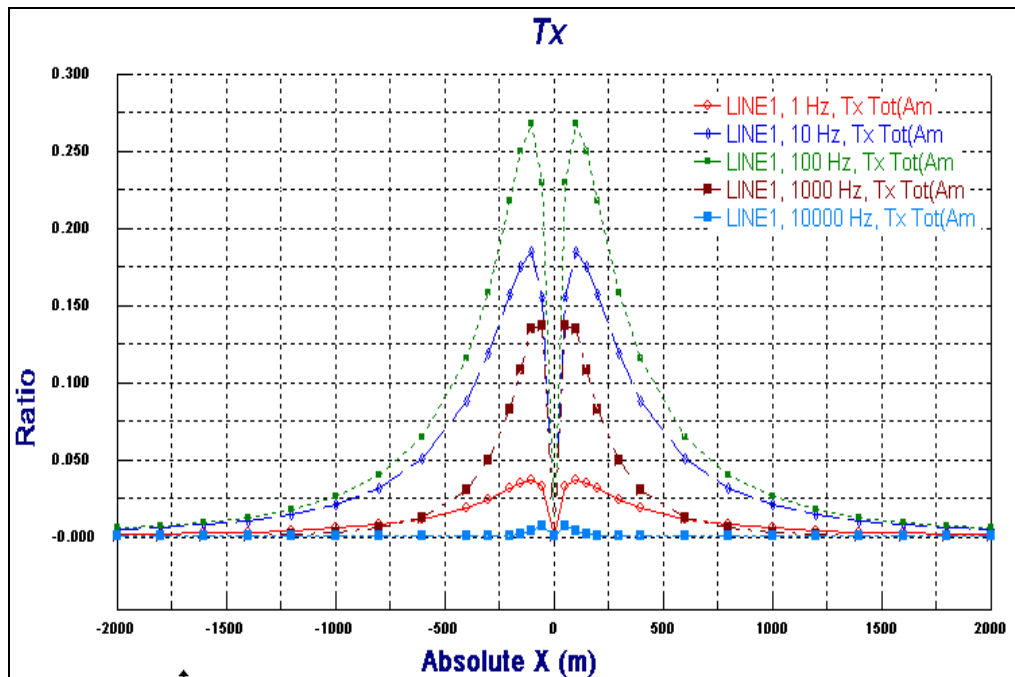


Figure D-2 – Calculated Tx component of the Tipper at various frequencies

The (Tx) response amplitude at 1,10,100,1000,10000 Hz. Peak amplitude at 100Hz

Inphase and Quadrature Response

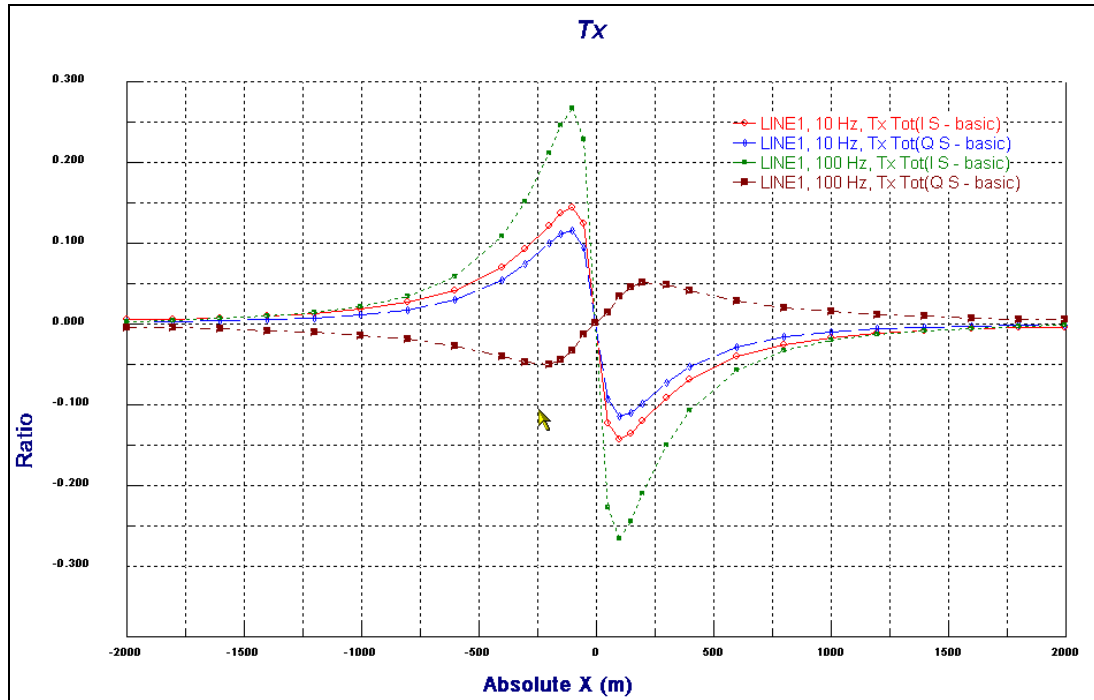


Figure D-3 – Calculated In-phase and Quadrature of the Tx component at various frequencies

Figure D-3 shows the In-phase and Quadrature response at 10 and 100Hz. Note the crossovers in the In-phase and Quadrature, and the phase reversal in the Quadrature responses from low to high frequencies.

Bo Lo, P.Eng, B.Sc. (Geophysics), Consultant
Geotech Ltd.
September, 2007

AFMAG Source Fields and ZTEM method¹

AFMAG uses naturally occurring audio frequency magnetic fields as the source of the primary field signal, and therefore requires no transmitter (Ward, 1959). The primary fields resemble those from VLF except that they are lower frequency (tens & hundreds of Hz versus tens of kHz) and are usually not as strongly directionally polarized (Labson et al., 1985). These EM fields used in AFMAG are derived from worldwide atmospheric thunderstorm activity, have the unique characteristic of being uniform, planar and horizontal, and also propagate vertically into the earth – to great depth, up to several km, as determined by the magnetotelluric (MT) skin depth (Vozoff, 1972), which is directly proportional to the ratio of the bedrock resistivity to the frequency (Figure D4).

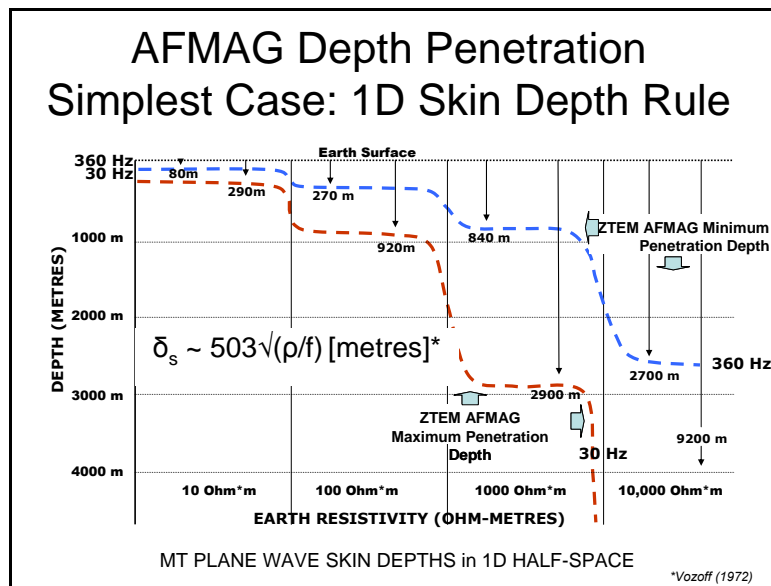


Figure D4: MT Skin Depth Penetrations for ZTEM in 30-360Hz and 10-1000 ohm resistivity

At the frequencies used for ZTEM, the penetration depths likely range between approx. 600m to 2km in this region (approx. 1k ohm-m avg. resistivity assumed), according to the following equation for the Bostick skin depth $\delta_B = 356 * \sqrt{(\rho / f)}$ metres (Bostick, 1977), which is considered appropriate as a rule of thumb equivalent depth estimate.

The other unique aspect of AFMAG fields is that they react to relative contrasts in the resistivity, and therefore do not depend on the absolute conductance, as measured using inductive EM systems, such as VTEM. Hence poorly, conductive targets, such as alteration zones and fault zones can be mapped, as well as higher conductance features, like graphitic units. Conversely, resistive targets can also be detected using AFMAG— provided they are of a sufficient size and contrast to produce a vertical field anomaly. Indeed resistors produce reversed anomalies relative to conductive features. Hence AFMAG can be effective as an all-round resistivity mapping tool, making it unique among airborne EM methods. A series of 2D synthetic models that illustrate these aspects have been created using the 2D forward

¹ From: Legault, J.M., Kumar, H., and Milicevic, B. (2009): ZTEM tipper AFMAG and 2D inversion results over an unconformity uranium target in northern Saskatchewan, Expanded Abstract submitted to Society of Exploration Geophysics SEG conference, Houston, Tx, Nov-2009, 5 pp.

MT modelling code of Wannamaker et al. (1987) and are presented in figures D5-D7.

The tipper from a single site contains information on the dimensionality of the subsurface (Pedersen, 1998), for example, in a horizontally stratified or 1D earth, $T=0$ and as such H_z is absent. For a 2D earth with the y-axis along strike, $T_y=0$ and $H_z = T_x \cdot H_x$. In 3D earths, both T_x and T_y will be non-zero. H_z is therefore only present, as a secondary field, due to a lateral resistivity contrast, whereas the horizontal H_x and H_y fields are a mixture of secondary and primary fields (Stodt et al., 1981). But, as an approximation, as in the telluric-magnetotelluric method (T-MT; Hermance and Thayer, 1975) used by distributed MT acquisition systems, the horizontal fields are assumed to be practically uniform, which is particularly useful for rapid reconnaissance mapping purposes. By measuring the vertical magnetic field H_x , using a mobile receiver and the orthogonal horizontal H_x and H_y fields at a fixed base station reference site, ZTEM is a direct adaptation of this technique for airborne AFMAG surveying.

Jean M. Legault, M.Sc.A., P.Eng., P.Geo.
Geotech Ltd.

References

- Bostick, F.X., 1977, A simple almost exact method of MT analysis. Proceedings of the University of Utah Workshop on Electrical methods in Geothermal Exploration, 175-188.
- Hermance, J.F., and Thayer, R.E., 1975, The telluric-magnetotelluric method, *Geophysics*, **37**, 349-364.
- Labson, V. F., A. Becker, H. F. Morrison, and U. Conti, 1985, Geophysical exploration with audio-frequency natural magnetic fields: *Geophysics*, **50**, 656-664.
- Murakami, Y., 1985, Short Note: Two representations of the magnetotelluric sounding survey, *Geophysics*, **50**, 161-164.
- Pedersen, L.B., 1998, Tensor VLF measurements: Our first experiences, *Exploration Geophysics*, **29**, 52-57.
- Stodt, J.A., Hohmann, G.W., and Ting, S.C., 1981, The telluric-magnetotelluric method in two- and three-dimensional environments, *Geophysics*, **46**, 1137-1147.
- Vozoff, K., 1972, The magnetotelluric method in the exploration of sedimentary basins, *Geophysics*, **37**, 98-141.
- Ward, S. H., 1959, AFMAG—Airborne and ground: *Geophysics*, **24**, 761-787.
- Wannamaker, P.E., Stodt, J.A., and Rijo, L., 1987, A stable finite element solution for two-dimensional magnetotelluric modelling, *Geophy. J. Roy. Astr. Soc.*, **88**, 227-296.

Interpretations R Us

1234 Main Street
Anytown, State 12345

MT Workstation

MT Data for: ztem-test

by
Geotools Corporation
5808 Balcones Dr, Suite 202
Austin, Texas 78731 USA

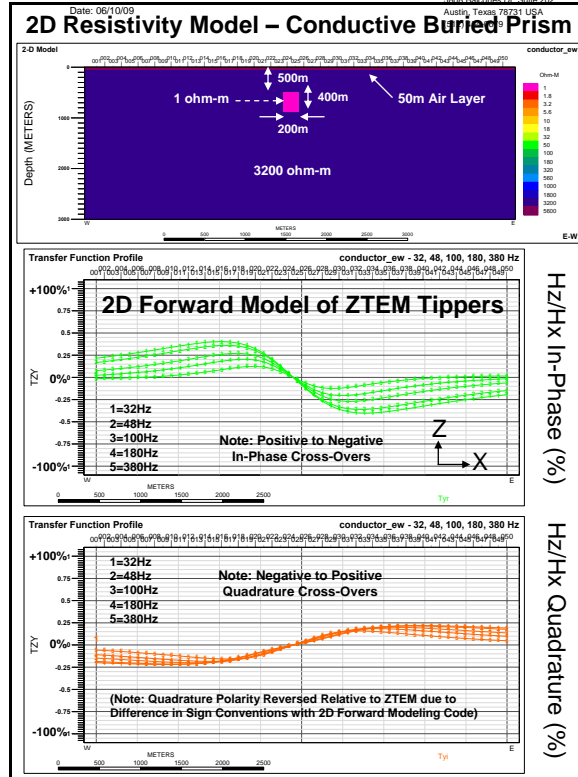


Figure D5: 2D synthetic f

Interpretations R Us

1234 Main Street
Anytown, State 12345

MT Workstation

MT Data for: ztem-test

by
Geotools Corporation
5808 Balcones Dr, Suite 202
Austin, Texas 78731 USA

conductive brick model.

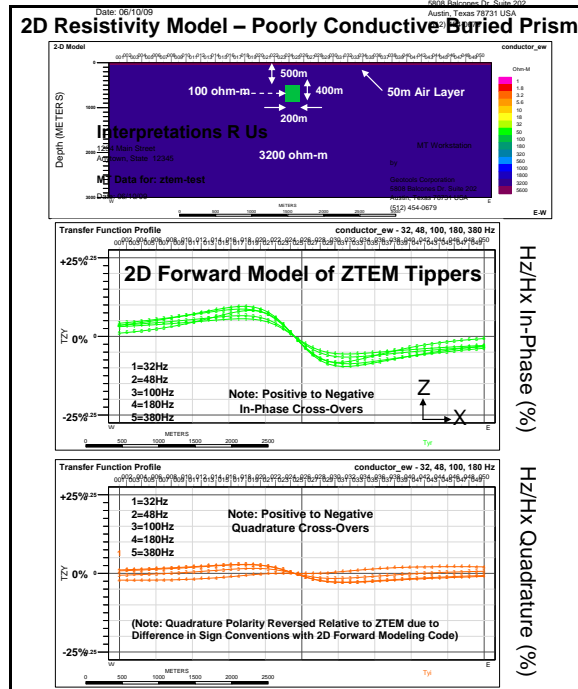


Figure D6: 2D synthetic forward model Tipper response (Tzx) for poorly conductive brick model.

Interpretations R Us

1234 Main Street
Anytown, State 12345

MT Workstation

MT Data for: ztem-test

Geotools Corporation
5808 Balcones Dr., Suite 202
Austin, Texas 78731 USA

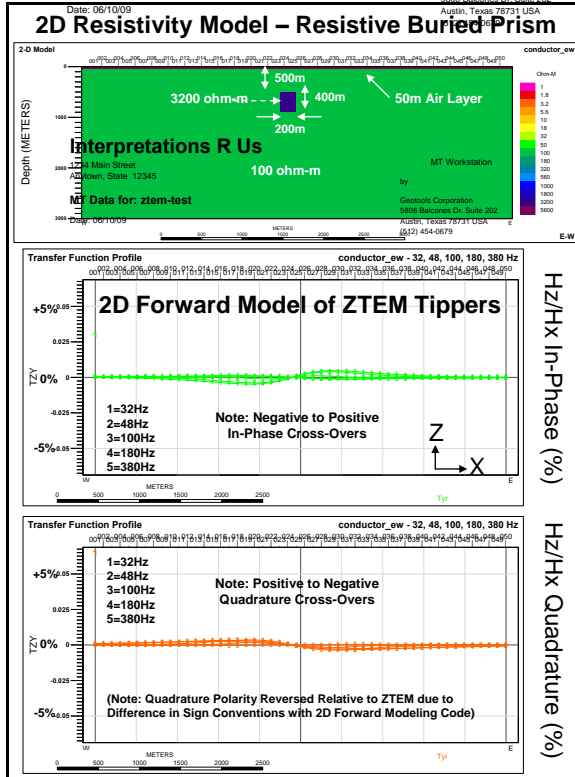


Figure D7: 2D synthetic forward model Tipper response (Tzx) for resistive brick model.

APPENDIX E

ZTEM (AIRBORNE AFMAG) TESTS OVER UNCONFORMITY URANIUM DEPOSITS⁶

Bob Lo^{1}, Jean Legault², Petr Kuzmin^{3,1} Formerly Geo Equipment Manufacturing Ltd., now Exploration Syndicate, Inc., bob.lo@expsyn.com,² Geotech Ltd., jean@geotech.ca,³ Geo Equipment Manufacturing Ltd., petr@geotech.ca*

Key Words: ZTEM, AFMAG, electromagnetic, airborne, uranium, Athabasca.

INTRODUCTION

A series of demonstration tests were conducted using the ZTEM, airborne AFMAG system over deep targets in the Athabasca Basin of Saskatchewan, Canada. These tests were conducted in mid-2008 and were flown to test ZTEM's ability to detect large conductive targets at depth; deeper than conventional airborne EM methods. Data are presented over areas where the conductors are located 450-600 metres beneath the surface. As well, a case of ZTEM following the plunge of a conductor to over 800 metres depth is shown.

BACKGROUND

The ZTEM system is the latest implementation of an airborne AFMAG system first commercialized in late 2006. ZTEM uses a large, 8 metre diameter airborne air core coil, slung from a helicopter, to measure the vertical component of the AFMAG signal. Two 4 metre square coils are deployed on the ground to measure the horizontal field. The ZTEM system has flown successful demonstration surveys over porphyry copper deposits in the southwest USA (Zang et al., 2008).

ZTEM was tested in the Athabasca Basin in Canada in May of 2008 to determine its depth of investigation and to determine its suitability for mapping deep conductors in the crystalline basement. Over 30% of the world's U3O8 is mined in the Athabasca Basin from unconformity uranium deposits. Unconformity uranium deposits of the Athabasca Basin are often associated with conductors located in the crystalline basement. The search for economic uranium deposits is moving to areas of the basin which are deeper and beyond the detection limits of modern airborne instrumentation. This creates the requirement for a system which can detect conductivity past the detection limits of modern traditional EM systems. This was the motivation behind the field trials of the ZTEM system in the Athabasca Basin. Several areas where known deep conductors (450-600m+) were located were flown. Also, a test survey block in the northern part of the basin was able to trace a deep and plunging conductor to depths that no other airborne EM system has been able to achieve.

ATHABASCA BASIN GEOLOGY

The high-grade uranium deposits within the Athabasca Basin are associated with the unconformity between the essentially flat-lying Proterozoic Athabasca Group sandstones and the underlying Archean-Paleoproterozoic metamorphic and igneous basement rocks. The deposits occupy a range of positions from wholly basement-hosted to wholly sediment-hosted, at structurally favourable sites in the interface between the deeply weathered basement and overlying sediments of the Athabasca Basin (Ruzicka, 1997). The locations of These deposits are lithologically and structurally controlled

⁶ Extended abstract submitted to 20TH ASEG International Geophysical Conference & Exhibition, Adelaide, AU, 22-26 Feb, 2009.

by the sub-Athabasca unconformity and basement faults and fracture zones, which are localized in graphitic pelitic gneisses that may flank structurally competent Archean granitoid domes (Quirt, 1989).

In general, most of the known important deposits tend to occur within a few tens to a few hundred metres of the unconformity and within 500 m of the current ground surface. This may be more of a limitation of exploration techniques. There is no reason to believe that the distribution of the deposits is dependent on the modern day depth of burial.

Empirically, the geophysical exploration for unconformity type uranium targets have been to search for large basement structures which post date the sandstone deposition of the basement (Matthews et al, 1997). All the deposits located so far are associated with fault structures associated with a graphitic conductive basement. An alteration zone of clay silicification and enrichment around the deposits probably leads to magnetite destruction causing the magnetic low observed around the deposits. The clay alteration should give rise to a resistivity low signature about the deposits. The low conductivity of the clay alteration makes it a difficult target for airborne EM if it is buried at significant depth.

ZTEM INSTRUMENTATION AND PRESENTATION

ZTEM is an airborne AFMAG system introduced by Geotech Ltd. of Canada in early 2007 (Lo et al., 2008). In a ZTEM survey, a single vertical dipole air-core coil is flown over the survey area in a grid pattern similar to other airborne electromagnetic surveys. Two orthogonal, air-core, horizontal axis coils placed close to the survey site measures the horizontal EM fields for reference. A GPS array on the airborne coil monitors its attitude for post-flight corrections.

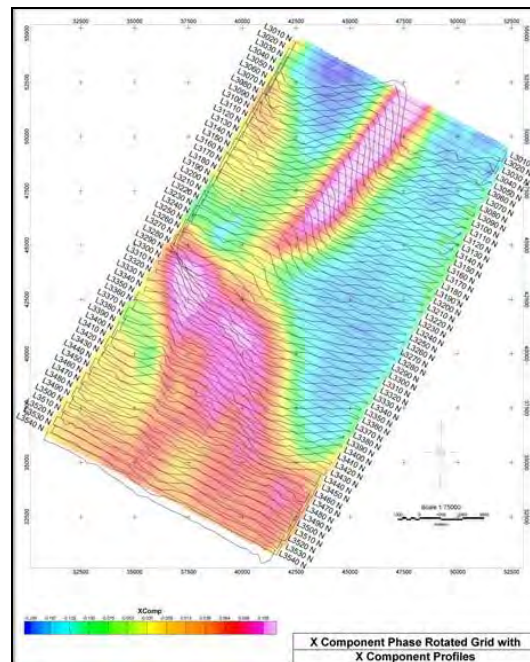


Figure 1 – Stacked profiles of the x-component Tipper over the gridded values of the phase rotated x-component data. Note that the cross-overs in the profiles are now peaks on the image.

As the source field is assumed to be far away, the excitation of the ground is more or less uniform. For large structures, the signal fall-off will be much slower than from a dipole source, such as those energized by traditional airborne systems. With the ZTEM system being less susceptible to terrain clearance, the planned ground clearance height is higher and the terrain drape is looser as compared to standard helicopter EM surveys.

The two Tippers obtained from the relationship between the vertical airborne coil and the two ground coils have a cross-over over a steeply dipping, plate-like body. The cross-overs can be made into local maxima via a 90 degree phase rotation which allows for easier interpretation of the gridded values. Figure 1 is an example of this transformation.

To present the data of both Tippers as one image, we calculate a parameter termed the DT which is the horizontal divergence of the two Tippers, much in the same manner as the “peaker” parameter in VLF (Pedersen, 1998). The DT is typically plotted with an inverted colour bar as it is negative over a steeply dipping thin body.

ZTEM RESULTS – NORTHERN ATHABASCA BASIN

Figure 2 shows gridded values from a number of ZTEM lines over an area where the sedimentary cover is approximately 450-600 metres thick. A number of traditional EM systems have also been flown over this block. While they were able to detect conductors, the resolution of the conductive features is not nearly as detailed as the information provided by ZTEM.

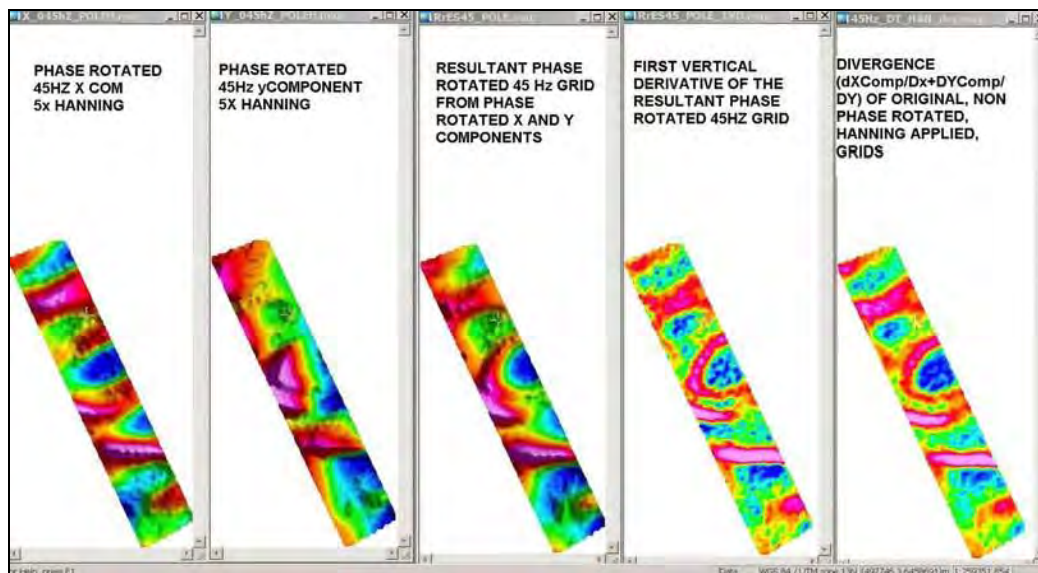


Figure 2 – ZTEM results over an area of 450-600 metre thick sedimentary cover.

Figure 3, from another area, shows the data from one of the larger blocks that was flown. It is a 3D composite image of the DT at various frequencies plotted at the equivalent skin depth assuming a 1,000 ohm-m average resistivity.

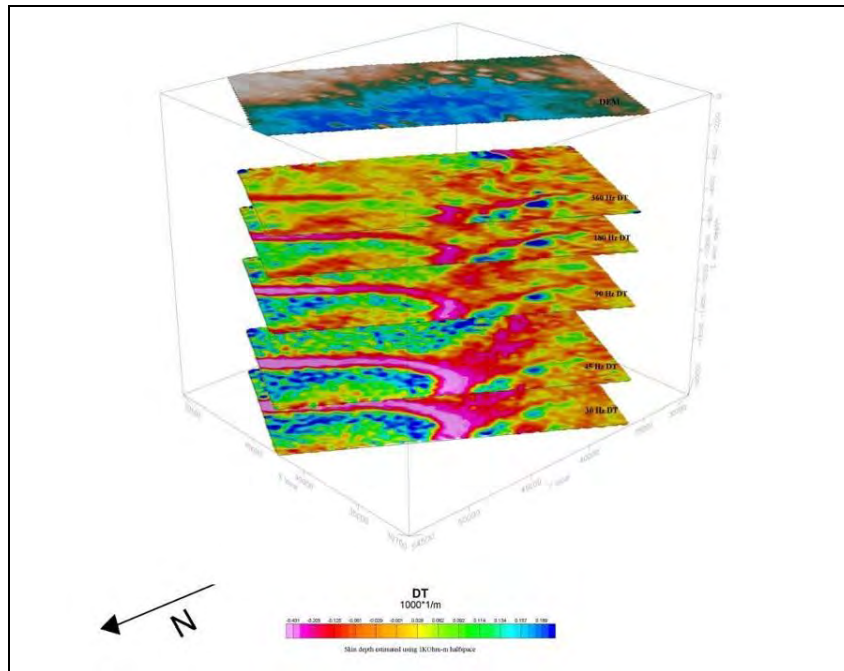


Figure 3 - Perspective view of DT's of different frequencies plotted at the skin depth (using a 1,000 ohm-m Earth).

The data in Figure 3 come from a survey over the north rim of the Athabasca Basin. The sandstone cover is about 500m on the left hand side of the image, and progressively getting deeper to the right. It is about 700m in the middle part of the image and over 800 metres thick on the right middle portion where exploration drilling is concentrated. Starting in the middle left and trending to the right of the image, there is a known graphitic shear.

In the uppermost (600m) “depth slice”, Figure 3 shows a linear conductive feature that progressively weakens as one moves to the right until it is no longer seen. This is interpreted to be due to the graphitic shear conductor plunging deeper past the depth of investigation of the 360 Hz data. The lower frequencies penetrate more into the sedimentary cover that is deeper towards the right. DT's of decreasing frequency show the linear conductive feature extending more and more to the right. The feature also strengthens/sharpens into a synformal shape with lower frequencies. This fits with what the known geology of a plunging conductor at depth is doing.

At the nose of the fold, in the right third of the images, we also see another, broader anomalous zone that trends towards the back of the image. At this location, two radioactive springs are situated. These spring waters which are anomalously high in uranium and radon may reflect the upward migration of deep waters along faults, suggesting structural targets in areas where basinal waters may have tapped a radioactive source. This broad DT trend might be the plunge of the fold axis that is aligned away from the front of the image. An anomaly along this trend, at the highest frequency, that steadily grows with each decreasing frequency can be seen. This might represent an alteration zone in the sandstone that is detected at the shallowest depth. By about the 90Hz DT depth slice or so, we are possibly in the deeper basement and into a basement graphitic unit.

CONCLUSIONS

A number of successful ZTEM tests were conducted over the Athabasca Basin. The tests demonstrated that ZTEM can easily detect conductivity to 800 metres beneath relatively resistive sedimentary cover. Assuming a 1,000 ohm-metre resistivity, the skin depth of the 30 Hz data is approximately 2,000 metres. The 30 Hz data presented have good signal to noise ratios indicating a deep depth of exploration. The observation that ZTEM may be detecting the clay alteration above the crystalline basement is a significant advantage for exploration of unconformity uranium deposits.

More demonstration surveys are planned in the Athabasca Basin later this year. And more target types for testing are also planned.

ACKNOWLEDGEMENTS

The authors thank Geotech Ltd. for allowing them to publish this work and for providing the support required to write this abstract and to present this paper.

REFERENCES

- Labson, V. F., Becker A., Morrison, H. F., and Conti, U., 1985, Geophysical exploration with audiofrequency natural magnetic fields, *Geophysics*, Vol. 50, p. 656-664.
- Lo, B., Zang, M., Kuzmin, P., 2008, Geotech's Z-TEM (Airborne AFMAG) Instrumentation, a paper presented at KEGS PDAC 2008 Symposium, Toronto.
- Matthews, R., Koch, R. and Leppin, M., 1997, Advances in Integrated Exploration for Unconformity Uranium Deposits in Western Canada; in *Proceeding of Exploration 97*, edited by Arnis Gubins, Prospectors and Developers Association of Canada, Toronto.
- McMullan, S.R., Matthews, R.B, and Robertshaw, P., 1990, Exploration geophysics for Athabasca Uranium Deposits, in: *Proceedings of Exploration 87*, Ontario Geological Survey.
- Pedersen, L.B, Qian, W., Dynesius, L., Zhang, P., 1994, An airborne tensor VLF system. From concept to realization, *Geophysical Prospecting*, Vol. 42.
- Ruzicka, V.R., 1997, Metallogenic features of the uranium-polymetallic mineralization of the Athabasca Basin, Alberta, and a comparison with other parts of the basin; in R.W. Macqueen, ed., *Geological Survey of Canada, Bulletin 500*, 31-79.
- Wheatley, K., Murphy, J., Leppin, M., and Climie, J.A., 1996, Advances in the Genetic Model and Exploration Techniques for Unconformity-type Uranium Deposits in the Athabasca Basin; in Ashton, K.E., Harper, C.T., eds., *MinExpo '96 Symposium – Advances in Saskatchewan Geology and Mineral Exploration: Saskatchewan Geological Society, Special Publication No 14*, p. 126-136.
- Quirt, D., 1989, Host rock alteration at Eagle Point South: Sask. Research Council, Publication no. R-855-1-E- 89, 95p.
- Ward, S. H., 1959, AFMAG - Airborne and Ground: *Geophysics*, Vol. 24, p. 761-787.
- Zang, M., Lo, B., 2008, The Application of Airborne Natural Field Electromagnetics (ZTEM): Some Examples from the Southwestern United States, a paper presented at the 2008 PDAC, Toronto

APPENDIX F

2D Inversions



GEOTECH LTD.

AIRBORNE
GEOPHYSICAL
SURVEYS

GEOPHYSICAL SURVEYS

2D ZTEM Inversion Start Model Test Results

for

Teck Resources Limited

Scud Block

Scud Peak, BC, Canada

Project: GL130332

By

Geotech Ltd.

245 Industrial Parkway North
Aurora, Ont., CANADA, L4G 4C4

Tel: 1.905.841.5004

Fax: 1.905.841.0611

www.geotech.ca

Email: info@geotech.ca

October, 2013



Start Model Test

ZTEM inversions require a suitable a priori resistivity starting model – usually the representative average/bulk resistivity for the survey area. The correct choice ensures the proper depth estimates for inversion models. When ground or borehole resistivity data are unavailable, the choice can be estimated using a range of starting models. The final model with smallest input error suggests the most optimal choice of half-space resistivity. We have tested L1030 and L2040 with various start models. The results are summarized in the table below. Overall the 2000 ohm-m start model needs the smallest input error.

Input Error (%)

Start Model (ohm-m)	L1030	L2400_01	L2400_02	L2400_03	Total
300	1.581	1.891	2.339	1.531	7.342
500	1.318	1.539	2.016	1.503	6.376
1000	1.124	1.420	1.623	1.480	5.647
2000	1.058	1.405	1.418	1.498	5.379
4000	1.112	1.462	1.392	1.573	5.539

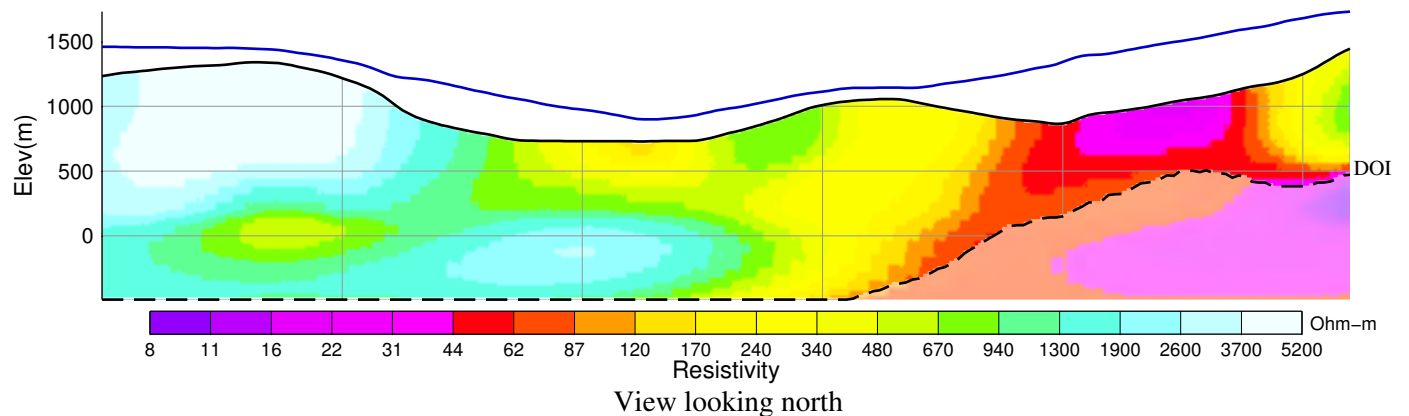
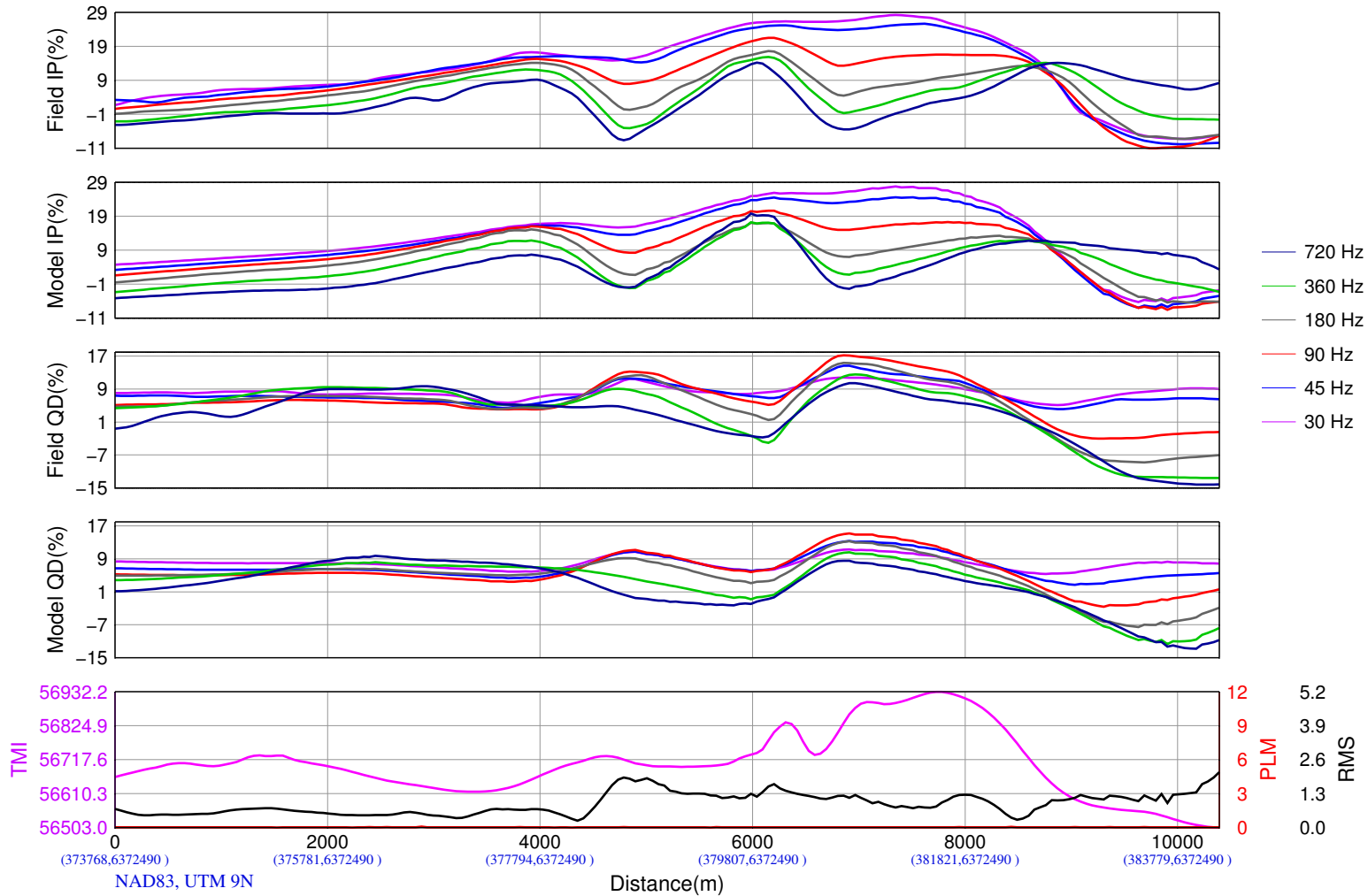
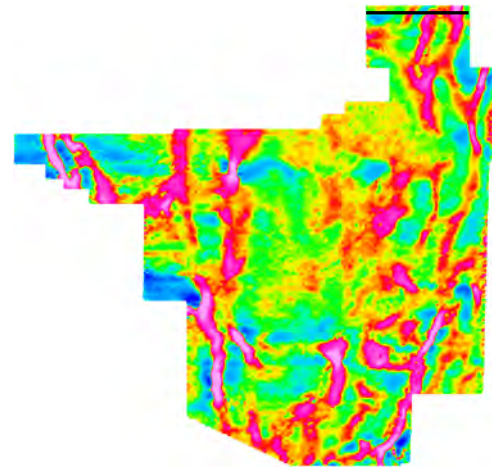


The following 5 slides are inversion results for
L1030

2D INVERSION PARAMETERS

Inversion Code: Geotech AV2DPTOPO
 Model Mesh: 440 wide x 112 vertical,
 Average cell width: 27.21 m
 Two (2) Cells between sites
 Input Data: In-Phase & Quadrature,
 Tzx In-Line (only)
 Average sampling rate: 4,400 points,
 Total data points: 2304
 Frequencies: 30 45 90 180 360 720
 Input error(%): 1.58 1.58 1.58 1.58 1.58 1.58
 Half-space resistivity: 300 ohm-m
 Output error: 0.997 RMS in 5 iterations

Line L1030 over IP 90 Hz DT image



Teck Resources Limited
 Scud Block
 Scud Peak, BC, Canada

Geotech ZTEM System
 Resistivity-Depth Image
 Project GL130332, Line L1030
 Flight 10, 2013/09/05

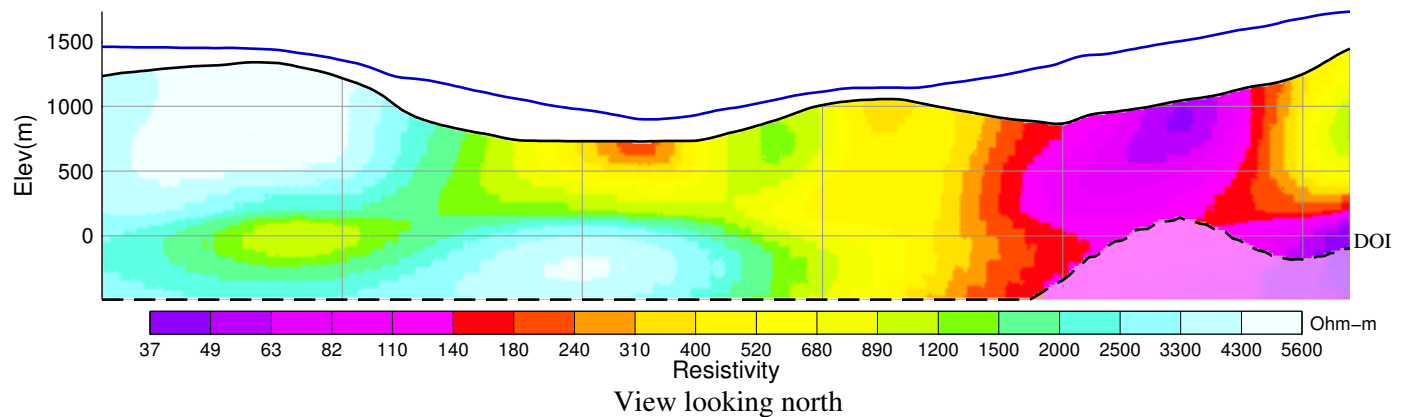
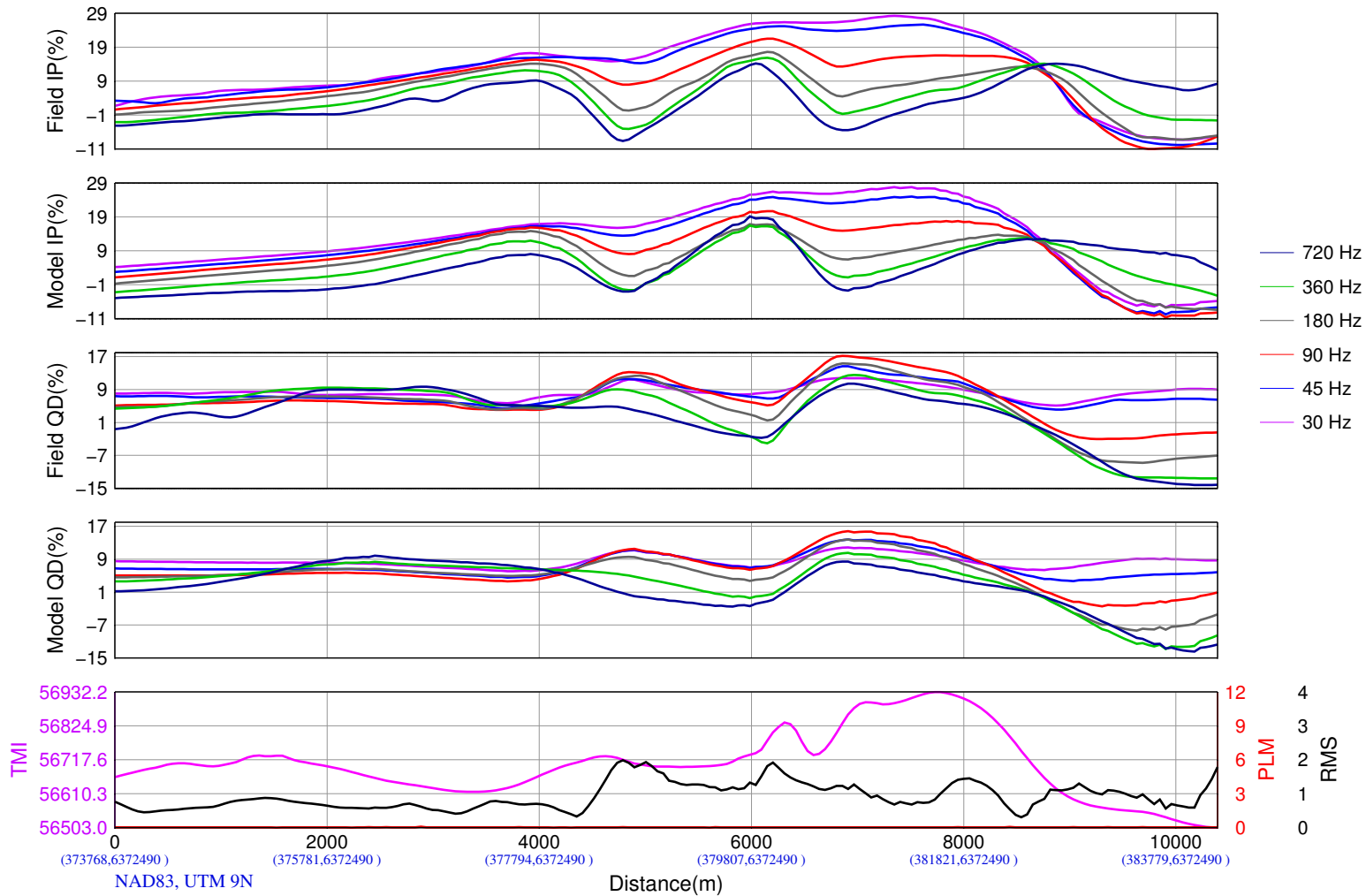
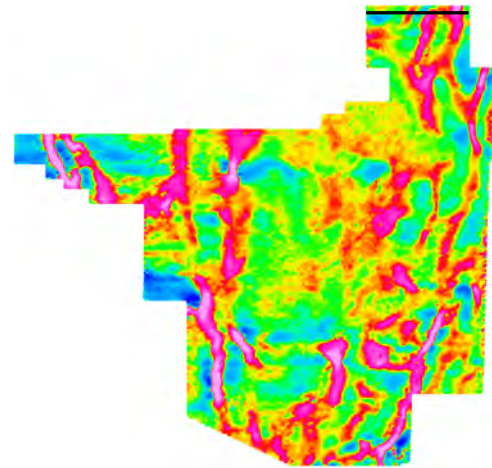
Flown and Processed by Geotech Ltd.
 245 Industrial Parkway North
 Aurora, Ontario, Canada L4G 4C4
 www.geotech.ca

2013/10/15

2D INVERSION PARAMETERS

Inversion Code: Geotech AV2D TOPO
 Model Mesh: 440 wide x 112 vertical,
 Average cell width: 27.21 m
 Two (2) Cells between sites
 Input Data: In-Phase & Quadrature,
 Tzx In-Line (only)
 Average sampling rate: 4,400 points,
 Total data points: 2304
 Frequencies: 30 45 90 180 360 720
 Input error(%): 1.32 1.32 1.32 1.32 1.32 1.32
 Half-space resistivity: 500 ohm-m
 Output error: 0.997 RMS in 5 iterations

Line L1030 over IP 90 Hz DT image



Teck Resources Limited
 Scud Block
 Scud Peak, BC, Canada

Geotech ZTEM System
 Resistivity-Depth Image
 Project GL130332, Line L1030
 Flight 10, 2013/09/05

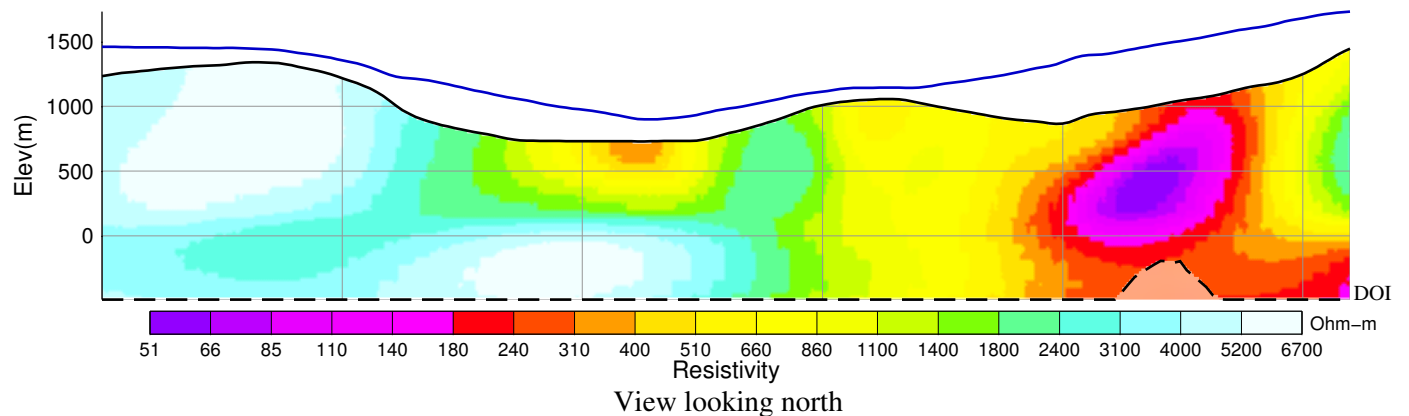
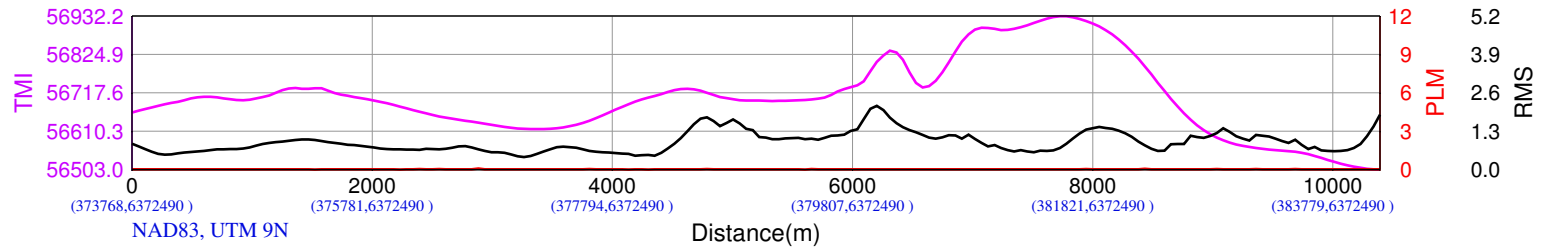
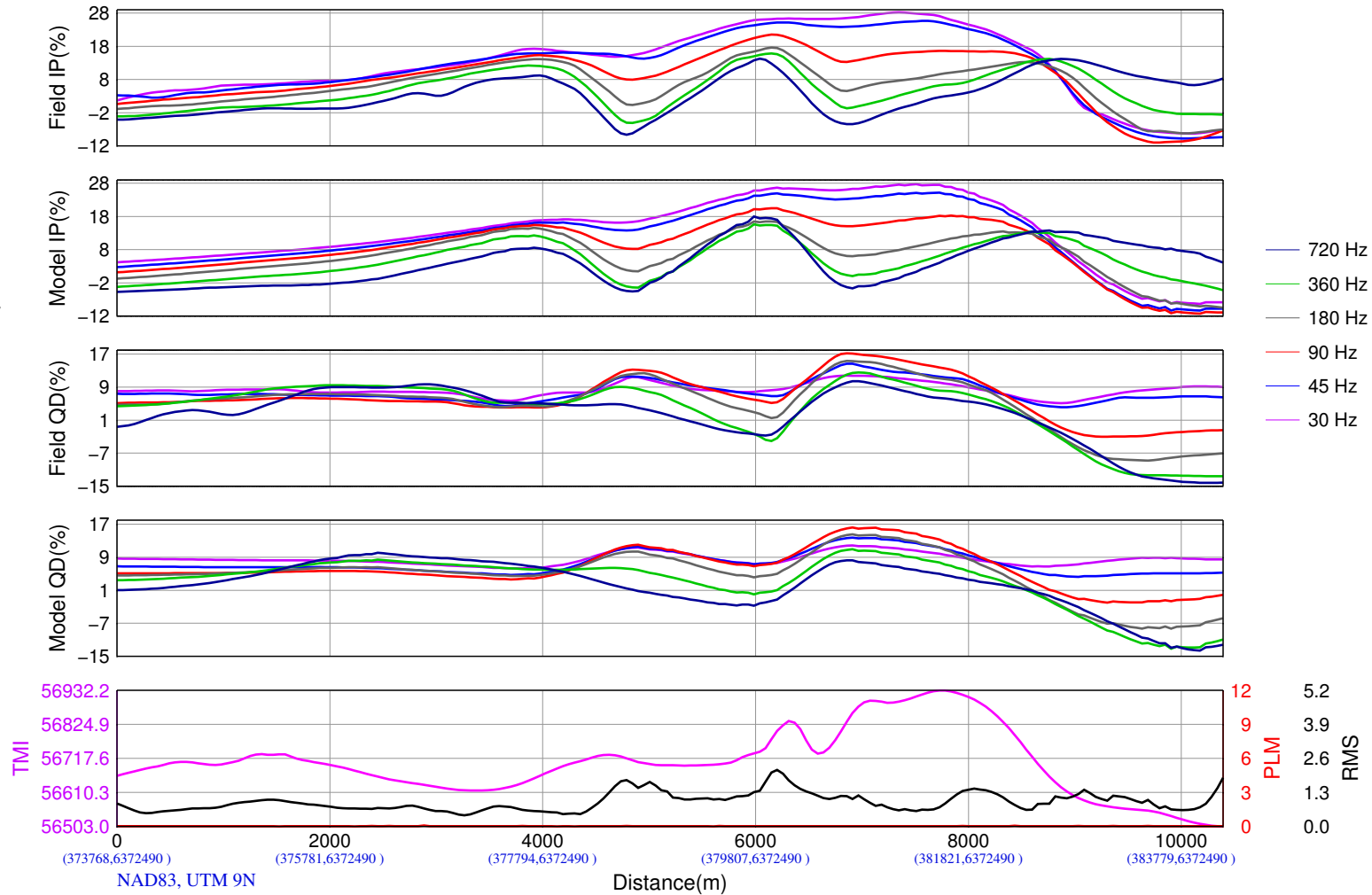
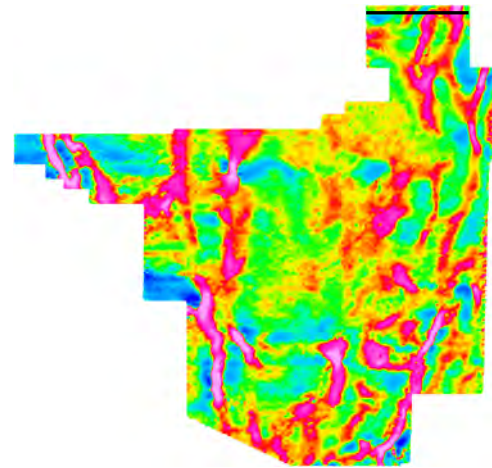
Flown and Processed by Geotech Ltd.
 245 Industrial Parkway North
 Aurora, Ontario, Canada L4G 4C4
 www.geotech.ca

2013/10/15

2D INVERSION PARAMETERS

Inversion Code: Geotech AV2DPTPO
 Model Mesh: 440 wide x 112 vertical,
 Average cell width: 27.21 m
 Two (2) Cells between sites
 Input Data: In-Phase & Quadrature,
 Tzx In-Line (only)
 Average sampling rate: 4,400 points,
 Total data points: 2304
 Frequencies: 30 45 90 180 360 720
 Input error(%): 1.12 1.12 1.12 1.12 1.12 1.12
 Half-space resistivity: 1000 ohm-m
 Output error: 0.997 RMS in 5 iterations

Line L1030 over IP 90 Hz DT image



Teck Resources Limited
 Scud Block
 Scud Peak, BC, Canada

Geotech ZTEM System
 Resistivity-Depth Image
 Project GL130332, Line L1030
 Flight 10, 2013/09/05

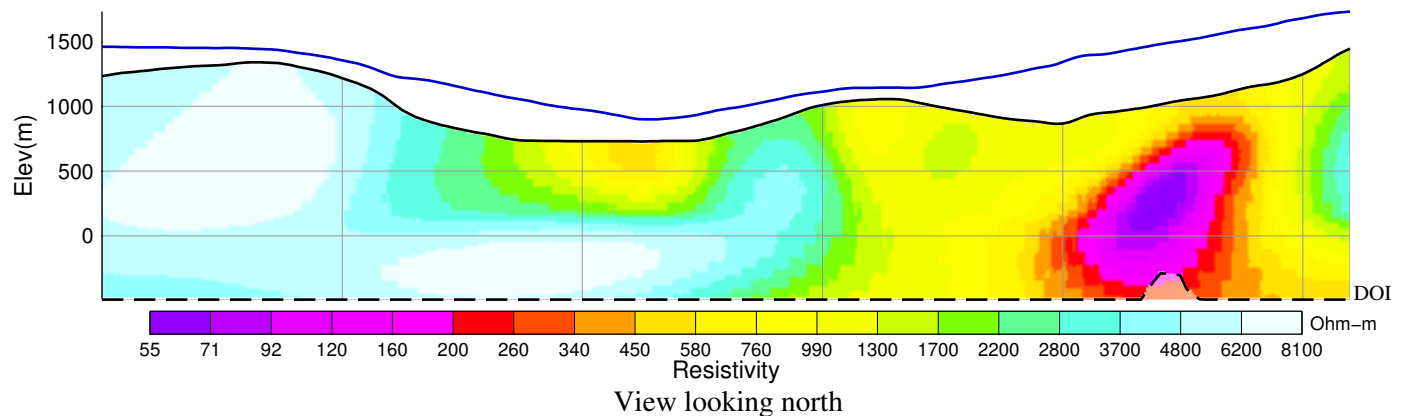
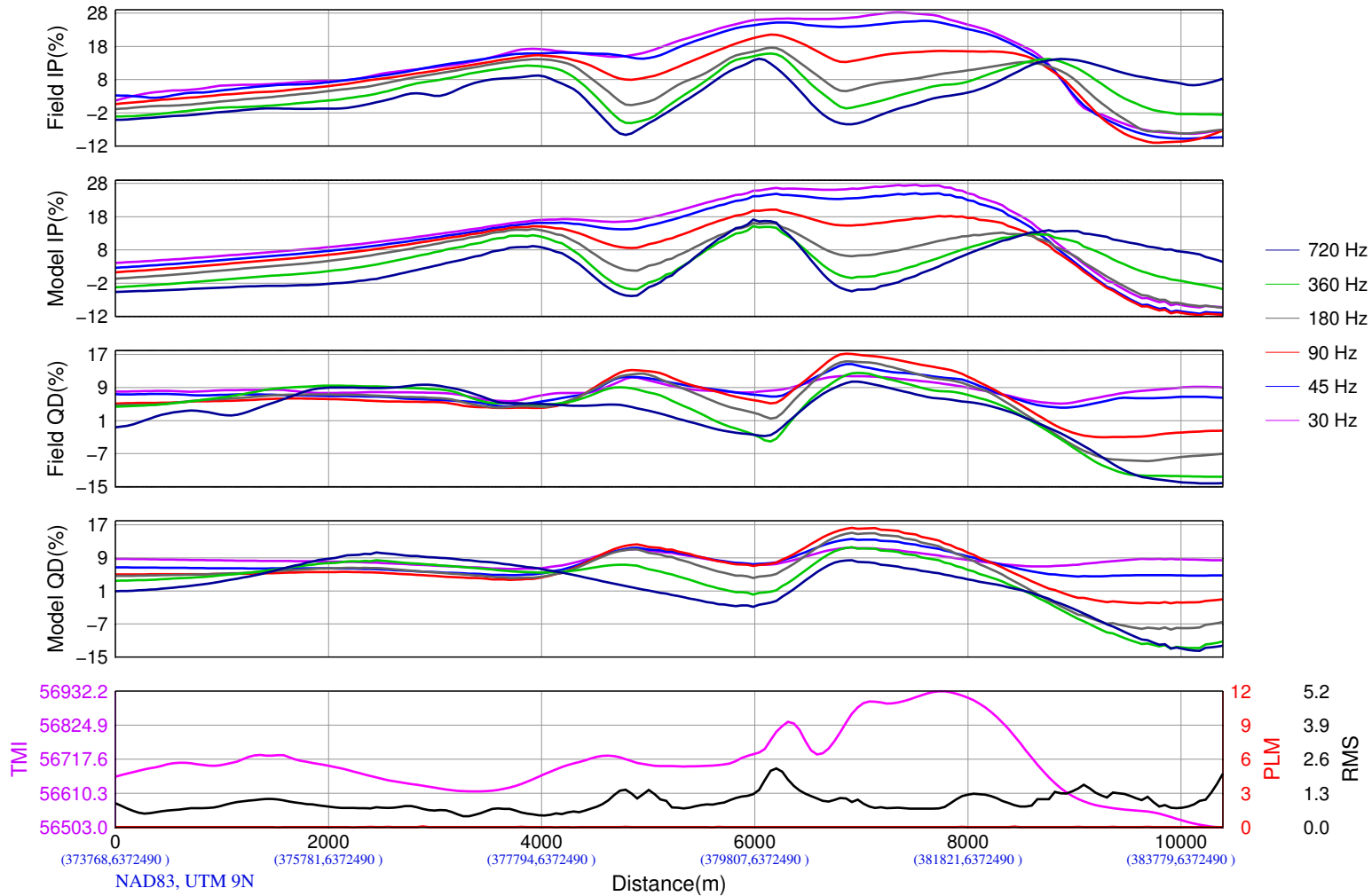
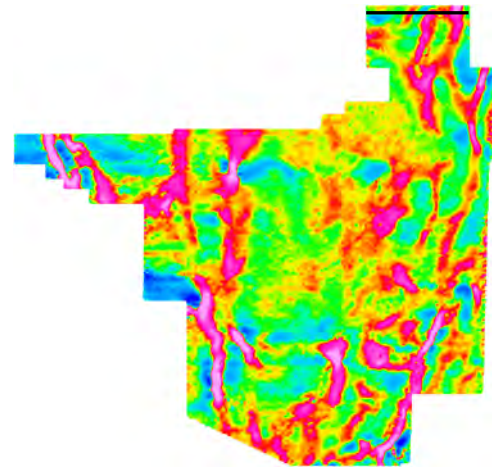
Flown and Processed by Geotech Ltd.
 245 Industrial Parkway North
 Aurora, Ontario, Canada L4G 4C4
 www.geotech.ca

2013/10/15

2D INVERSION PARAMETERS

Inversion Code: Geotech AV2DTPPO
 Model Mesh: 440 wide x 112 vertical,
 Average cell width: 27.21 m
 Two (2) Cells between sites
 Input Data: In-Phase & Quadrature,
 Tzx In-Line (only)
 Average sampling rate: 4,400 points,
 Total data points: 2304
 Frequencies: 30 45 90 180 360 720
 Input error(%): 1.06 1.06 1.06 1.06 1.06 1.06
 Half-space resistivity: 2000 ohm-m
 Output error: 0.997 RMS in 5 iterations

Line L1030 over IP 90 Hz DT image



Teck Resources Limited
 Scud Block
 Scud Peak, BC, Canada

Geotech ZTEM System
 Resistivity-Depth Image
 ProjectGL130332, Line L1030
 Flight 10, 2013/09/05

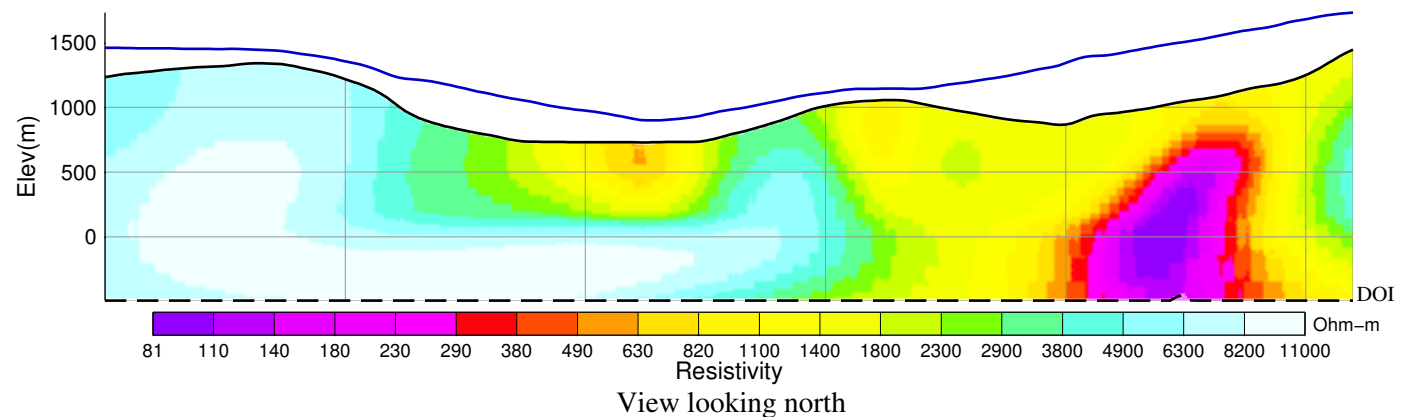
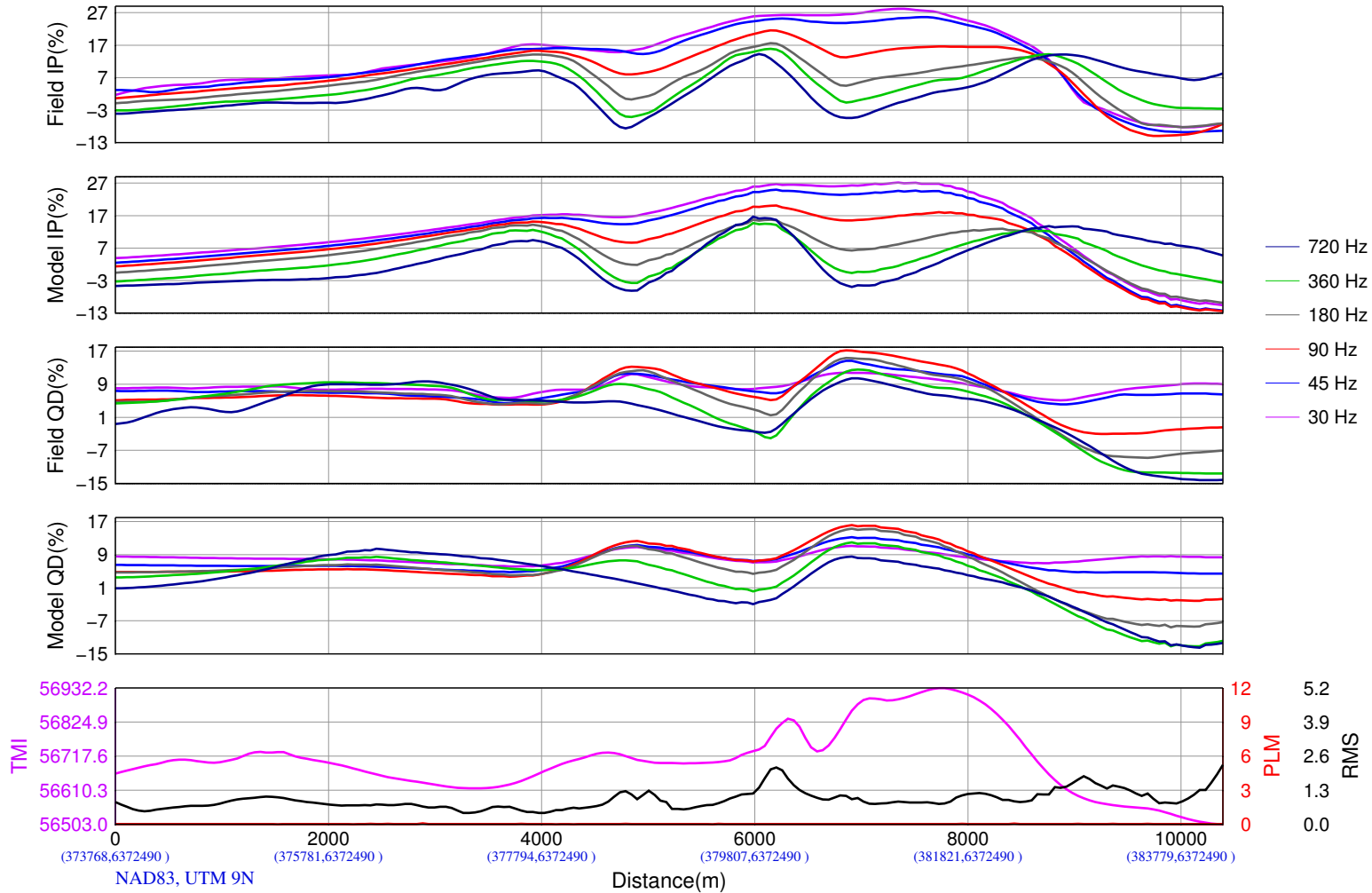
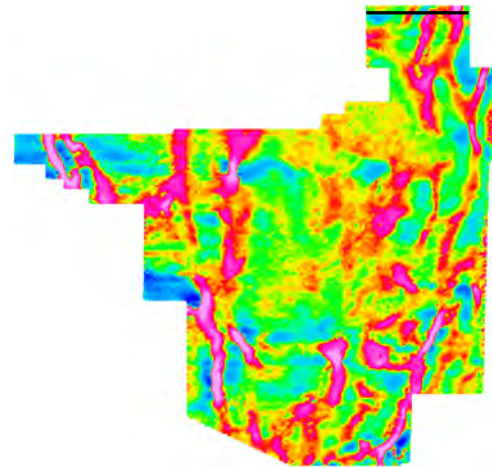
Flown and Processed by Geotech Ltd.
 245 Industrial Parkway North
 Aurora, Ontario, Canada L4G 4C4
 www.geotech.ca

2013/10/15

2D INVERSION PARAMETERS

Inversion Code: Geotech AV2DTPPO
 Model Mesh: 440 wide x 112 vertical,
 Average cell width: 27.21 m
 Two (2) Cells between sites
 Input Data: In-Phase & Quadrature,
 Tzx In-Line (only)
 Average sampling rate: 4,400 points,
 Total data points: 2304
 Frequencies: 30 45 90 180 360 720
 Input error(%): 1.11 1.11 1.11 1.11 1.11 1.11
 Half-space resistivity: 4000 ohm-m
 Output error: 0.997 RMS in 5 iterations

Line L1030 over IP 90 Hz DT image



Teck Resources Limited
 Scud Block
 Scud Peak, BC, Canada

Geotech ZTEM System
 Resistivity-Depth Image
 Project GL130332, Line L1030
 Flight 10, 2013/09/05

Flown and Processed by Geotech Ltd.
 245 Industrial Parkway North
 Aurora, Ontario, Canada L4G 4C4
 www.geotech.ca

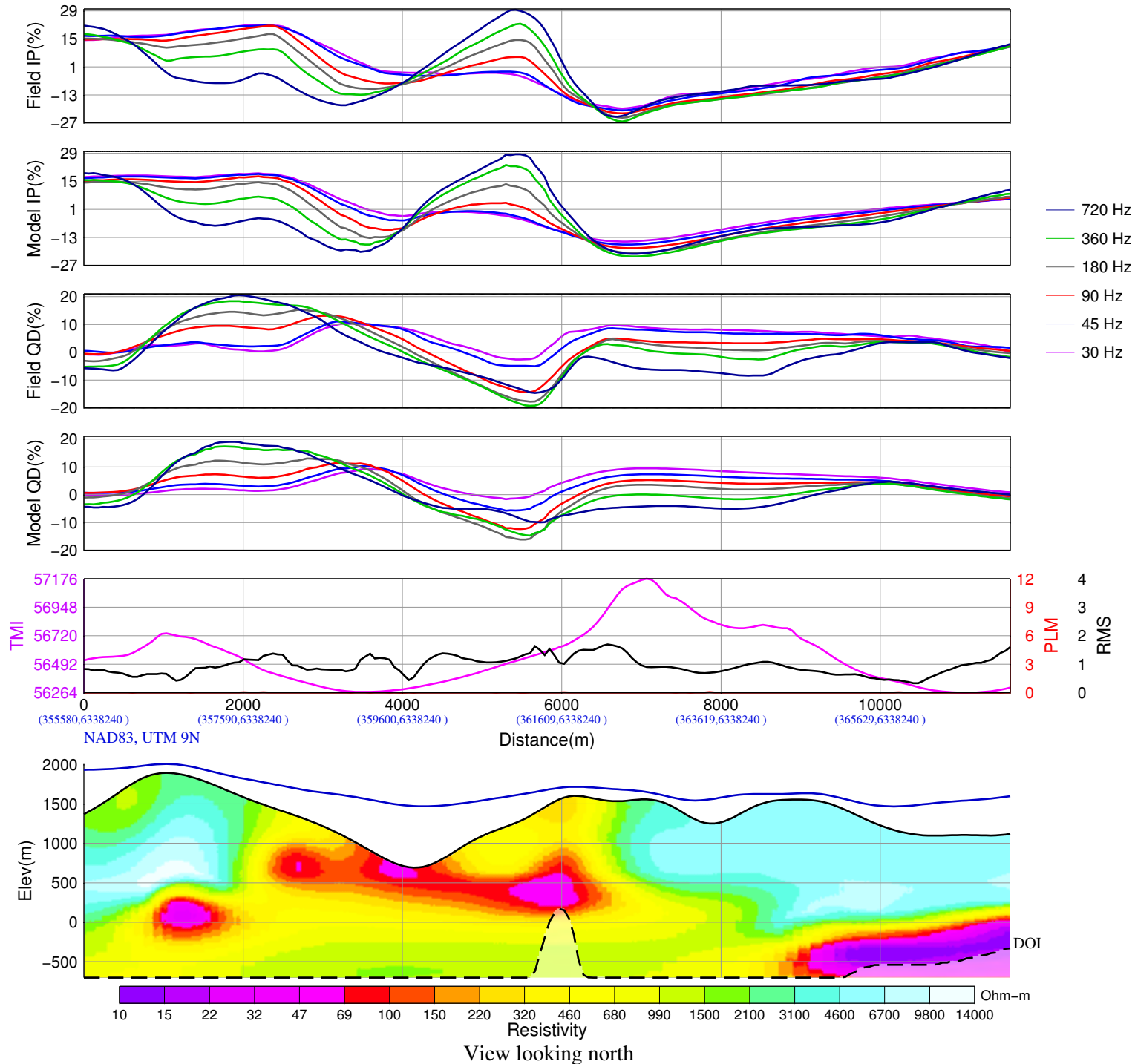
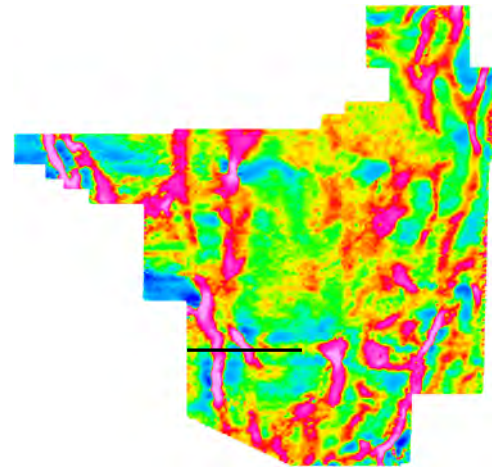
2013/10/15



The following 5 slides are inversion results for
L2400_01

2D INVERSION PARAMETERS

Inversion Code: Geotech AV2DTOPO
 Model Mesh: 440 wide x 112 vertical,
 Average cell width: 15.23 m
 Two (2) Cells between sites
 Input Data: In-Phase & Quadrature,
 Tzx In-Line (only)
 Average sampling rate: 2.560 points,
 Total data points: 2304
 Frequencies: 30 45 90 180 360 720
 Input error(%): 1.89 1.89 1.89 1.89 1.89 1.89
 Half-space resistivity: 300 ohm-m
 Output error: 0.999 RMS in 5 iterations
 Line L2400_01 over IP 90 Hz DT image



Teck Resources Limited
 Scud Block
 Scud Peak, BC, Canada

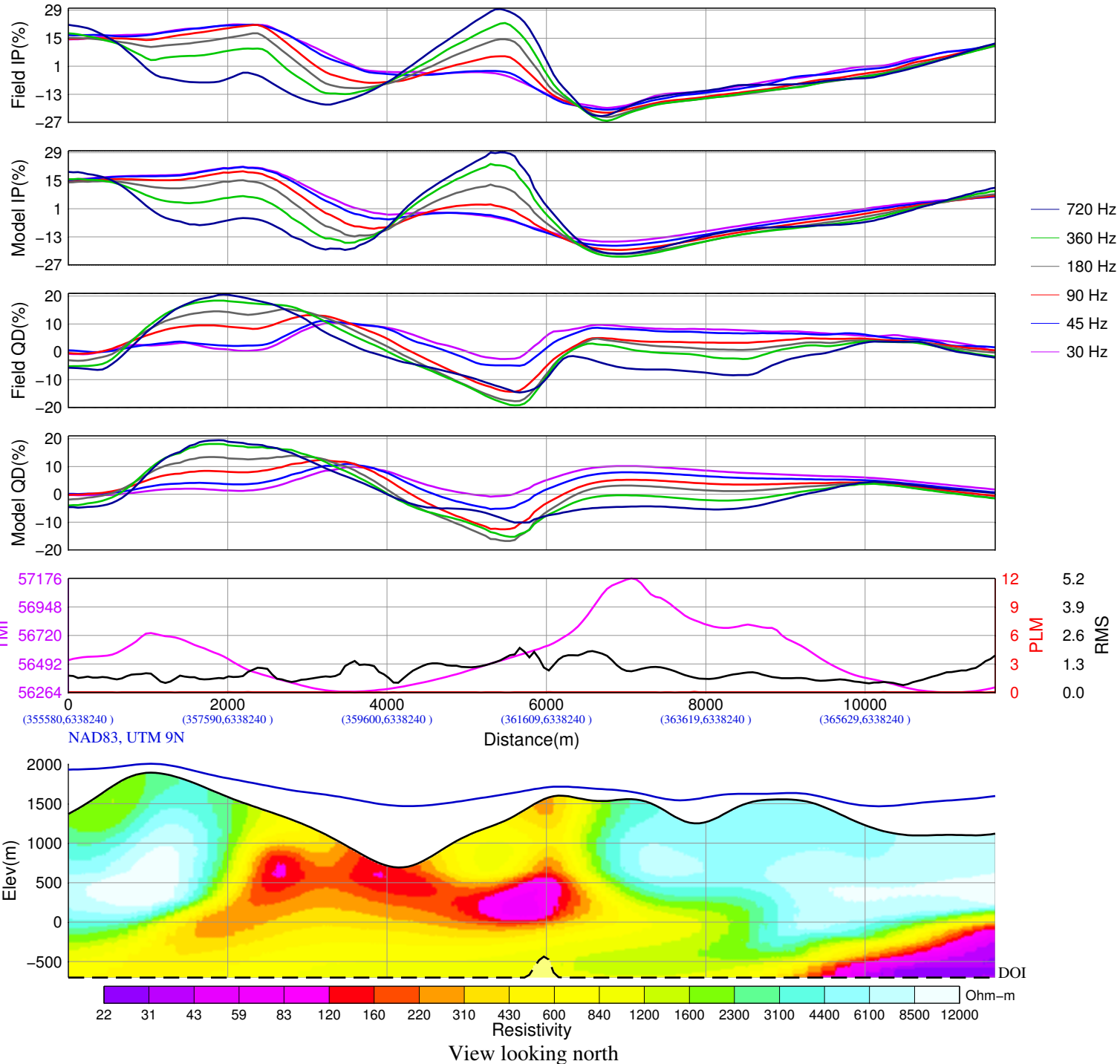
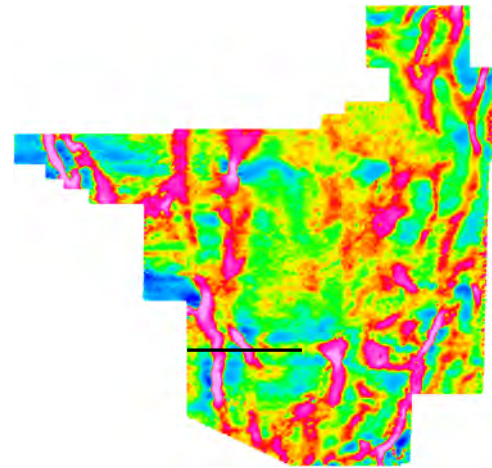
Geotech ZTEM System
 Resistivity-Depth Image
 ProjectGL130332, Line L2400_01
 Flight 27, 2013/09/13

Flown and Processed by Geotech Ltd.
 245 Industrial Parkway North
 Aurora, Ontario, Canada L4G 4C4
 www.geotech.ca

2013/10/16

2D INVERSION PARAMETERS

Inversion Code: Geotech AV2DTPPO
 Model Mesh: 440 wide x 112 vertical,
 Average cell width: 15.23 m
 Two (2) Cells between sites
 Input Data: In-Phase & Quadrature,
 Tzx In-Line (only)
 Average sampling rate: 2.560 points,
 Total data points: 2304
 Frequencies: 30 45 90 180 360 720
 Input error(%): 1.54 1.54 1.54 1.54 1.54 1.54
 Half-space resistivity: 500 ohm-m
 Output error: 0.999 RMS in 5 iterations
 Line L2400_01 over IP 90 Hz DT image



Teck Resources Limited
 Scud Block
 Scud Peak, BC, Canada

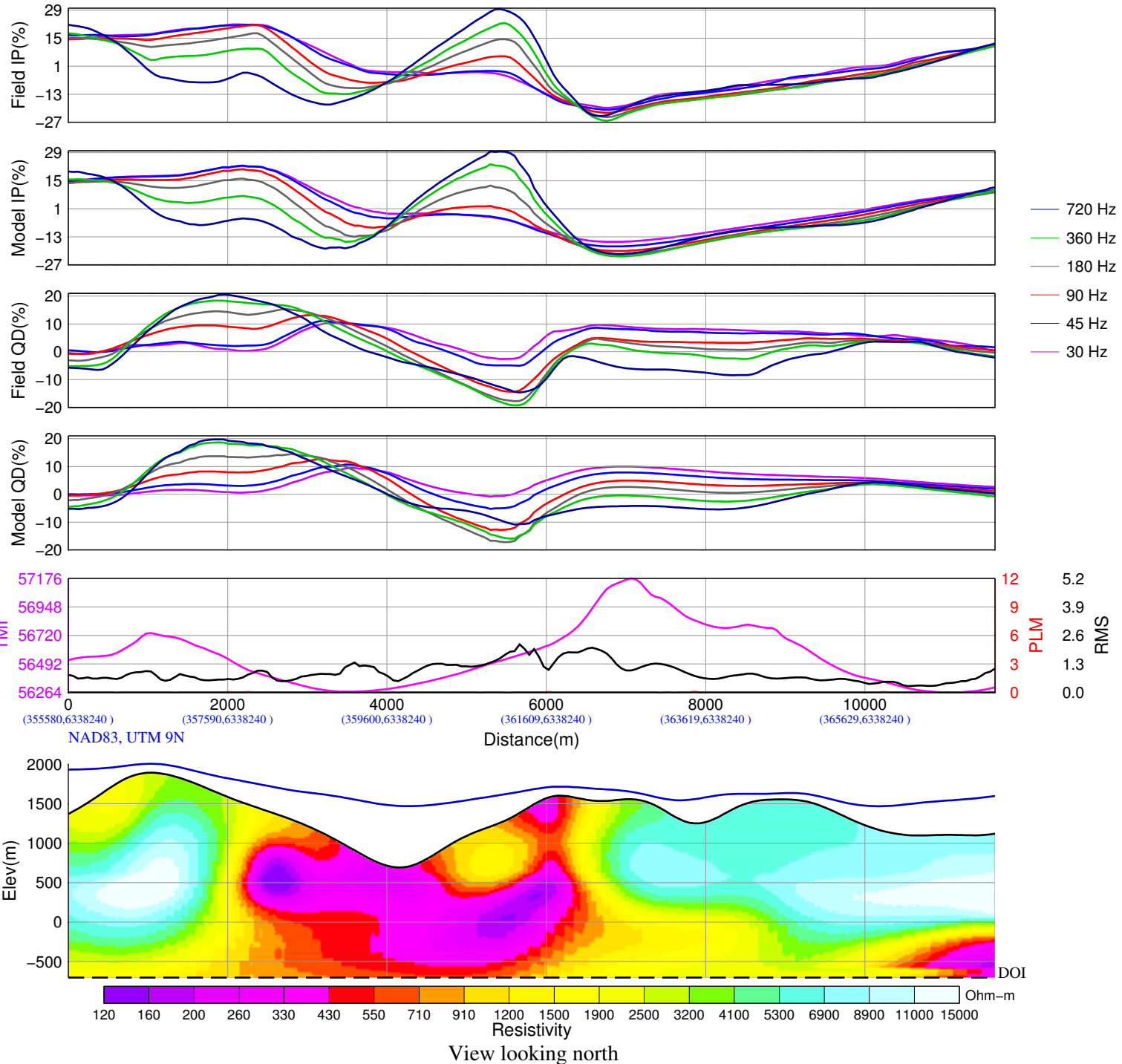
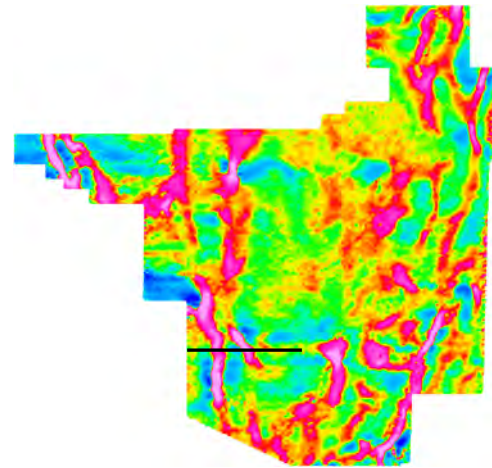
Geotech ZTEM System
 Resistivity-Depth Image
 ProjectGL130332, Line L2400_01
 Flight 27, 2013/09/13

Flown and Processed by Geotech Ltd.
 245 Industrial Parkway North
 Aurora, Ontario, Canada L4G 4C4
 www.geotech.ca

2013/10/16

2D INVERSION PARAMETERS

Inversion Code: Geotech AV2DPTOP
 Model Mesh: 440 wide x 112 vertical,
 Average cell width: 15.23 m
 Two (2) Cells between sites
 Input Data: In-Phase & Quadrature,
 Tzx In-Line (only)
 Average sampling rate: 2.560 points,
 Total data points: 2304
 Frequencies: 30 45 90 180 360 720
 Input error(%): 1.42 1.42 1.42 1.42 1.42 1.42
 Half-space resistivity: 1000 ohm-m
 Output error: 0.999 RMS in 5 iterations
 Line L2400_01 over IP 90 Hz DT image



Teck Resources Limited
 Scud Block
 Scud Peak, BC, Canada

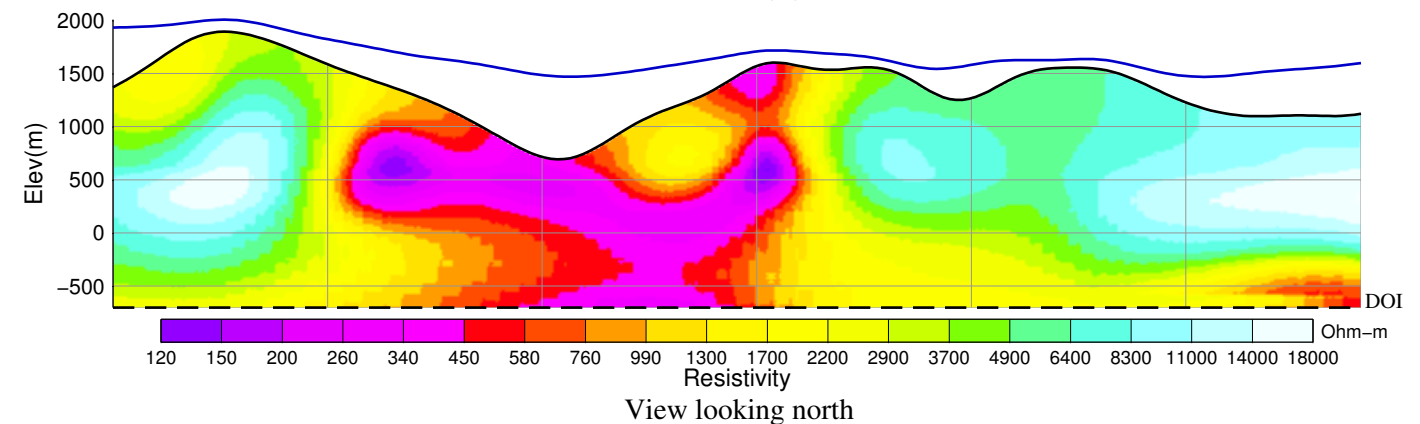
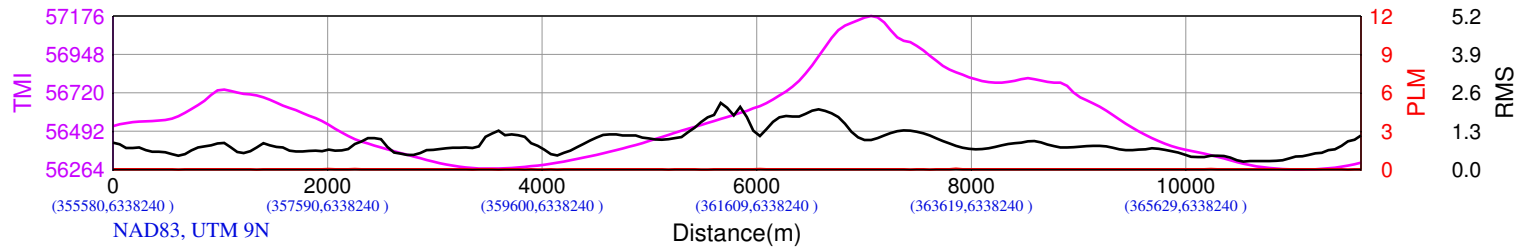
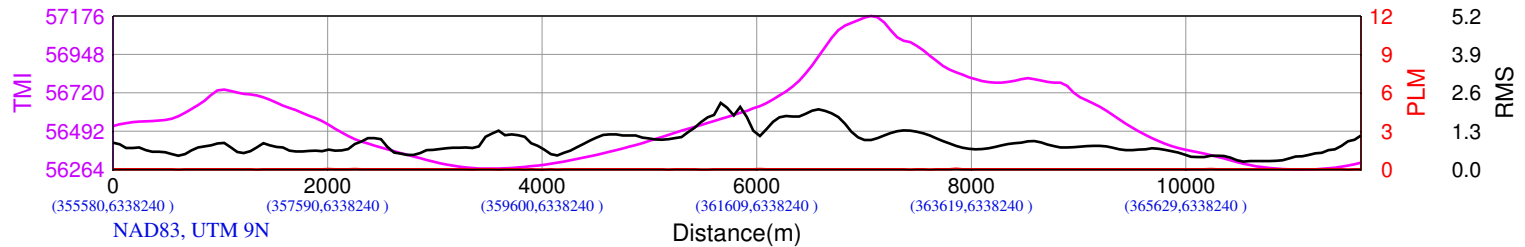
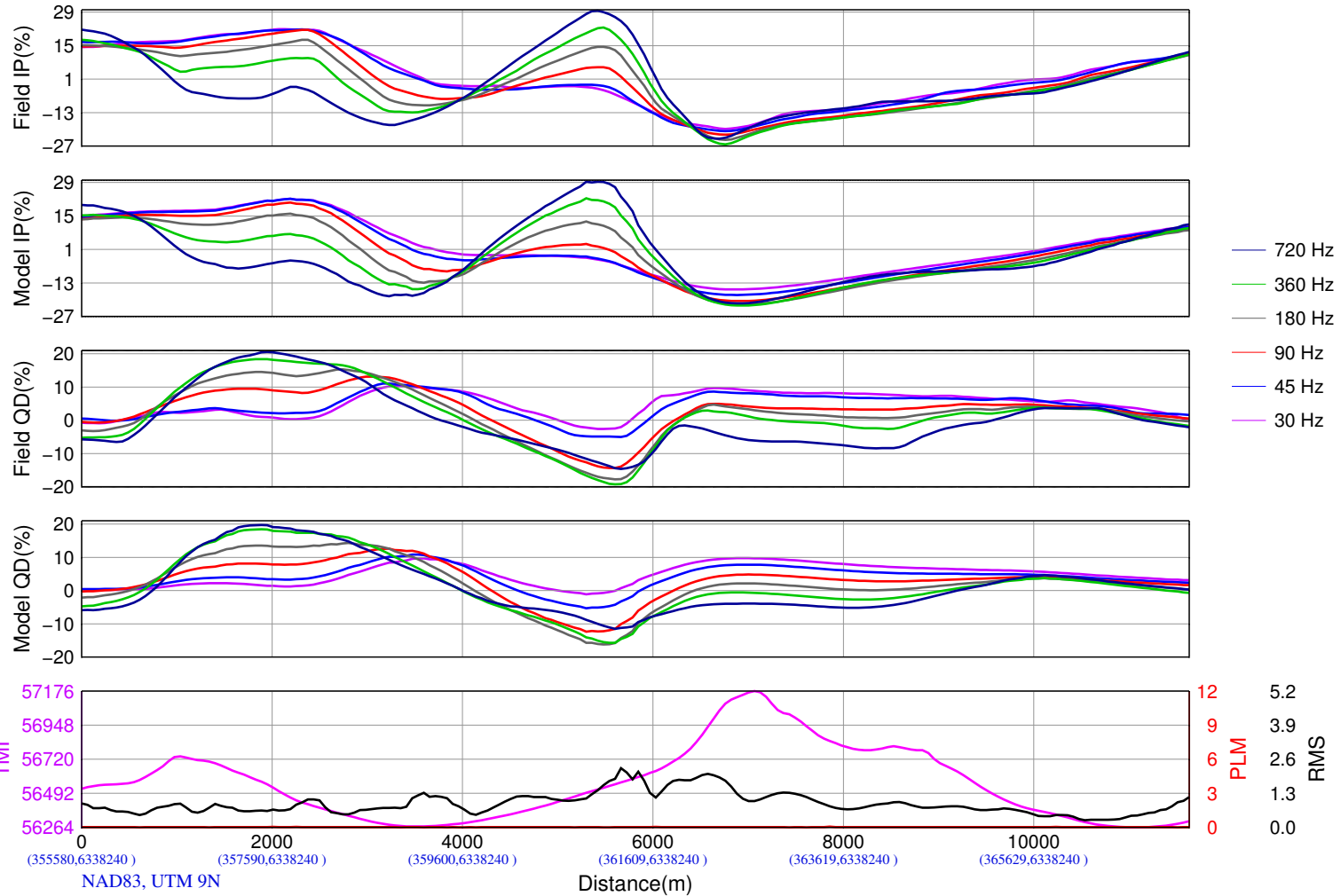
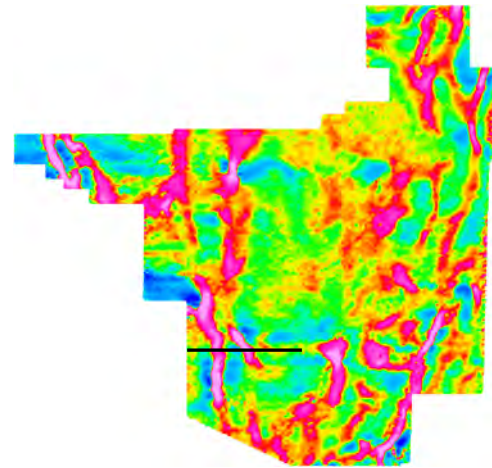
Geotech ZTEM System
 Resistivity-Depth Image
 ProjectGL130332, Line L2400_01
 Flight 27, 2013/09/13

Flown and Processed by Geotech Ltd.
 245 Industrial Parkway North
 Aurora, Ontario, Canada L4G 4C4
 www.geotech.ca

2013/10/16

2D INVERSION PARAMETERS

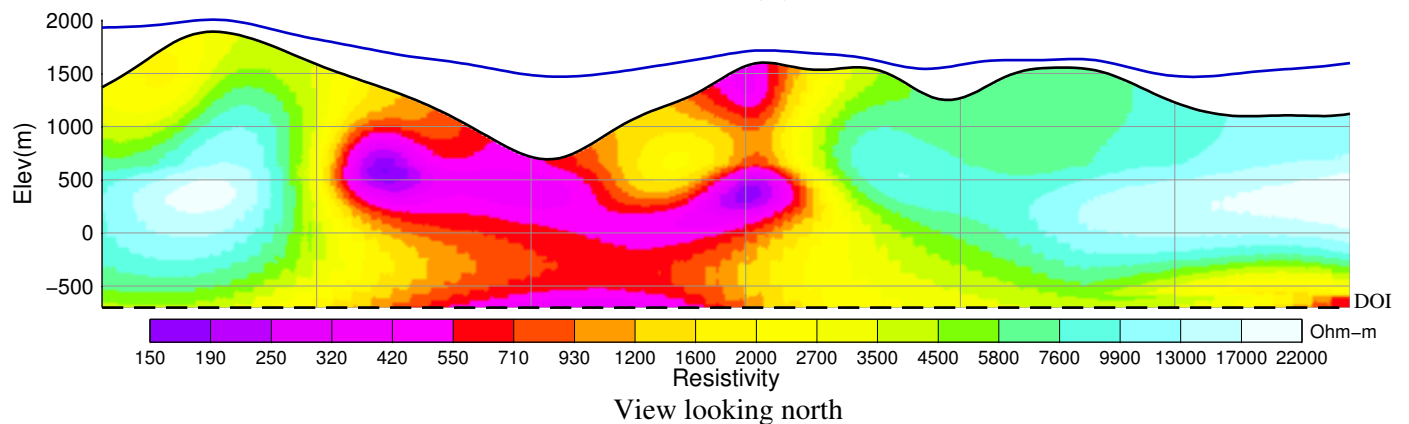
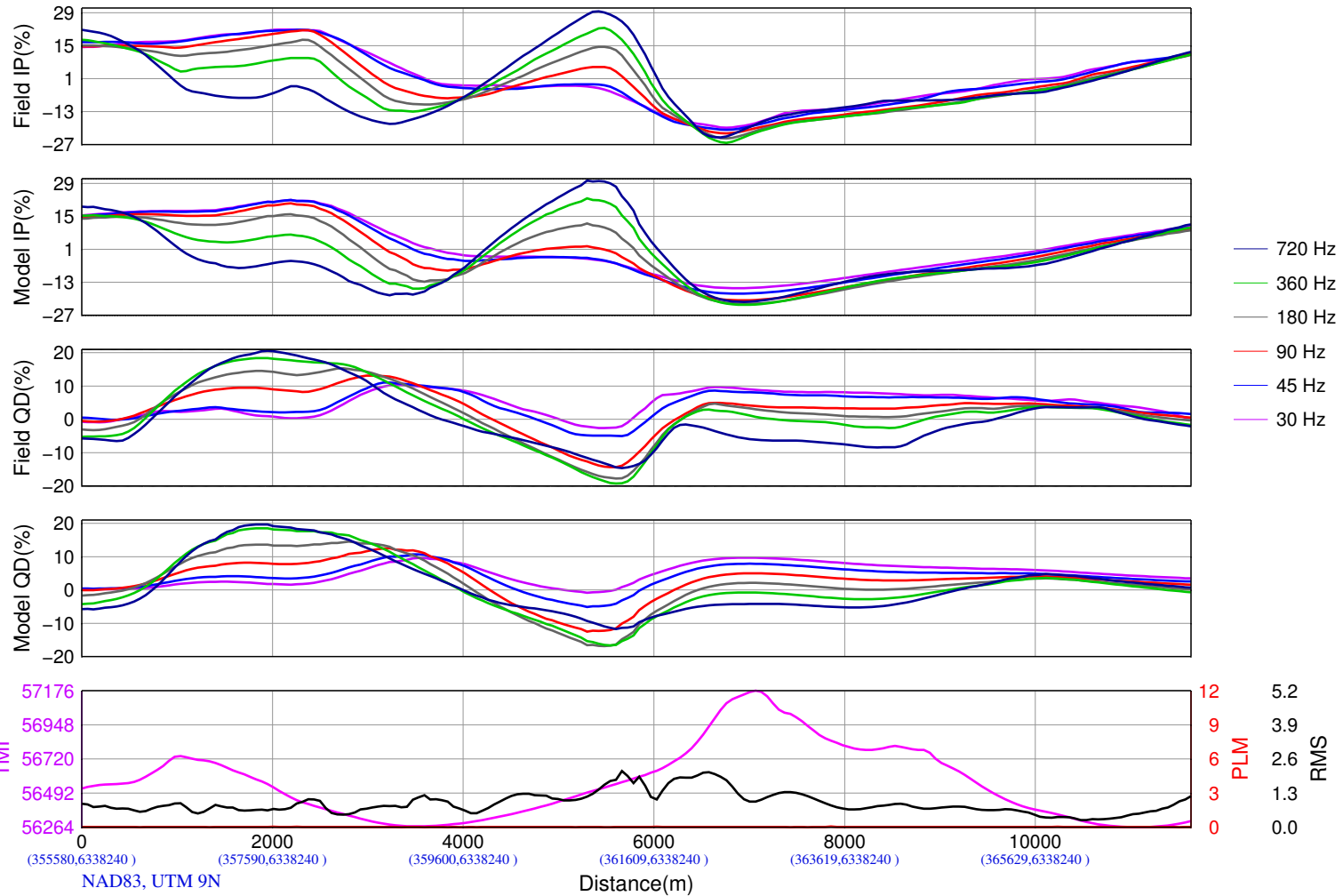
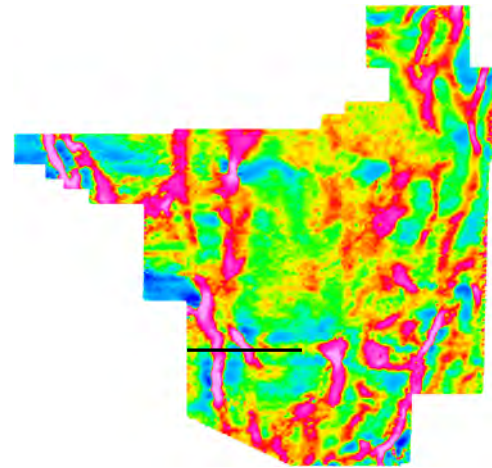
Inversion Code: Geotech AV2DPTOP
 Model Mesh: 440 wide x 112 vertical,
 Average cell width: 15.23 m
 Two (2) Cells between sites
 Input Data: In-Phase & Quadrature,
 Tzx In-Line (only)
 Average sampling rate: 2.560 points,
 Total data points: 2304
 Frequencies: 30 45 90 180 360 720
 Input error(%): 1.41 1.41 1.41 1.41 1.41 1.41
 Half-space resistivity: 2000 ohm-m
 Output error: 0.999 RMS in 4 iterations
 Line L2400_01 over IP 90 Hz DT image



Teck Resources Limited Scud Block Scud Peak, BC, Canada
Geotech ZTEM System Resistivity-Depth Image ProjectGL130332, Line L2400_01 Flight 27, 2013/09/13
Flown and Processed by Geotech Ltd. 245 Industrial Parkway North Aurora, Ontario, Canada L4G 4C4 www.geotech.ca
2013/10/16

2D INVERSION PARAMETERS

Inversion Code: Geotech AV2DPTOPO
 Model Mesh: 440 wide x 112 vertical,
 Average cell width: 15.23 m
 Two (2) Cells between sites
 Input Data: In-Phase & Quadrature,
 Tzx In-Line (only)
 Average sampling rate: 2.560 points,
 Total data points: 2304
 Frequencies: 30 45 90 180 360 720
 Input error(%): 1.46 1.46 1.46 1.46 1.46 1.46
 Half-space resistivity: 4000 ohm-m
 Output error: 0.999 RMS in 5 iterations
 Line L2400_01 over IP 90 Hz DT image



Teck Resources Limited
 Scud Block
 Scud Peak, BC, Canada

Geotech ZTEM System
 Resistivity-Depth Image
 ProjectGL130332, Line L2400_01
 Flight 27, 2013/09/13

Flown and Processed by Geotech Ltd.
 245 Industrial Parkway North
 Aurora, Ontario, Canada L4G 4C4
 www.geotech.ca

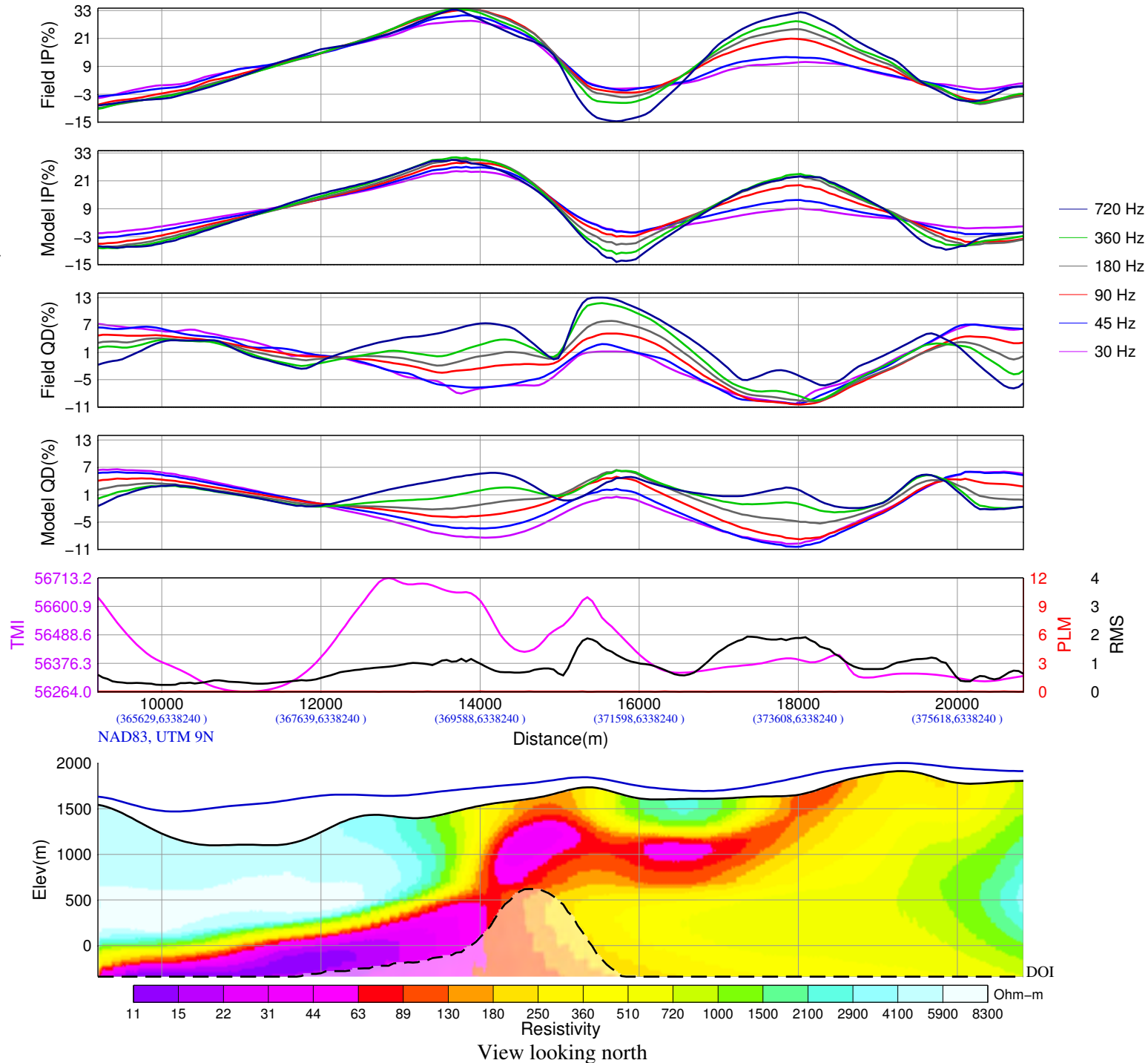
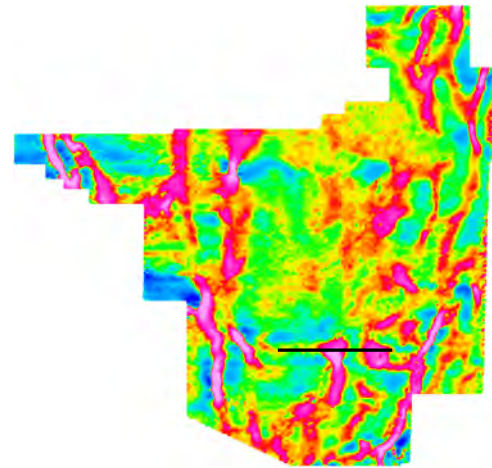
2013/10/16



The following 5 slides are inversion results for
L2400_02

2D INVERSION PARAMETERS

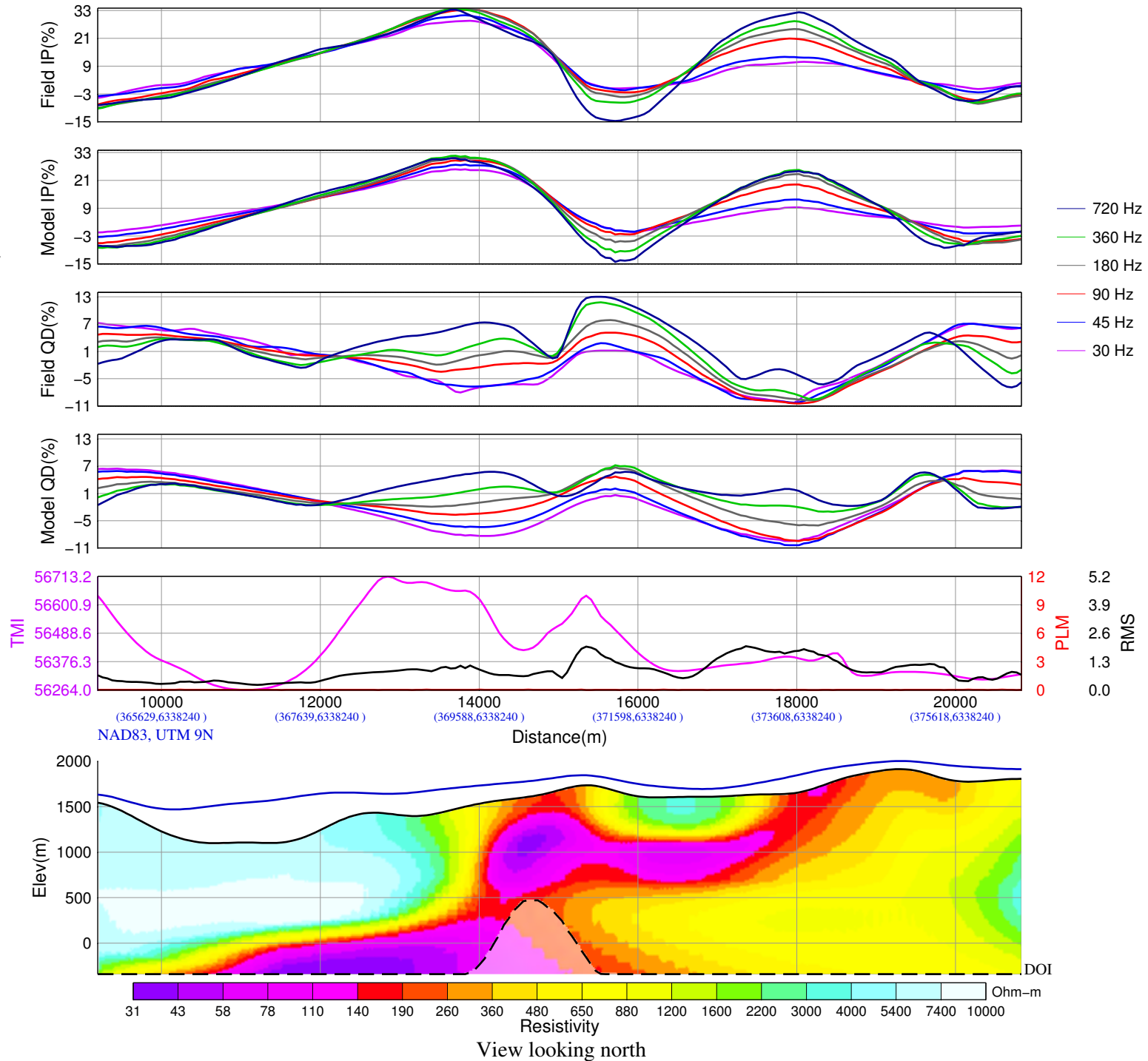
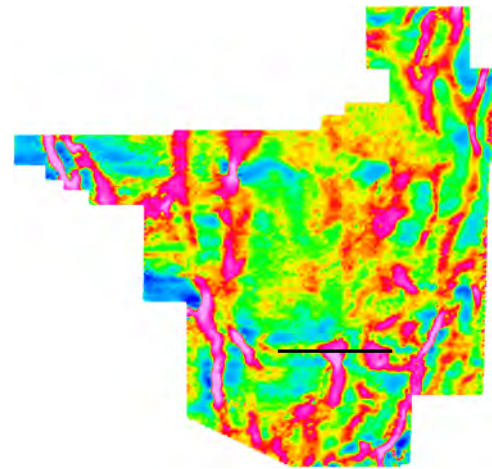
Inversion Code: Geotech AV2DPTOP
 Model Mesh: 440 wide x 112 vertical,
 Average cell width: 15.23 m
 Two (2) Cells between sites
 Input Data: In-Phase & Quadrature,
 Tzx In-Line (only)
 Average sampling rate: 2.560 points,
 Total data points: 2304
 Frequencies: 30 45 90 180 360 720
 Input error(%): 2.34 2.34 2.34 2.34 2.34 2.34
 Half-space resistivity: 300 ohm-m
 Output error: 0.999 RMS in 5 iterations
 Line L2400_02 over IP 90 Hz DT image



Teck Resources Limited Scud Block Scud Peak, BC, Canada
Geotech ZTEM System Resistivity-Depth Image ProjectGL130332, Line L2400_02 Flight 27, 2013/09/13
Flown and Processed by Geotech Ltd. 245 Industrial Parkway North Aurora, Ontario, Canada L4G 4C4 www.geotech.ca
2013/10/16

2D INVERSION PARAMETERS

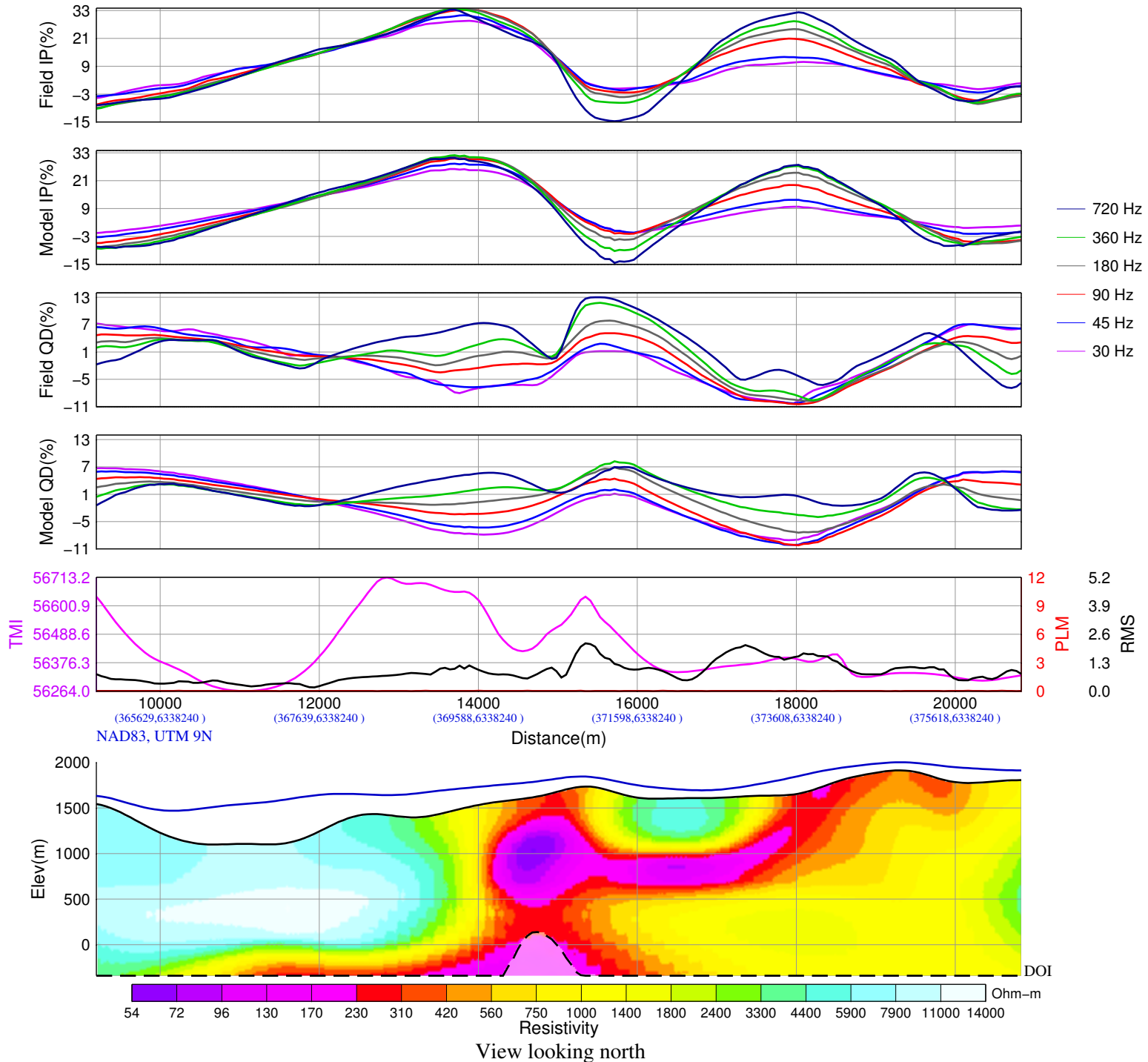
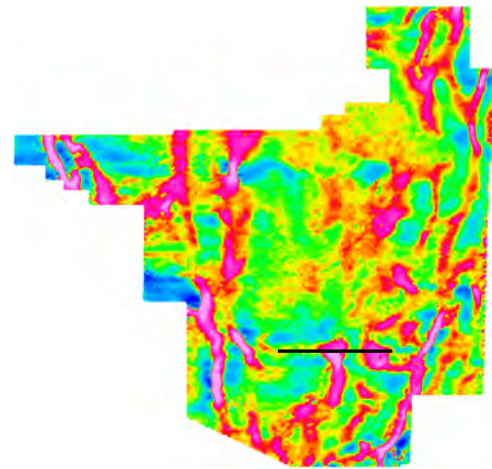
Inversion Code: Geotech AV2DPTOPO
 Model Mesh: 440 wide x 112 vertical,
 Average cell width: 15.23 m
 Two (2) Cells between sites
 Input Data: In-Phase & Quadrature,
 Tzx In-Line (only)
 Average sampling rate: 2.560 points,
 Total data points: 2304
 Frequencies: 30 45 90 180 360 720
 Input error(%): 2.02 2.02 2.02 2.02 2.02 2.02
 Half-space resistivity: 500 ohm-m
 Output error: 0.999 RMS in 5 iterations
 Line L2400_02 over IP 90 Hz DT image



Teck Resources Limited Scud Block Scud Peak, BC, Canada
Geotech ZTEM System Resistivity-Depth Image ProjectGL130332, Line L2400_02 Flight 27, 2013/09/13
Flown and Processed by Geotech Ltd. 245 Industrial Parkway North Aurora, Ontario, Canada L4G 4C4 www.geotech.ca
2013/10/16

2D INVERSION PARAMETERS

Inversion Code: Geotech AV2DTPPO
 Model Mesh: 440 wide x 112 vertical,
 Average cell width: 15.23 m
 Two (2) Cells between sites
 Input Data: In-Phase & Quadrature,
 Tzx In-Line (only)
 Average sampling rate: 2.560 points,
 Total data points: 2304
 Frequencies: 30 45 90 180 360 720
 Input error(%): 1.62 1.62 1.62 1.62 1.62 1.62
 Half-space resistivity: 1000 ohm-m
 Output error: 0.999 RMS in 5 iterations
 Line L2400_02 over IP 90 Hz DT image



Teck Resources Limited
 Scud Block
 Scud Peak, BC, Canada

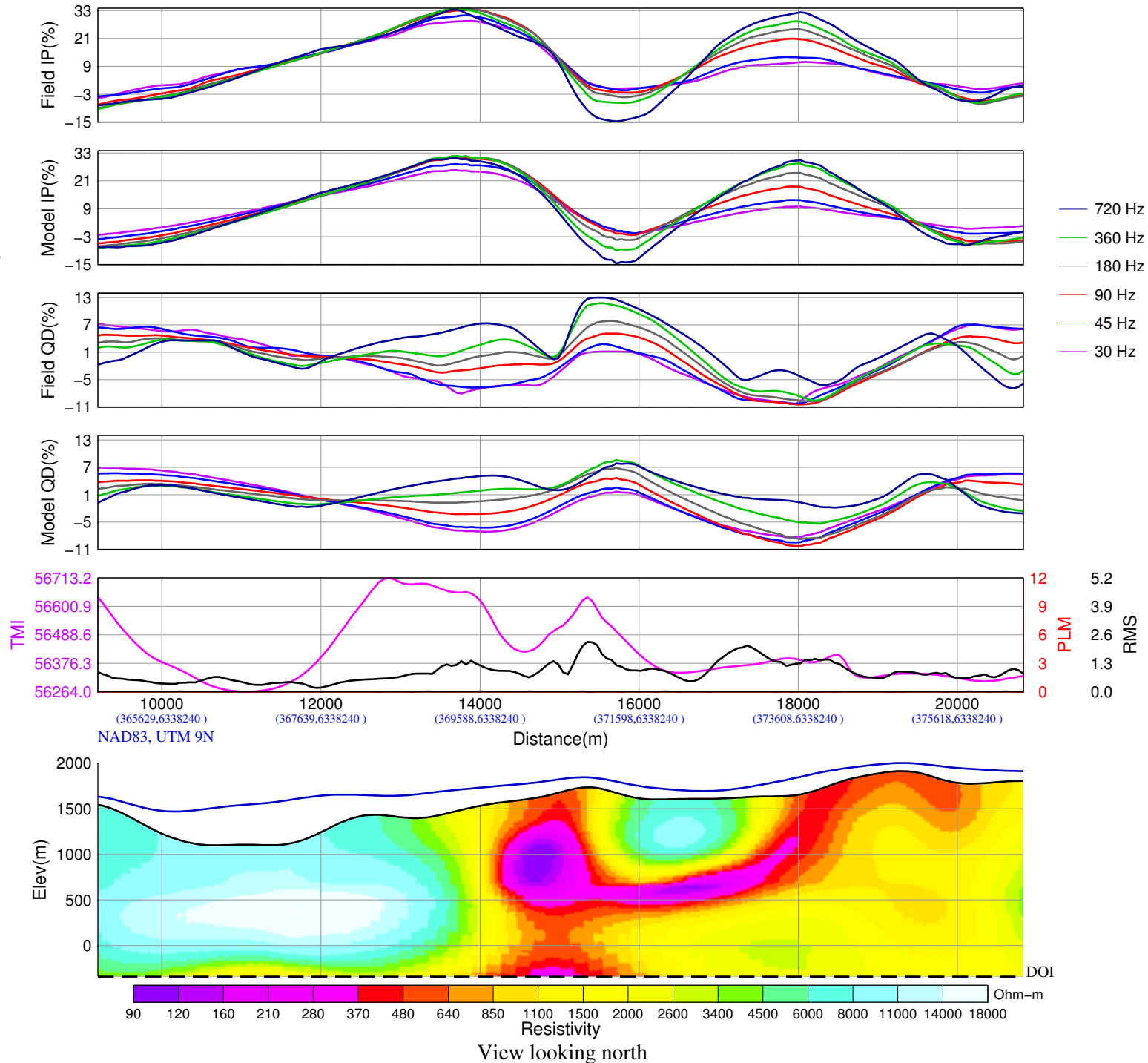
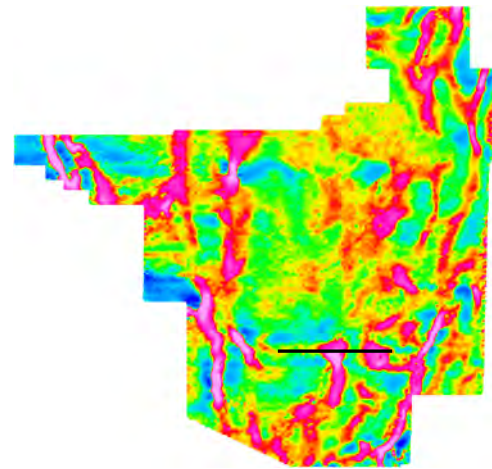
Geotech ZTEM System
 Resistivity-Depth Image
 Project GL130332, Line L2400_02
 Flight 27, 2013/09/13

Flown and Processed by Geotech Ltd.
 245 Industrial Parkway North
 Aurora, Ontario, Canada L4G 4C4
 www.geotech.ca

2013/10/16

2D INVERSION PARAMETERS

Inversion Code: Geotech AV2DTPPO
 Model Mesh: 440 wide x 112 vertical,
 Average cell width: 15.23 m
 Two (2) Cells between sites
 Input Data: In-Phase & Quadrature,
 Tzx In-Line (only)
 Average sampling rate: 2.560 points,
 Total data points: 2304
 Frequencies: 30 45 90 180 360 720
 Input error(%): 1.42 1.42 1.42 1.42 1.42 1.42
 Half-space resistivity: 2000 ohm-m
 Output error: 0.999 RMS in 5 iterations
 Line L2400_02 over IP 90 Hz DT image



Teck Resources Limited
 Scud Block
 Scud Peak, BC, Canada

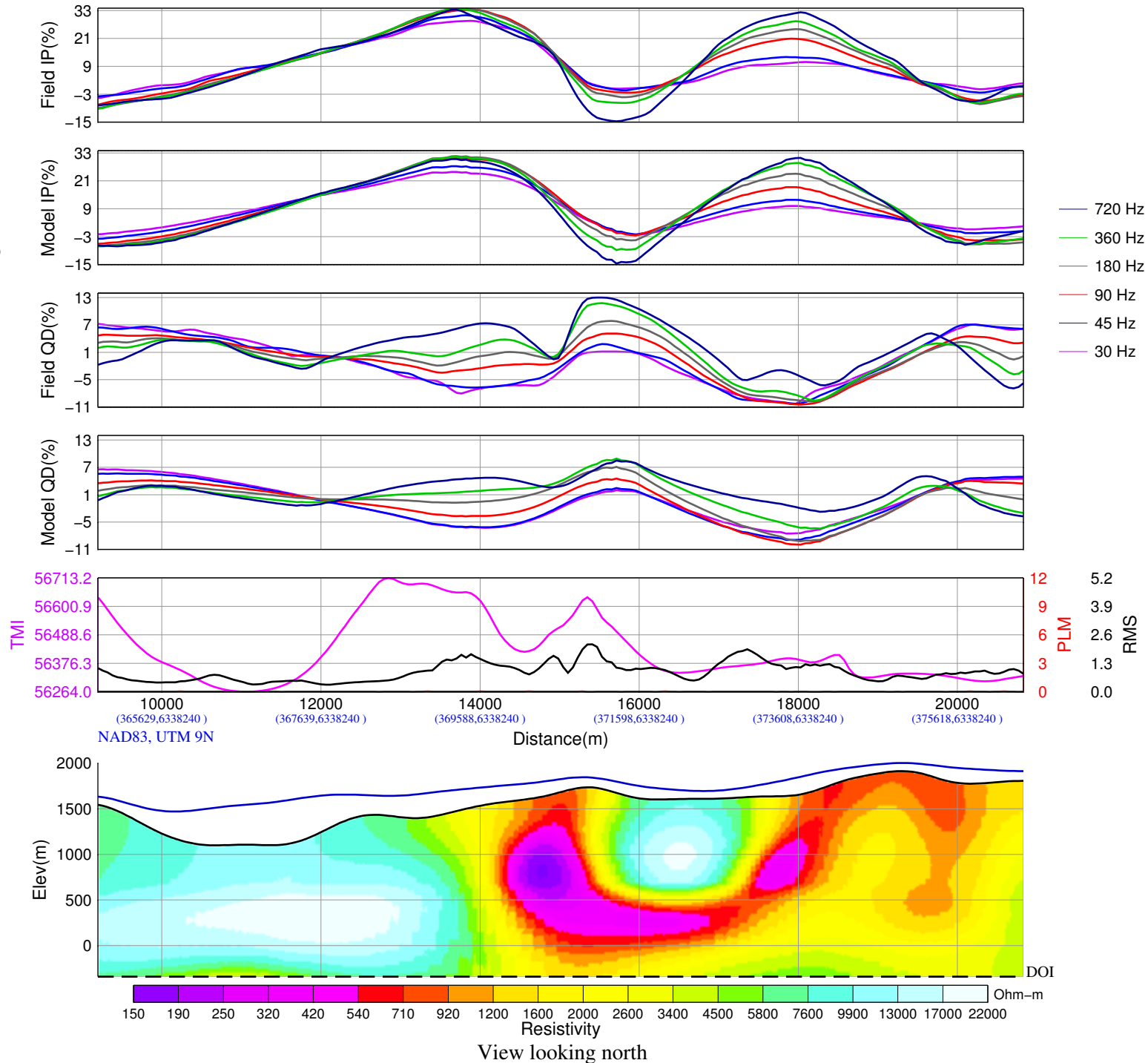
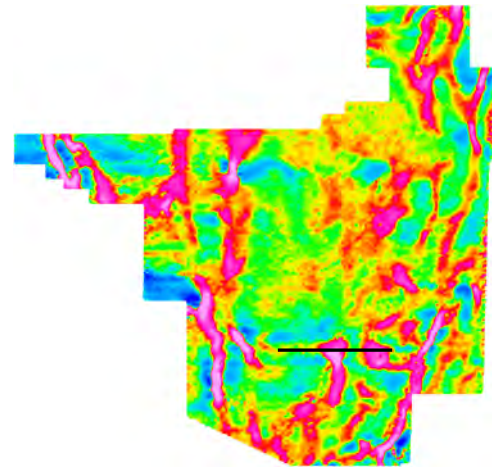
Geotech ZTEM System
 Resistivity-Depth Image
 ProjectGL130332, Line L2400_02
 Flight 27, 2013/09/13

Flown and Processed by Geotech Ltd.
 245 Industrial Parkway North
 Aurora, Ontario, Canada L4G 4C4
 www.geotech.ca

2013/10/16

2D INVERSION PARAMETERS

Inversion Code: Geotech AV2DTPPO
 Model Mesh: 440 wide x 112 vertical,
 Average cell width: 15.23 m
 Two (2) Cells between sites
 Input Data: In-Phase & Quadrature,
 Tzx In-Line (only)
 Average sampling rate: 2.560 points,
 Total data points: 2304
 Frequencies: 30 45 90 180 360 720
 Input error(%): 1.39 1.39 1.39 1.39 1.39 1.39
 Half-space resistivity: 4000 ohm-m
 Output error: 0.999 RMS in 5 iterations
 Line L2400_02 over IP 90 Hz DT image



Teck Resources Limited
 Scud Block
 Scud Peak, BC, Canada

Geotech ZTEM System
 Resistivity-Depth Image
 ProjectGL130332, Line L2400_02
 Flight 27, 2013/09/13

Flown and Processed by Geotech Ltd.
 245 Industrial Parkway North
 Aurora, Ontario, Canada L4G 4C4
 www.geotech.ca

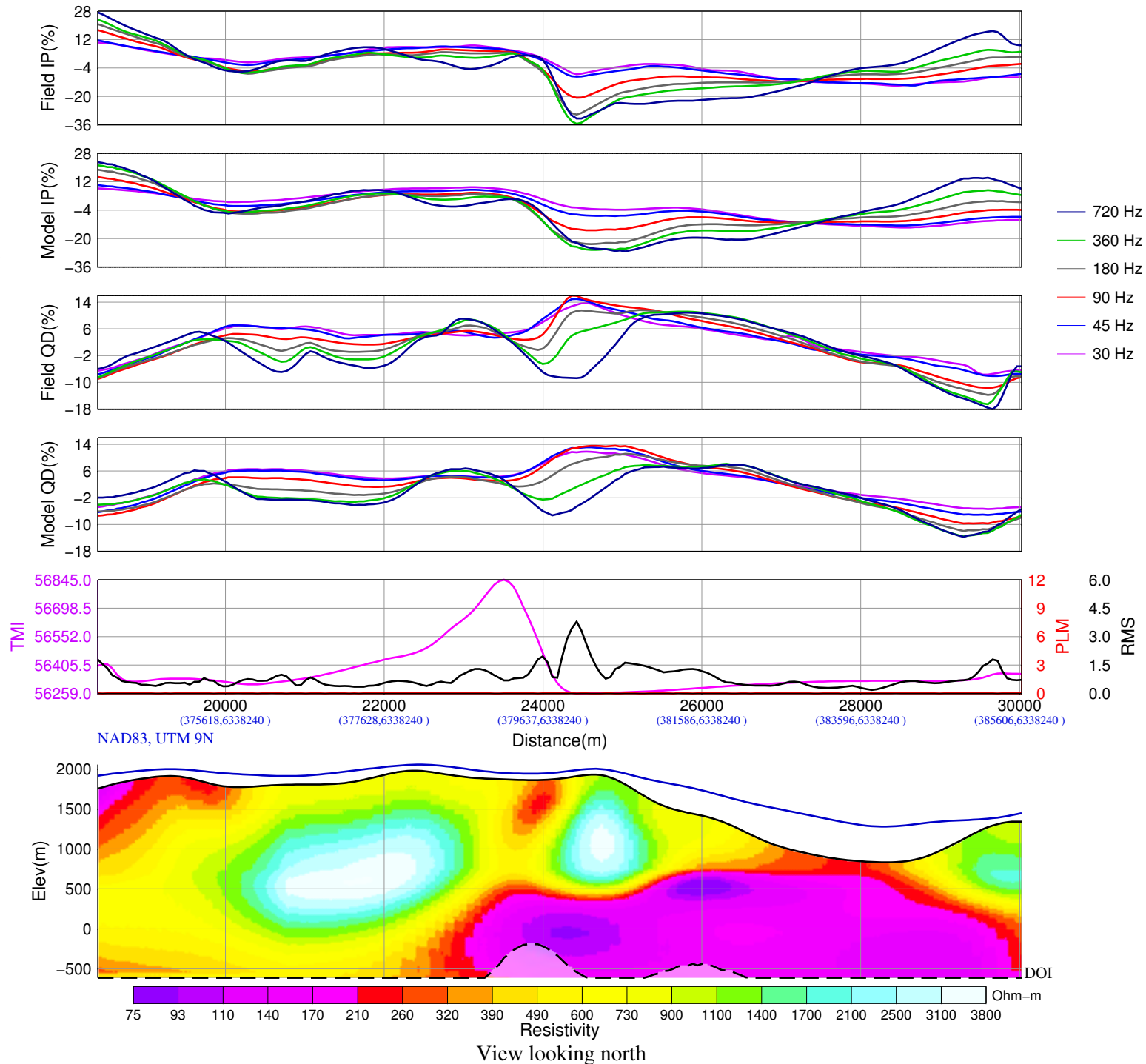
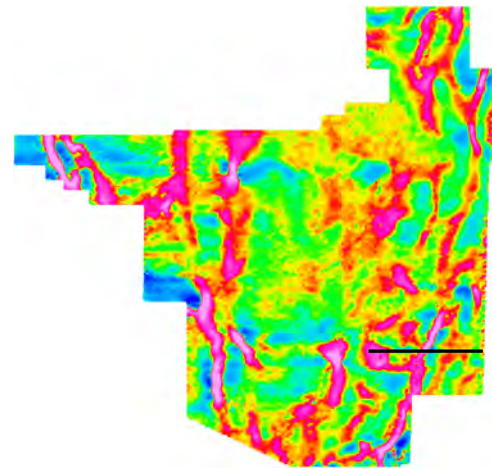
2013/10/16



The following 5 slides are inversion results for
L2400_03

2D INVERSION PARAMETERS

Inversion Code: Geotech AV2DPTOP
 Model Mesh: 440 wide x 112 vertical,
 Average cell width: 15.23 m
 Two (2) Cells between sites
 Input Data: In-Phase & Quadrature,
 Tzx In-Line (only)
 Average sampling rate: 2.560 points,
 Total data points: 2304
 Frequencies: 30 45 90 180 360 720
 Input error(%): 1.53 1.53 1.53 1.53 1.53 1.53
 Half-space resistivity: 300 ohm-m
 Output error: 0.999 RMS in 5 iterations
 Line L2400_03 over IP 90 Hz DT image



Teck Resources Limited
 Scud Block
 Scud Peak, BC, Canada

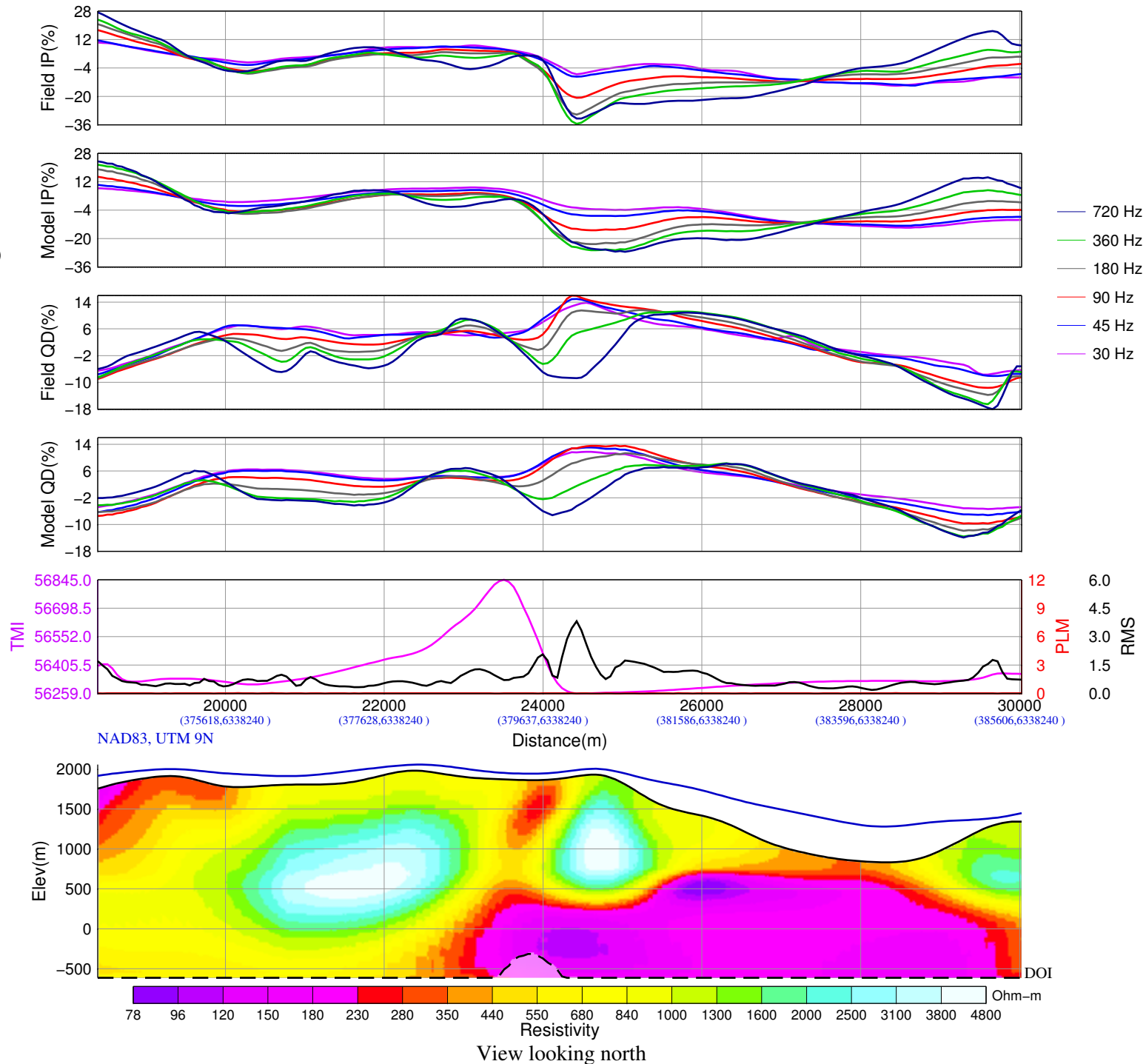
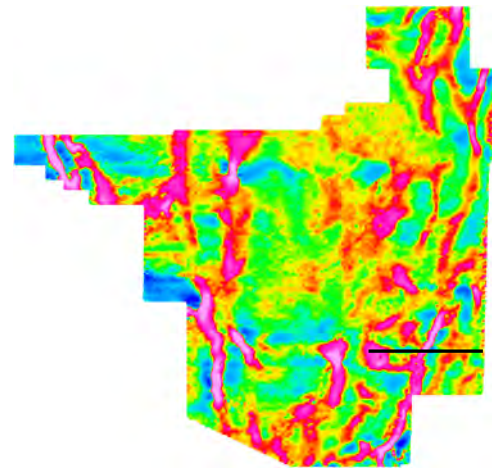
Geotech ZTEM System
 Resistivity-Depth Image
 ProjectGL130332, Line L2400_03
 Flight 27, 2013/09/13

Flown and Processed by Geotech Ltd.
 245 Industrial Parkway North
 Aurora, Ontario, Canada L4G 4C4
 www.geotech.ca

2013/10/16

2D INVERSION PARAMETERS

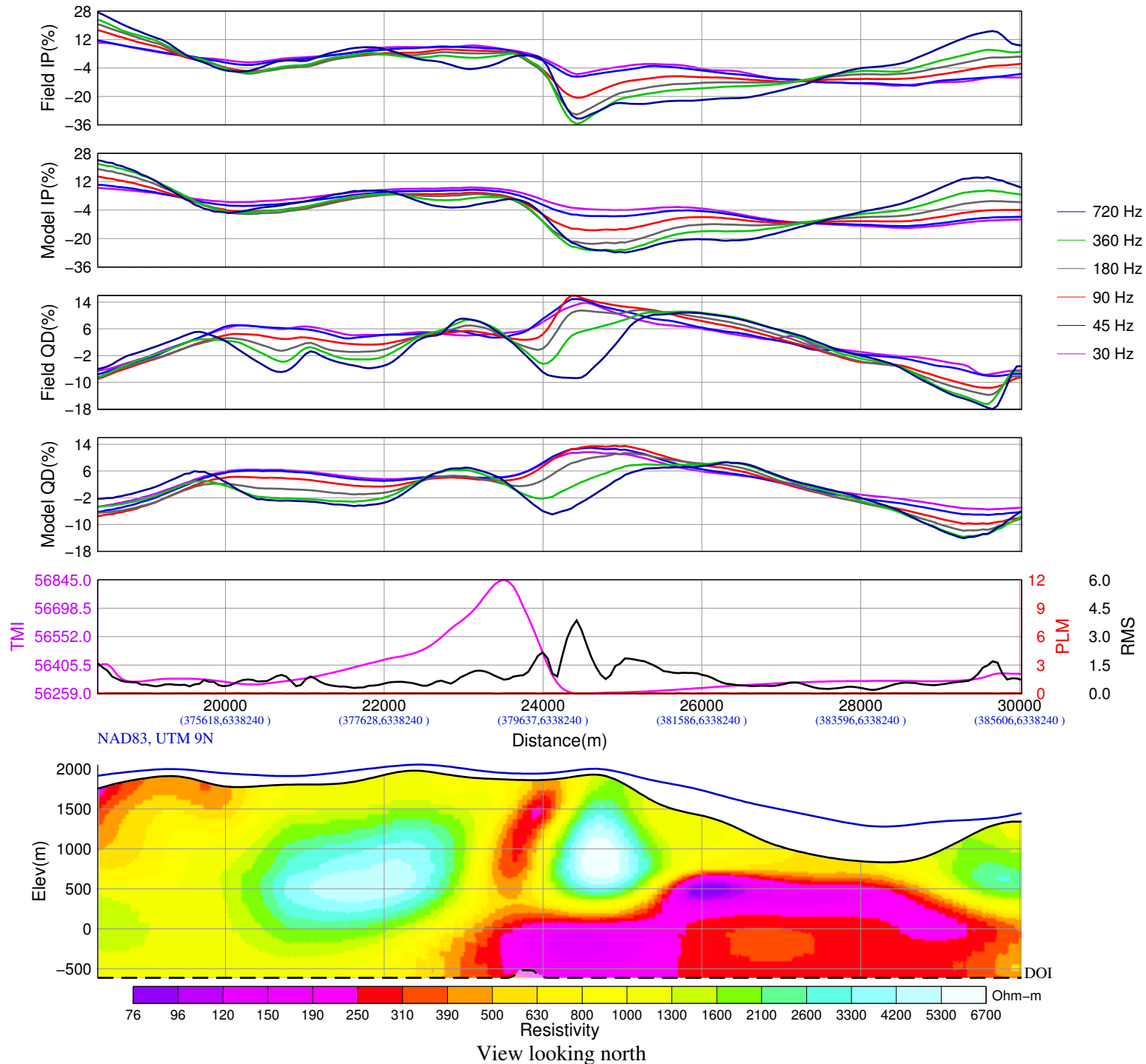
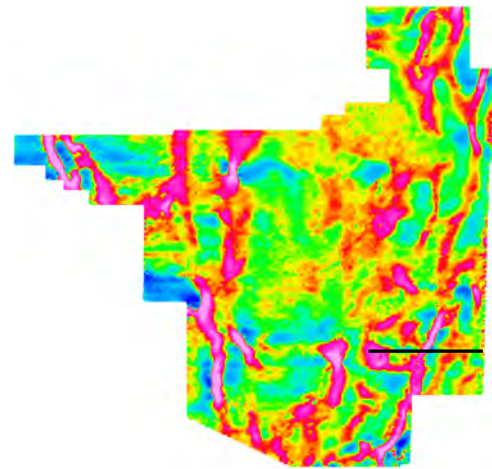
Inversion Code: Geotech AV2DTOPO
 Model Mesh: 440 wide x 112 vertical,
 Average cell width: 15.23 m
 Two (2) Cells between sites
 Input Data: In-Phase & Quadrature,
 Tzx In-Line (only)
 Average sampling rate: 2.560 points,
 Total data points: 2304
 Frequencies: 30 45 90 180 360 720
 Input error(%): 1.50 1.50 1.50 1.50 1.50 1.50
 Half-space resistivity: 500 ohm-m
 Output error: 0.999 RMS in 5 iterations
 Line L2400_03 over IP 90 Hz DT image



Teck Resources Limited Scud Block Scud Peak, BC, Canada
Geotech ZTEM System Resistivity-Depth Image ProjectGL130332, Line L2400_03 Flight 27, 2013/09/13
Flown and Processed by Geotech Ltd. 245 Industrial Parkway North Aurora, Ontario, Canada L4G 4C4 www.geotech.ca
2013/10/16

2D INVERSION PARAMETERS

Inversion Code: Geotech AV2DTPPO
 Model Mesh: 440 wide x 112 vertical,
 Average cell width: 15.23 m
 Two (2) Cells between sites
 Input Data: In-Phase & Quadrature,
 Tzx In-Line (only)
 Average sampling rate: 2.560 points,
 Total data points: 2304
 Frequencies: 30 45 90 180 360 720
 Input error(%): 1.48 1.48 1.48 1.48 1.48 1.48
 Half-space resistivity: 1000 ohm-m
 Output error: 0.999 RMS in 5 iterations
 Line L2400_03 over IP 90 Hz DT image



Teck Resources Limited
 Scud Block
 Scud Peak, BC, Canada

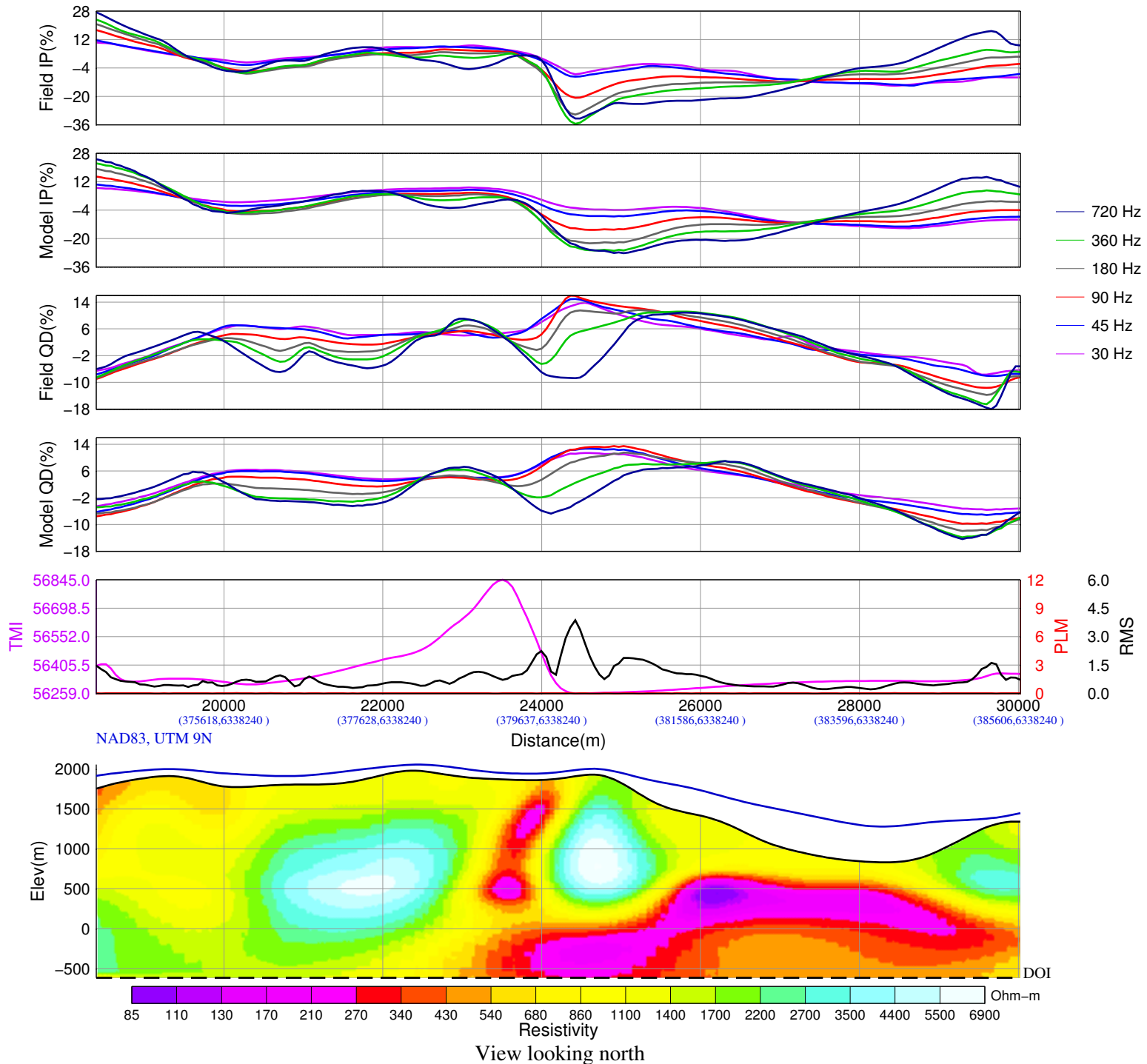
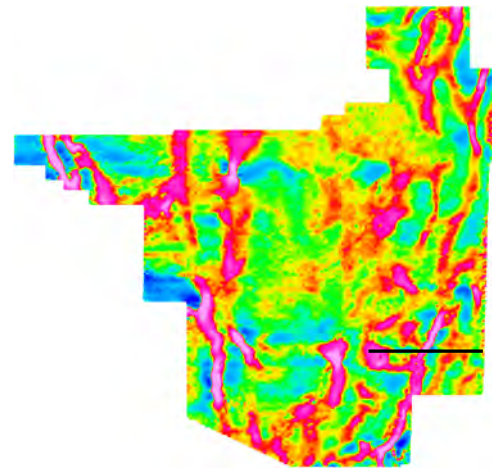
Geotech ZTEM System
 Resistivity-Depth Image
 ProjectGL130332, Line L2400_03
 Flight 27, 2013/09/13

Flown and Processed by Geotech Ltd.
 245 Industrial Parkway North
 Aurora, Ontario, Canada L4G 4C4
 www.geotech.ca

2013/10/16

2D INVERSION PARAMETERS

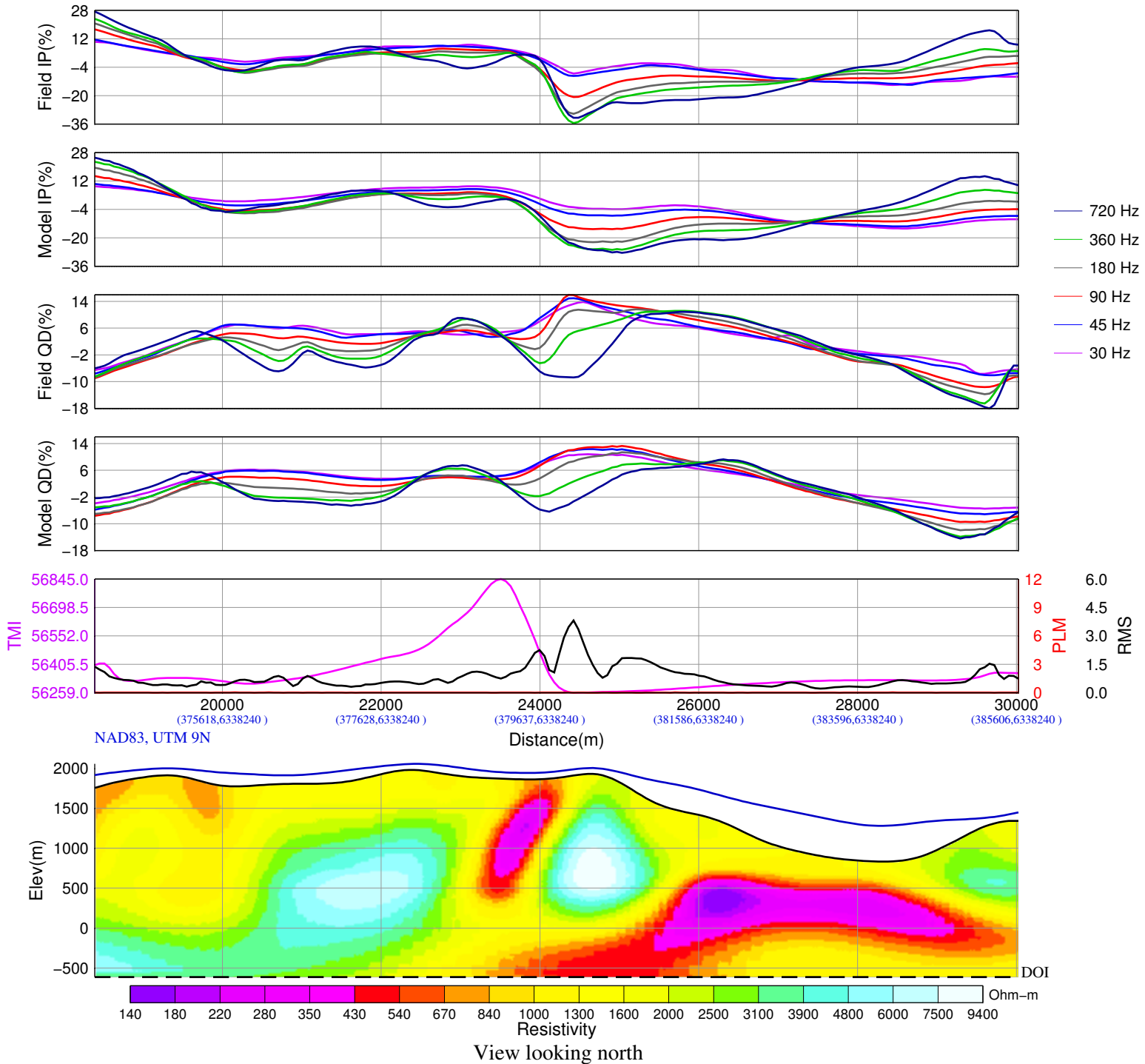
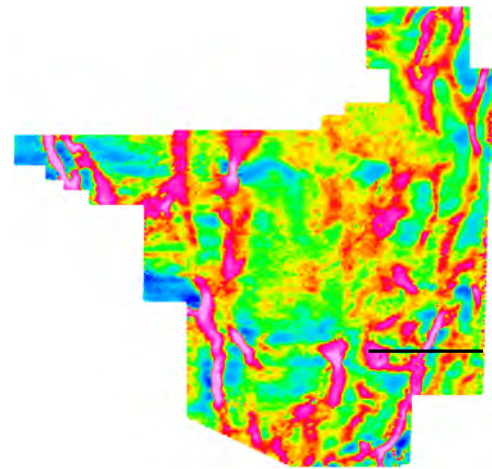
Inversion Code: Geotech AV2DTOPO
 Model Mesh: 440 wide x 112 vertical,
 Average cell width: 15.23 m
 Two (2) Cells between sites
 Input Data: In-Phase & Quadrature,
 Tzx In-Line (only)
 Average sampling rate: 2.560 points,
 Total data points: 2304
 Frequencies: 30 45 90 180 360 720
 Input error(%): 1.50 1.50 1.50 1.50 1.50 1.50
 Half-space resistivity: 2000 ohm-m
 Output error: 0.999 RMS in 5 iterations
 Line L2400_03 over IP 90 Hz DT image



Teck Resources Limited Scud Block Scud Peak, BC, Canada
Geotech ZTEM System Resistivity-Depth Image ProjectGL130332, Line L2400_03 Flight 27, 2013/09/13
Flown and Processed by Geotech Ltd. 245 Industrial Parkway North Aurora, Ontario, Canada L4G 4C4 www.geotech.ca
2013/10/16

2D INVERSION PARAMETERS

Inversion Code: Geotech AV2DPTOP
 Model Mesh: 440 wide x 112 vertical,
 Average cell width: 15.23 m
 Two (2) Cells between sites
 Input Data: In-Phase & Quadrature,
 Tzx In-Line (only)
 Average sampling rate: 2.560 points,
 Total data points: 2304
 Frequencies: 30 45 90 180 360 720
 Input error(%): 1.57 1.57 1.57 1.57 1.57 1.57
 Half-space resistivity: 4000 ohm-m
 Output error: 0.999 RMS in 5 iterations
 Line L2400_03 over IP 90 Hz DT image



Teck Resources Limited Scud Block Scud Peak, BC, Canada
Geotech ZTEM System Resistivity-Depth Image ProjectGL130332, Line L2400_03 Flight 27, 2013/09/13
Flown and Processed by Geotech Ltd. 245 Industrial Parkway North Aurora, Ontario, Canada L4G 4C4 www.geotech.ca
2013/10/16